Kübra Nur ŞAHİN

Ph.D. Thesis

AGU 2025

OPTIMAL DECISION-MAKING FOR OPERATIONS OF SMART GRIDS AND MICROGRIDS

Ph.D. THESIS
SUBMITTED TO THE DEPARTMENT OF INDUSTRIAL ENGINEERING
AND THE GRADUATE SCHOOL OF ENGINEERING AND SCIENCE OF
ABDULLAH GUL UNIVERSITY
IN PARTIAL FULFILLMENT OF THE REQUIREMENTS
FOR THE DEGREE OF
DOCTOR OF PHILOSOPHY

By

Kübra Nur ŞAHİN

June 2025

OPTIMAL DECISION-MAKING FOR OPERATIONS OF SMART GRIDS AND MICROGRIDS

A THESIS
SUBMITTED TO THE DEPARTMENT OF INDUSTRIAL ENGINEERING
AND THE GRADUATE SCHOOL OF ENGINEERING AND SCIENCE OF
ABDULLAH GUL UNIVERSITY
IN PARTIAL FULFILLMENT OF THE REQUIREMENTS
FOR THE DEGREE OF
DOCTOR OF PHILOSOPHY

By
Kübra Nur ŞAHİN
June 2025

SCIENTIFIC ETHICS COMPLIANCE

I hereby declare that all information in this document has been obtained in accordance with academic rules and ethical conduct. I also declare that, as required by these rules and conduct, I have fully cited and referenced all materials and results that are not original to this work.

Name-Surname: Kübra Nur ŞAHİN

Signature :

REGULATORY COMPLIANCE

Ph.D. thesis titled "**Optimal Decision-Making for Operations of Smart Grids and Microgrids**" has been prepared in accordance with the Thesis Writing Guidelines of the Abdullah Gül University, Graduate School of Engineering & Science.

Prepared By	Advisor
Kübra Nur ŞAHİN	Assoc. Prof. Muhammed Sütçü
Signature	Signature

Head of the Industrial Engineering Graduate Program
Assoc. Prof. Ramazan ÜNLÜ
Signature

ACCEPTANCE AND APPROVAL

Ph.D. thesis titled "**Optimal Decision-Making for Operations of Smart Grids and Microgrids**" and prepared by Kübra Nur ŞAHİN has been accepted by the jury in the Industrial Engineering Graduate Program at Abdullah Gül University, Graduate School of Engineering & Science.

19 /06 /2025

JURY:

Advisor : Assoc. Prof. Muhammed SÜTÇÜ

Member : Prof. Niğmet UZAL

Member : Assist. Prof. Betül ÇOBAN

Member : Prof. Bülent Yılmaz

Member : Prof. Özgür Demirtaş

APPROVAL:

The acceptance of this Ph.D. thesis has been approved by the decision of the Abdullah Gül University, Graduate School of Engineering & Science, Executive Board dated ….. /….. / ……….. and numbered ……………..……. .

19/06 /2025

Graduate School Dean
Prof. İrfan ALAN

ABSTRACT

OPTIMAL DECISION-MAKING FOR OPERATIONS OF SMART GRIDS AND MICROGRIDS

Kübra Nur ŞAHİN
Ph.D. in Industrial Engineering
Advisor: Assoc. Prof. Muhammed SÜTÇÜ
June 2025

The rising adoption of renewable energy sources and decentralized electricity production has introduced new challenges in power system coordination, uncertainty management, and reliability. This study presents a multi-stage framework combining probabilistic modelling, centralized optimization, and adaptive control for smart energy communities. First, a hybrid model integrating copula theory, deep learning, and decision trees is developed for probabilistic wind energy assessment. Second, a Mixed-Integer Linear Programming (MILP) model is formulated to optimize distributed energy resource scheduling and peer-to-peer (P2P) energy trading across various household types. Finally, a rule-based control environment is extended with a Deep Deterministic Policy Gradient (DDPG) reinforcement learning algorithm to enable real-time pricing and decentralized decision-making. The proposed model adapts to dynamic conditions, optimizes energy dispatch, and improves long-term system performance under uncertainty.

Collectively, this study introduces an integrated paradigm that combines resource evaluation, system optimization, and adaptive control. The findings highlight the potential for intelligent energy management to enhance grid flexibility, encourage decentralized operation, and facilitate the transition towards sustainable and resilient power systems.

Keywords: Smart Grid Energy Management, Reinforcement Learning, Peer-to-Peer Trading, Renewable Energy Integration, Distributed Energy Resources

ÖZET

AKILLI ŞEBEKE VE MIKROŞEBEKE OPERASYONLARINDA OPTIMAL KARAR VERME

Kübra Nur ŞAHİN
Endüstri Mühendisliği Anabilim Dalı Doktora
Tez Danışmanı: Doç. Dr. Muhammed SÜTÇÜ
Haziran - 2025

Yenilenebilir enerji kaynaklarının artan entegrasyonu ve elektrik üretiminin merkeziyetsizleşerek dağıtık hale gelmesi, güç sistemlerinde koordinasyon ve sistem güvenilirliği açısından önemli zorlukları beraberinde getirmiştir. Bu çalışma, akıllı enerji toplulukları için, olasılıksal modelleme, merkezî optimizasyon ve uyarlanabilir kontrol yaklaşımlarını bir araya getiren çok katmanlı bir metodolojik çerçeve sunmaktadır. İlk aşamada, meteorolojik değişkenler arasındaki karmaşık doğrusal olmayan ilişkileri modelleyebilen ve rüzgâr enerjisi potansiyelini belirsizlik altında değerlendirebilen, kopula teorisi, derin öğrenme ve karar ağaçlarını birleştiren hibrit bir yöntem geliştirilmiştir. İkinci aşamada, farklı hane yapılarını içeren bir şebekede, dağıtık enerji kaynaklarının zamanlaması ve eşler arası (P2P) enerji ticaretinin optimizasyonu için Karışık Tamsayılı Doğrusal Programlama (MILP) tabanlı model tasarlanmıştır. Son aşamada ise, kural tabanlı karar verme yapısı, Derin Deterministik Politika Gradyanı (DDPG) algoritması ile geliştirilerek, gerçek zamanlı fiyatlandırma ve merkezsiz karar alma yeteneklerine sahip bir operasyonel kontrol ortamı oluşturulmuştur. Geliştirilen model, değişken sistem koşullarına uyum sağlamakta, enerji yönetimini optimize etmekte ve belirsizlik altında uzun vadeli sistem performansını artırmaktadır.

Bu çalışma, enerji sistemlerinde kaynak değerlendirmesinden operasyonel kontrole uzanan; deterministik planlamayı gerçek zamanlı, öğrenen yapılarla bütünleştiren kapsamlı bir karar destek mimarisi sunmaktadır. Elde edilen bulgular, dağıtık yenilenebilir kaynakların entegrasyonunu destekleyen, esnek, dayanıklı ve sürdürülebilir enerji sistemlerinin geliştirilmesine katkı sunmaktadır.

Anahtar kelimeler: Akıllı Şebeke Enerji Yönetimi, Pekiştirmeli Öğrenme, Eşler Arası Ticaret, Yenilenebilir Enerji Entegrasyonu, Dağıtık Enerji Kaynakları

Acknowledgements

I would like to express my deepest gratitude to my advisor, Associate Professor Dr. Muhammed SÜTÇÜ, for his invaluable guidance, insight, and encouragement throughout the course of this research. His mentorship has been instrumental in shaping both the direction and quality of this work.

I would also like to thank the members of my thesis monitoring committee, Prof. Dr. Niğmet UZAL and Assist. Prof. Dr. Betül ÇOBAN, for their insightful feedback and guidance during the research. I am also thankful for their time and continuous encouragement throughout the progress tracking phases of my doctoral journey.

I am profoundly grateful to my parents, Muammer ŞAHİN and Sema ŞAHİN, whose unwavering support, patience, and belief in me provided the foundation for this achievement. I would also like to thank my beloved siblings Zeliha KAYA, Muhammed Emirhan ŞAHİN, Hayrunnisa ŞAHİN, Celal KAYA, and Maviş ŞAHİN and my dear nieces Hafsa Hüma KAYA and Mehmet Emir KAYA, whose encouragement and love have been a constant source of motivation throughout this journey.

A heartfelt thank you goes to my best friend, Dr. Refika Sultan DOĞAN. Her unwavering support, contagious positivity, and constant belief in me made even the toughest days bearable. This journey would not have been the same without her friendship, laughter, and endless encouragement.

I would also like to acknowledge my heartfelt appreciation to TÜBİTAK for their generous support through the 2211-A National PhD Scholarship Program and the 2214 International Research Fellowship Programme for PhD Students. Their commitment to fostering scientific research and empowering young scholars was instrumental in enabling this work and expanding its academic impact both nationally and internationally.

TABLE OF CONTENTS

LIST OF FIGURES

LIST OF TABLES

LIST OF ABBREVIATIONS

RES	Renewable Energy Sources
P2P	Peer-To-Peer
MILP	Mixed-Integer Linear Programming
DDPG	Deep Deterministic Policy Gradient
MCDM	Multi-Criteria Decision-Making
AHP	Analytical Hierarchy Process
TOPSIS	Technique for Order of Preference by Similarity to Ideal Solution
PROMETHEE	Secure Multiparty Computation
ELECTRE	Elimination Et. Choice Translating Reality
LSTM	Long Short-Term Memory
RMSE	Root Mean Squared Error
MSE	Mean Squared Error
MOM	Method Of Moments
CML	Canonical Maximum Likelihood
MDM	Minimum Distance Model
MPL	Maximum Pseudo-Likelihood
MCS	McNamee-Celona Shortcut
EMS	Extended Swanson-Megill
EPT	Extended Pearson-Tukey
ZDI	Zaino-D'Errico "Improved"
ZDT	Zaino-D'Errico-Tagichi
MRO	Miller-Rice One Step
RNN	Recurrent Neural Network
PV	Photovoltaic
BESS	Battery Energy Storage System
EV	Electric Vehicle
DER	Distributed Energy Resources
PSO	Particle Swarm Optimization
DQN	Deep Q Network
SoC	State Of Charge
CSSR	Community-Supported Self-Sufficiency Rate

GDR	Grid Dependency Ratio
V2G	Vehicle-to-Grid
G2V	Grid-to-Vehicle
H2G	Home-to-Grid
DR	Demand Response
RTP	Real-time Pricing
TOU	Time-of-Use
CPP	Critical peak pricing
PSA	P2P PV Surplus Allocation
P2P-BSET	P2P BESS-Supported Energy Trading
MDP	Markov Decision Process
DRL	Deep Reinforcement Learning
DPG	Deep Policy Gradient

To my lovely family

Chapter 1

Introduction

Energy systems are the cornerstone of modern economic and social development. Urbanization, industrialization, and digital transformation have all contributed to an increase in energy demand, emphasizing the importance of sustainable and intelligent energy solutions. At the same time, environmental concerns, fossil fuel depletion, and international frameworks like the Paris Agreement and the UN 2030 Agenda [1,2] have highlighted the importance of shifting to low-carbon, decentralized energy systems. Smart grid technologies, which may incorporate renewable and distributed energy resources (DERs), are critical to this shift [3].

Implementing smart grids introduces complex challenges, especially in optimizing energy flow, coordinating markets, and ensuring system reliability. The variability of renewable energy sources (RESs) and the dynamic nature of prosumers require advanced, data-driven management strategies [4]. This thesis addresses the challenges by developing comprehensive control frameworks tailored to smart energy communities.

This study progresses from resource assessment and centralized scheduling to real-time adaptive control, reflecting the evolution of energy management. It begins with the probabilistic evaluation of renewable energy potential, continues with the optimization of DERs scheduling and Peer-to-Peer (P2P) trading, and culminates in reinforcement learning-based control mechanisms.

Chapter 2 presents a hybrid model for assessing wind energy potential, combining copula theory, deep learning, and decision trees. This model effectively captures nonlinear meteorological dependencies, supporting uncertainty-aware planning and renewable integration.

Chapter 3 introduces a Mixed-Integer Linear Programming (MILP) framework for managing residential power systems with diverse household types. It optimizes energy scheduling and P2P trading across grid-dependent users, PV-only, and PV–BESS prosumers, highlighting the impact of storage and user diversity on system efficiency.

Chapter 4 shifts to decentralized control by first modeling operational logic with rule-based strategies. This environment is then enhanced with a Deep Deterministic Policy Gradient (DDPG) algorithm that enables real-time pricing and adaptive prosumer behavior in response to grid conditions and market dynamics.

This thesis offers an integrated structure that addresses three critical components of smart energy systems: evaluation, planning, and control. The thesis provides a scalable, intelligent framework for fostering the development of robust, adaptive, and sustainable energy infrastructures.

Chapter 2

Probabilistic Assessment of Wind Power Plant Energy Potential through a Copula-Deep Learning Approach in Decision Trees[5]

*This study has been published on Heliyon, and the content has been reprinted with permission

Abstract

In the face of environmental degradation and diminished energy resources, there is an urgent need for clean, affordable, and sustainable energy solutions, which highlights the importance of wind energy. In the global transition to renewable energy sources, wind power has emerged as a key player that is in line with the Paris Agreement, the Net Zero Target by 2050, and the UN 2030 Goals, especially SDG-7. It is critical to consider the variable and intermittent nature of wind to efficiently harness wind energy and evaluate its potential. Nonetheless, since wind energy is inherently variable and intermittent, a comprehensive assessment of a prospective site's wind power generation potential is required. This analysis is crucial for stakeholders and policymakers to make well-informed decisions because it helps them assess financial risks and choose the best locations for wind power plant installations. In this study, a Copula-Deep Learning based framework is presented within the context of decision trees. The main objective is to enhance the assessment of the wind power potential of a site by exploiting the intricate and non-linear dependencies among meteorological variables through the fusion of copulas and deep learning techniques. An empirical study was carried out using wind power plant data from Turkey. This dataset includes hourly power output measurements as well as comprehensive meteorological data for 2021. The results show that acknowledging and addressing the non-independence of variables through innovative frameworks like the Copula-LSTM based decision tree approach can significantly improve the accuracy and reliability of wind power plant potential assessment and analysis in other real-world data scenarios. The implications of this research extend beyond wind energy to inform decision-making processes critical for a sustainable energy future.

2.1 Introduction

Under the pressure of environmental degradation and the depletion of energy resources, achieving clean, cheap, and sustainable energy has become an important issue that needs to be tackled. At the forefront of this imperative is the energy sector, the largest contributor to global greenhouse gas emissions, accounting for approximately 73.2%. (see Figure 2.1[6])

Given the central role of the energy sector, it is clear that transformative action is essential to reduce its negative impact on the environment. Strategies aimed at reducing emissions, switching to renewable energy sources, and improving energy efficiency are of paramount importance. In addition, encouraging innovation and implementing sound policies can further advance the energy sector towards a more sustainable future.

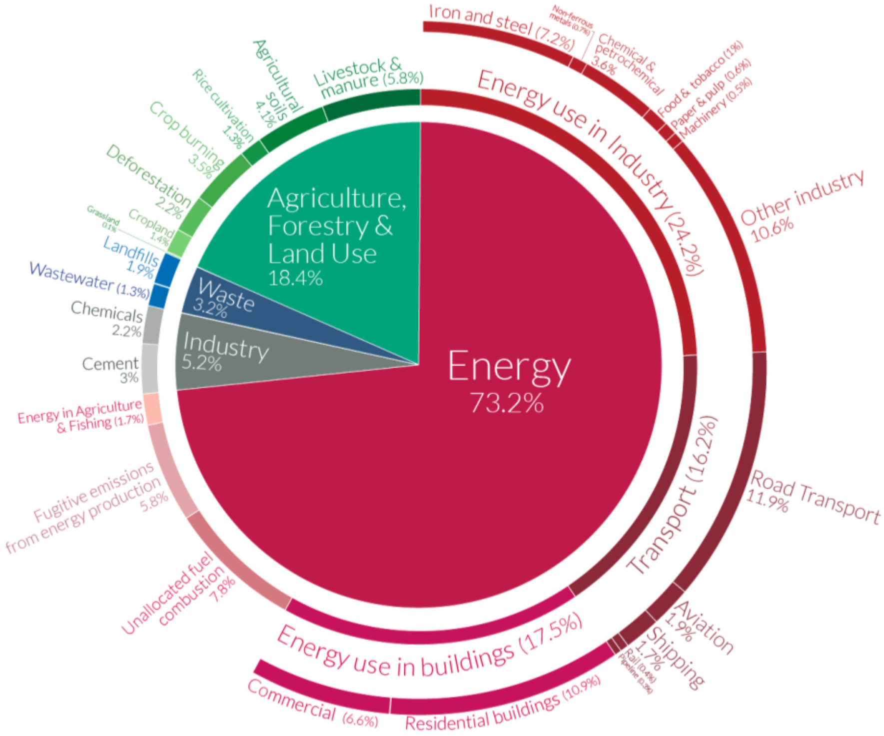

Figure 2.1 Global greenhouse gas emissions by sector

The importance of wind energy as a clean and sustainable energy source has increased due to the urgent need to reduce emissions in the energy sector and switch to renewable energy sources. Wind energy plays a crucial role in achieving the ambitious goals in agreements such as the Paris Agreement, the Net Zero Target by 2050, and the United Nations 2030 goals, in particular SDG-7 (Affordable and Clean Energy). This growing recognition underlines the central role of wind energy in mitigating climate change and advancing the global agenda for a sustainable and low-carbon future. Consequently, the expansion of wind power plants is essential to meet the growing demand for clean energy and to fulfill global sustainability goals.

However, when establishing wind power plants, the assessment of wind energy potential is crucial in the construction of wind turbines, as it determines the success and efficiency of the project. While current assessment tools are valuable, they are often not practical or comprehensive enough. Furthermore, existing tools may lack the precision required to identify and mitigate the risks associated with specific sites, potentially exposing projects to unforeseen challenges. Given these limitations, there is an urgent need for more comprehensive and practical tools to assess the potential of wind power plants. These tools should go beyond the current limitations and provide a more nuanced understanding of wind patterns, speeds, and variability at potential sites. In this way, they can facilitate optimal site selection and ensure not only maximum energy yield but also the long-term sustainability and resilience of wind power plants. Additionally, enhanced assessment tools would contribute to more accurate financial evaluations, enabling decision-makers to take well-informed decisions regarding the technical feasibility, viability, and profitability of wind energy projects [7]. Therefore, investing in developing advanced, practical, and comprehensive assessment tools is essential to guide the wind energy sector towards a more efficient, sustainable, and resilient future [8].

With these tools analyzing the output characteristics of wind power emerges as a strategic and effective response to the inherent uncertainties associated with wind energy. These tools involve a thorough examination of the patterns and behaviors in power generation, empowering stakeholders to devise resilient strategies for risk mitigation and enhanced optimization of energy production [9-12]. Wind power output P_w is the most accurate way to assess the technical potential of wind power plants to decide whether the site is financially feasible [13]. Understanding the output characteristics of wind power is imperative, given the noteworthy power fluctuations and the intricate influence of challenging site locations [11,14]. Furthermore, recognizing that the fluctuation in wind power output is attributed to changes in wind speed, precise determination of the distribution and fluctuation characteristics of wind speed within the wind power plant becomes instrumental for a comprehensive understanding of its overall output [15-17].

The most common techniques when assessing wind energy potential are statistical time series models, distribution fitting such as Weibull distribution methods and estimation models [18-22]. Due to the unpredictable nature of factors that affect wind energy production, multivariate analysis is required. By using multivariate analysis, which takes into consideration the interactions between several varied factors, it is possible to attain a more thorough understanding of wind patterns and their behavior [23]. In the literature, when wind power plant energy potential is analyzed, wind-related meteorological uncertainties are generally assumed to be completely independent variables, and the joint probability distributions of these uncertainties were constructed by approaches such as isotropic Gaussian distribution [24], anisotropic Gaussian distribution [25], and anisotropic logarithmic Gaussian distribution [26], etc. As expected, these approaches fall short at some points because the meteorological uncertainties are not independent by their nature. Although the techniques used in the literature offered helpful insights, they may sometimes fail to capture the complex dependencies and non-linear interactions that are inherently present in wind data, which results in limited accuracy and reliability. Among the multivariate techniques, copulas have gained substantial attention in recent studies due to their potential to reflect complex dependence structures and wide application areas such as finance, risk management, rainfall analysis, drought analysis, insurance, etc. [27-30].

Concurrently, in multivariate modeling and analysis, a "dependence tree" approach is applied to assess dependence measures in a hierarchical manner [31]. Despite this, integrating multivariate dependencies in a decision tree is computationally expensive in general since the generation of conditional distributions for each branch of the tree is a challenging task [32]. If the marginal distributions of the variates belong to different distribution families, generating the conditional distributions becomes even more challenging. In this context, it is practical to specify the variable marginal distributions and use copulas to compute joint distributions to describe the hierarchical structure of multivariate dependence. There has been limited study on the application of copulas to discrete probability trees in decision analysis [32].

Furthermore, in the literature, the application of Multi-Criteria Decision-Making (MCDM) models, notably Analytical Hierarchy Process (AHP), TOPSIS (Technique for Order of Preference by Similarity to Ideal Solution), PROMETHEE (Preference Ranking Organization Method for Enrichment Evaluation), ELECTRE (Elimination Et. Choice Translating Reality), and Fuzzy has been widespread for assessment of wind energy site. Studies by Emeksiz and Demirci et al.[33] in Turkey, Şahin et al. [34] in the Netherlands, Solangi et al. [35] in Pakistan, and Islam et al. [36] in Bangladesh exemplify the utilization of these methods to assess various criteria for identifying optimal locations for wind power plants. However, alongside overseeing interdependencies among critical factors, the literature underscores challenges in MCDM models assuming linear relationships between variables. This assumption has the potential to lead to suboptimal site assessment, emphasizing the need for advanced methodologies that can capture the non-linear dynamics inherent in wind energy production. Addressing these limitations is imperative to ensure accurate and robust decision-making processes in selecting wind energy sites.

The copula-based dependent tree approach can be an effective and practical approach to statistically representing the multivariate dependence structure of wind data. Meanwhile, in order to estimate the wind power potential of a site, there is a need to develop a model to generate wind farm power outputs for each branch of the dependent tree. Therefore, in that study, a Long Short-Term Memory (LSTM) architecture was adopted for this purpose.

Using multivariate analysis, it is possible to gain a better understanding of the relationships among meteorological variables. Despite the complexity of the interactions between these variables, the determination of the joint distributions of the variables and their conditional distributions and the estimation of the power output values are crucial for evaluating the potential of wind power plants. However, the earlier methods have some limitations in terms of their effectiveness and computational complexity. To overcome this limitation, a copula-deep learning based multivariate modelling framework has been developed. The main goal of this study is, therefore, to provide a comprehensive and robust framework for evaluating the potential of a wind power plant while capturing the complex dependencies and patterns in the data and leveraging the capabilities of deep learning. Through the use of this framework, energy stakeholders will be able to make more informed decisions about the planning, development, and operation of wind power plants.

The main contributions of the study can be summarized as follows: (1) dependence between the meteorological variables is often disregarded, and the independence assumption has been generally applied since defining a multivariate joint distribution is challenging and computationally expensive. A copula-based dependence structure is adopted, and complex and nonlinear dependencies and tendencies that are limited in other studies are incorporated; (2) a comprehensive Copula-Deep Learning fusion in decision trees approach has been employed for the first time to evaluate wind power plant energy potential assessment at a certain location taking into consideration the meteorological uncertainties; and (3) the findings from this study will provide insights into the techno-economic feasibility of wind power projects and a decision support mechanism for policymakers and stakeholders of wind power plants thereby realizing effective utilization of this abundant resource.

The rest of the chapter is structured as follows: Section 2.2 introduces the Copula-LSTM-based decision tree framework. The implementation of the proposed framework and the performance analysis are provided in Section 2.3. Finally, Section 2.4 concludes Chapter 2.

2.2 Methodology

The main steps of the proposed methodology are data analysis, feature selection, identifying the most suitable marginal probability distributions, modeling multivariate distributions with copulas, parameter estimation for the underlying copula, copula-based transient tree structure, inverse marginal transformation, and LSTM neural networks.

2.2.1 Data Analysis

The correlations between meteorological conditions are investigated to gain a comprehensive understanding of their interactions. Tests of Spearman, Kendall [37], and Pearson [38] are applied to measure the dependencies between the variables; temperature, humidity, pressure, wind speed, wind gust, and wind bearing.

Significant relationships emerged from the analysis. Notably, a negative correlation was observed between temperature and humidity (Spearman's $\rho = -0.620$, $p < 0.05$), indicating their interconnectedness. Similarly, a negative correlation was found between temperature and pressure (Kendall's $\tau = -0.454$, $p < 0.05$), highlighting the interplay between these meteorological factors.

Additionally, a positive monotonic relationship surfaced between wind speed and wind gust (Pearson's $r = 0.907$, $p < 0.05$), suggesting a consistent variation in wind speed corresponding to changes in wind gust.

To deepen the interpretation of these correlations, effect size measures were calculated. For example, Cohen's d for the negative correlation between temperature and humidity yielded $d = -0.612$, indicating a moderate effect size. Likewise, for the correlation between temperature and pressure, Kendall's effect size τ-b was calculated as $\tau\text{-b} = -0.616$, signifying a moderate effect.

These effect size measures enhance the understanding of the correlations, providing valuable insights into the magnitude and practical significance of the observed meteorological dependencies. The findings contribute to the robustness and applicability of the research, offering nuanced insights into the relationships among meteorological variables. However, for a more comprehensive exploration of complex dependence structures, copulas provide a versatile framework. They excel in modeling multivariate dependencies beyond linear correlations, capturing intricate patterns such as tail dependencies, asymmetric relations, and non-monotonic behaviors. Incorporating copulas into the analysis further refines the understanding of meteorological dependencies, acknowledging the nuanced nature of these relationships and contributing to the depth and applicability of the research findings.

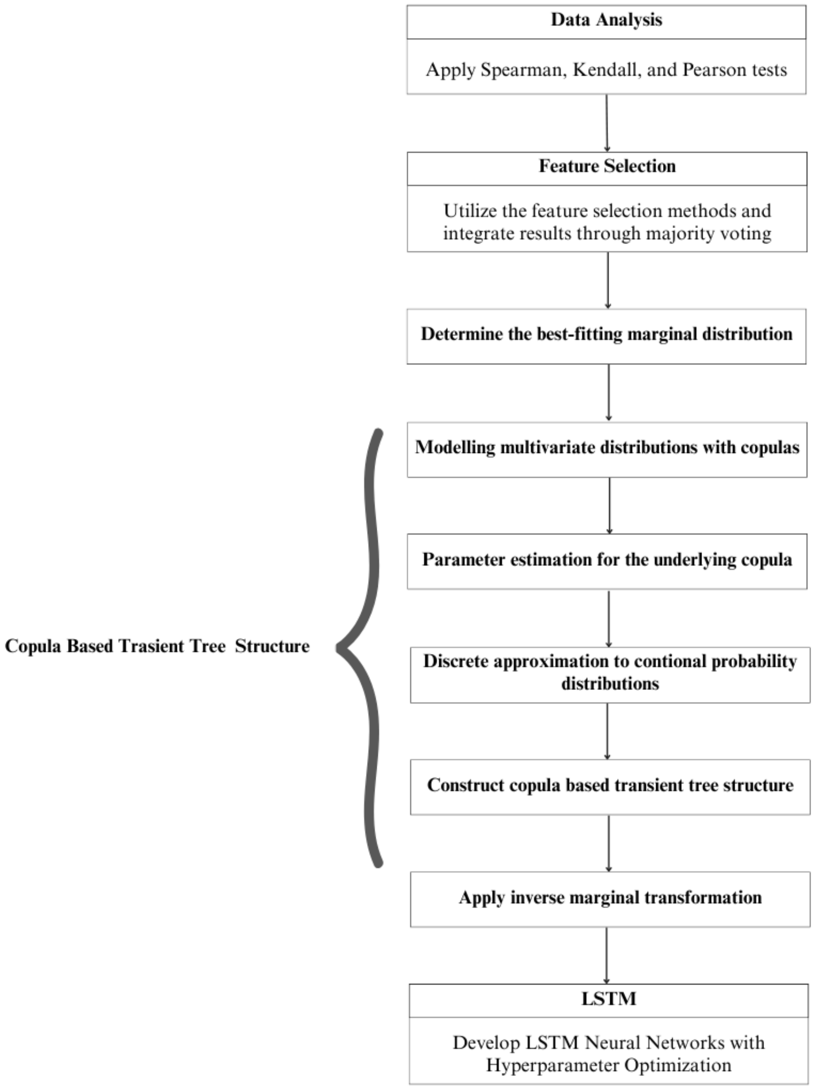

Figure 2.2 The flowchart of proposed methodology

2.2.2 Feature Selection and Identifying the Most Suitable Marginal Probability Distributions

In the context of the dependent decision tree approach, feature selection is essential to identify the most relevant variables that significantly contribute, since it helps to reduce the complexity of the model and enhance its performance. When the number of variables increases, the depth of the decision tree grows linearly, but the number of branches grows exponentially with the number of features.

Forward selection, backward elimination, lasso regularization, decision tree importance, recursive feature elimination, and mutual info techniques are used in this study to reduce the computational complexity of the model and determine the most informative set of features. Feature selection through various techniques followed by a voting approach is used as a tool to improve model performance. The voting approach aggregates the selection of the individual feature selection techniques. The ensemble of various feature selection techniques with majority voting helps in making robust predictions, reducing overfitting, and improving the model's generalization performance. With this approach, the set of selected features that is likely to capture relevant information while minimizing computational burden is determined.

In addition, to accurately capture the inherent characteristics of a variable, deriving the best-fitted marginal probability distribution is crucial. The evaluation metrics mainly used to measure the fitting performance of the theoretical distribution are the Root Mean Squared Error (RMSE), Mean Squared Error (MSE), Kolmogorov-Smirnov and Chi-square tests. In that study, MSE is used to evaluate the fitting performance of the distribution.

2.2.3 Modelling Multivariate Distributions with Copulas

In recent years, there has been growing interest in copula models to examine the structure of interdependence between variables in a variety of research fields such as energy, medical science, banking, and economics. Copulas are powerful statistical tools to develop a dependent structure of multivariate random variables where the marginal distributions of random variables are independently determined. The term "Copula" was first introduced by Sklar, in 1959 [39]. The proposed idea is that a joint distribution can be expressed as a function of the marginal distributions [39]. Variations in the correlation of the variables in different parts of marginal distributions can be explained by copula models [40]. Mathematically, it can be expressed as

$$C\big(F_1(x_1), F_2(x_2), .., F_n(x_n)\big) = F(x_1, x_2, \dots, x_n) \quad \textbf{(2.1)}$$

and,

$$F(X_1) = U_1, F(X_2) = U_2, .., F(X_n) = U_n \quad \textbf{(2.2)}$$

Thus,

$$C(u) = C(u_1, u_2, \dots, u_n) = P(U_1 \leq u_1, U_2 \leq u_2, \dots, U_n \leq U_n) \quad \textbf{(2.3)}$$

where $x = (x_1, x_2, .., x_n) \in R^n$ and $U = (U_1, U_2, .., U_n)$ is a n-dimensional random vector with $U_i \sim \mathrm{Unif}(0,1),\ \forall i = 1,2, \dots, n$. This is well-known Sklar's Theorem (1) enables us to express any multivariate distribution in terms of its marginal distributions and a copula that captures dependencies between the variables. If X is a continuous random vector, then the copula C is unique [39].

With the cumulative distribution function of a joint distribution, the joint probability distribution function (PDF) can be derived as follows:

$$\begin{aligned} f(x_1, x_2, \dots, x_n) &= \frac{\partial^n F(x_1, x_2, \dots, x_n)}{\partial x_1 \partial x_2 \dots \partial x_n} \\ &= \frac{\partial^n C\big(F_1(x_1), F_2(x_2), .., F_n(x_n)\big)}{\partial F_1(x_1)\, \partial F_2(x_2) .. \partial F_n(x_n)} \frac{\partial F_1(x_1)}{\partial x_1} \frac{\partial F_2(x_2)}{\partial x_2} \dots \frac{\partial F_n(x_n)}{\partial x_n} \\ &= c(F_1(x_1), F_2(x_2), .., F_n(x_n)) \prod_{i=1}^{n} f_i(x_i) \end{aligned} \quad \textbf{(2.4)}$$

where $f_i(x_i)$ denotes the marginal PDF of X_i and $c(F_1(x_1), F_2(x_2), .., F_n(x_n))$ denotes the copula density that is obtained from the partial derivative of the copula. Thus, any joint probability density function can be written as the product of its marginal probability density functions. Detailed information about copulas in general can be found in the books by Nelsen [41].

In the literature, numerous families of copulas emphasizing various distributional properties have been proposed, i.e., the Archimedean, Elliptical, Plackett, etc. These copula families include a wide range of patterns of tail dependences and various types of asymmetries. The well-known elliptical copulas are the Gaussian and Student's t copula. The elliptical copulas represent symmetrical tail dependencies. In addition to elliptical copulas, the most known Archimedean copulas are Frank, Gumbel, and Clayton. These types of copulas capture various types of tail dependence. The Frank is symmetric with no tail dependence [42]. While the Gumbel copula has upper-tail dependence [43], the Clayton copula has lower-tail dependence [44]. Table 2.1 illustrates mathematical descriptions of the copula families used in this study.

The characteristics of copula theory allow for the construction of decision tree structures that incorporate the dependence structure obtained by copulas and marginal densities. A transient probability tree can be created based on copulas, which can capture the various types of multivariate dependencies. After the determination of the marginal distributions of the variables, the conditional distributions of each branch of the dependent decision tree can be obtained.

The generation of random uniform variables from multivariate copulas is performed to build a transient probability tree. This process can be called sampling. One approach for sampling a uniform random variable $(u_1, u_2, \dots, u_n)$ from n-dimensional normal copula is to use Cholesky decomposition for the generation of the uniform variables [45]. After the Cholesky factorization process is applied to the correlation matrix $\boldsymbol{\Sigma_n}$; i.e., $\boldsymbol{\Sigma_n} = \boldsymbol{AA'}$, we can generate n independent $\boldsymbol{z} = (z_1, z_2, \dots, z_n)$ and $\boldsymbol{x} = (x_1, x_2, \dots, x_n)$ which is $\boldsymbol{Az}$ [46]. N-dimensional t-copula can be obtained similarly with parameters $\boldsymbol{\Sigma_n}$ and d. For Archimedean copulas, as a first step to generate two-dimensional random variable (u_1, u_2), two independent uniform random variables u_1 and w will be generated. To obtain u_2 value using the quasi-inverse function of conditional distribution $P(U_2 \leq u_2 | U_1 = u_1)$ that is $u_2 = C_{2|1}^{-1}(w|u_1)$. We calculate the conditional copula as following,

$$C_{2|1}(u_2|u_1) = \frac{\partial C_2(u_1, u_2)}{\partial u_1} \tag{2.5}$$

For multivariate case (n-dimensional, $n \geq 3$) u_1 and $w_1, w_2, \dots, w_{n-1}$ are generated as bivariate case and $u_2, u_3, \dots, u_n$ random variables are obtained by [46]

$$\begin{aligned} u_2 &= C_{2|1}^{-1}(w_1|u_1) \\ u_3 &= C_{3|1,2}^{-1}(w_2|u_1, u_2), \\ &\vdots \\ u_n &= C_{n|1,2,\dots,n-1}^{-1}(w_{n-1}|u_1, u_2, \dots, u_{n-1}), \end{aligned}$$

where

$$\begin{aligned} C_{n|1,2,\dots,n-1}(u_n|u_1, u_2, \dots, u_{n-1}) &= P(U_n \leq u_n | U_1 = u_1, U_2 = u_2, \dots, U_{n-1} = u_{n-1}) \\ &= \frac{\left(\partial^{n-1} C_n(u_1, u_2, \dots, u_n)\right) / (\partial u_1 \partial u_2 \dots \partial u_{n-1})}{\left(\partial^{n-1} C_{n-1}(u_1, u_2, \dots, u_{n-1})\right) / (\partial u_1 \partial u_2 \dots \partial u_{n-1})} \end{aligned} \tag{2.6}$$

Let considers the bivariate Archimedean copula case. For any continuous random variables X_1 and X_2 to generate u_2 given that $u_1 = P(X_1 \leq x_1) = \alpha_1$, we need to obtain the conditional distribution of X_2 given $X_1 = x_1$ from the partial derivative of the copula function. For each given percentile $P(X_2 \leq x_2 | X_1 = x_1) = \alpha_2$ and $\partial C(u_1, u_2) / \partial u_1 = C_{u_1}(u_2) = \alpha_2$ then, $u_2 = C_{u_1}^{-1}(\alpha_2)$. Thus, with unconditional and conditional percentile values obtained by using copula functions, a transient probability tree structure can be built [32].

Table 2.1 Formulas of elliptical and archimedean copulas

Family	Mathematical Expression	Partial Derivative of the copula w.r.t $\boldsymbol{u_1}$	$\boldsymbol{u_2}$
Normal Copula	$C_n = \left(F_1(X_1), F_2(X_2)\right) = \phi_r\left(\phi^{-1}\left(F_1(X_1)\right), \phi^{-1}\left(F_2(X_2)\right)\right)$	$\phi\left(\frac{\phi^{-1}(u_2) - r\phi^{-1}(u_1)}{\sqrt{1-r^2}}\right)$	$u_2 = \phi\left(r\phi^{-1}(\alpha_1) + \sqrt{1-r^2\phi^{-1}(\alpha_2)}\right)$
t-copula	$C_T = \left(F_1(X_1), F_2(X_2)\right) = t_{r,v}\left(t_v^{-1}\left(F_1(X_1)\right), t_v^{-1}\left(F_2(X_2)\right)\right)$	$t_{r,v}\left(\sqrt{\frac{v+1}{v+(t_v^{-1}(u_1))^2}}.\frac{t_v^{-1}(u_2) - rt_v^{-1}(u_1)}{\sqrt{1-r^2}}\right)$	$u_2 = t_v\left(rt_v^{-1}(\alpha_1) + \sqrt{1-r^2}\sqrt{\frac{v+\left(t_v^{-1}(u_1)\right)^2}{v+1}}t_{v+1}^{-1}(\alpha_2)\right)$
Clayton Copula	$C_{Clayton}(u_1, u_2) = \left(u_1^{-\theta} + u_2^{-\theta} - 1\right)^{-1/\theta}$	$u_1^{-\theta-1}\left(u_1^{-\theta} + u_2^{-\theta} - 1\right)^{-1/\theta-1}$	$u_2 = \left(\left(\alpha_2^{-\theta/1+\theta} - 1\right)\alpha_1^{-\theta} + 1\right)^{-1/\theta}$
Gumbel Copula	$C_{gumbel}(u_1, u_2) = exp\left\{-\left[(-ln\, u_1)^\theta + (-ln\, u_2)^\theta\right]^{1/\theta}\right\}$	$\frac{\partial C}{\partial u_1}(u_1, u_2) = \frac{\varphi^{-1(1)}(c_2)}{\varphi^{-1(1)}(c_1)}$ where $c_1 = \varphi(u_1) = \left(-ln\,(u_1)\right)^\theta$ $c_2 = \varphi(u_1) + \varphi(u_2) = \left(-ln\,(u_1)\right)^\theta + \left(-ln\,(u_2)\right)^\theta$ and $\varphi^{-1(1)}(t) = -\frac{1}{\theta}e^{-t^{1/\theta}}\left(t^{1/\theta}\right)^{1-\theta}$	The value can be obtained by solving the given equations.
Frank Copula	$C_{Frank}(u_1, u_2) = -\frac{1}{\theta}ln\left(1 + \frac{(e^{-\theta u_1} - 1)(e^{-\theta u_2} - 1)}{e^{-\theta} - 1}\right)$	$\frac{\left(e^{-\theta u_2} - 1\right)\left(e^{-\theta u_1}\right)}{(e^{-\theta} - 1) + (e^{-\theta u_1} - 1)(e^{-\theta u_2} - 1)}$	$u_2 = -\frac{1}{\theta}ln\left(1 + \frac{\left(e^{-\theta} - 1\right)\alpha_2}{e^{-\theta\alpha_1} - (e^{-\theta\alpha_1} - 1)\alpha_2}\right)$

2.2.4 Parameter Estimation for the Underlying Copula

Since the dependency structure is modeled by copulas, specific parameters of copulas should be estimated. The methods that are proposed to estimate copula parameters are the method of moments (MOM) [47] known as inversion of Kendal's τ, inversion of Spearman's rho, canonical maximum likelihood (CML), minimum distance method (MDM) [48-50], and maximum pseudo-likelihood (MPL) [51].

For a normal copula, the product-moment correlation r should be estimated. To estimate the relationships between the product-moment correlation r for the normal copula, Spearman's rank order correlation ρ or Kendall's rank order correlation τ can be used [52].

$$r = 2\sin\left(\frac{\pi\rho}{6}\right) \text{ and } r = 2\sin\left(\frac{\pi\tau}{2}\right) \quad \textbf{(2.7)}$$

For the Archimedean family, using the MOM approach, the parameters are estimated using the relationship between Kendall's τ and the generator function φ of the copula [47].

$$\tau = 1 + \int_0^1 \frac{\varphi(t)}{\varphi'(t)} dt \quad \textbf{(2.8)}$$

The relationship between Kendall's rank order correlation τ and θ is summarized in Table 2.2 [41].

Table 2.2 The relation between Kendall's τ and θ for Archimedean copula

Copula Type	$\boldsymbol{\varphi(t)}$	**Kendall's Rank Order Correlation ($\boldsymbol{\tau}$)**	**Range of $\boldsymbol{\theta}$**
Clayton	$(t^{-\theta} - 1)/\theta$	$\frac{\theta}{\theta + 2}$	$(-1, \infty) - [0]$
Frank	$-\log\left(\frac{exp(t\theta) - 1}{exp(\theta)}\right)$	$1 + 4\theta^{-1}(D_1^*(\theta) - 1)$	$(-\infty, \infty) - [0]$
Gumbel	$-\log(t)^{\theta}$	$\frac{\theta - 1}{\theta}$	$[1, \infty)$

$$D_1^* = \frac{1}{\theta}\int_0^{\theta} \frac{t}{e^t - 1}$$

2.2.5. Copula-Based Transient Tree Structure

Discrete approximations to conditional probability distributions with the underlying copula are used to construct a probability tree. Discretization techniques are mostly used in decision analysis because using the true distribution is computationally costly, and using discretization techniques in the decision analysis approach enables us to estimate the expected value of the decision without any prior knowledge about the probability distribution function of any uncertainties. There are many methods for discretization in the literature such as McNamee-Celona Shortcut (MCS) [53], Extended Swanson-Megill (EMS) [48], Extended Pearson-Tukey (EPT) [49], Zaino-D'Errico "Improved" (ZDI) [50], Zaino-D'Errico-Tagichi (ZDT) [51] and Miller-Rice One Step (MRO) [52]. The mentioned methods all use the 50th percentile, and they differ in the distance to the mean and the probability values. This study focuses on MCS, which is widely used.

Table 2.3 Discretization methods

Discretization Method	Discretization Values	Probabilities
ESM	10th, 50th, 90th	0.3, 0.4, 0.3
MCS	10th, 50th, 90th	0.25, 0.5, 0.25
EPT	5th, 50th, 95th	0.185, 0.63, 0.185
ZDI	4.2nd, 50th, 95.8th	0.167, 0.667, 0.167
ZDT	11th, 50th, 89th	0.333, 0.333, 0.333
MRO	8.5th, 50th, 91.5th	0.248, 0.504, 0.248

The application of the MCS method at each layer of the tree is necessary for transient tree structures because the continuous random variables are required to be discretely represented. We used the 10th, 50th, and 90th percentiles, which correspond to realizations of 0.25, 0.5, and 0.25 to discretize each of the n features $X_1, X_2, \dots, X_n$. The dependent uniform random variables that are used as transient probabilities in the tree are calculated using copula functions. As an example, the dependent uniform random variable u_2 is computed based on the unconditional percentile value u_1 and the conditional percentile value for the second layer α_2 that were obtained after the discretization of the second feature X_2 using the chosen copula function that is listed in Table 2.1. Iteratively using this computational process, a complete transient tree structure is generated. Since the MCS method is used in discretization, the underlying marginal distributions of the feature are not used in this step.

2.2.6. Inverse Marginal Transformation

After the construction of the copula-based transient tree structure, we proceed with the stepwise inverse transformation after obtaining estimates for the multivariate joint probabilities for each quantile combination, which allows us to investigate the dependence structure across various subsets of the complex data sets. The inverse CDF transformation converts the copula-generated uniform u values to their original scales and distributions based on their marginal distributions. As a result, we obtain discrete approximations to the original variables. We construct a complete multivariate dependent tree structure by applying the inverse transformation to the transient tree, which provides a discrete approximation for the conditional distributions.

To generate discrete approximations of $X_1, X_2, \dots, X_n$, the inverse transformation needed to be applied to each level of $u_1, u_2, \dots, u_k$. In situations where expressing conditional density is difficult and computationally expensive, the dependent tree approach is a very useful and practical representation of the conditional relationship between the variables.

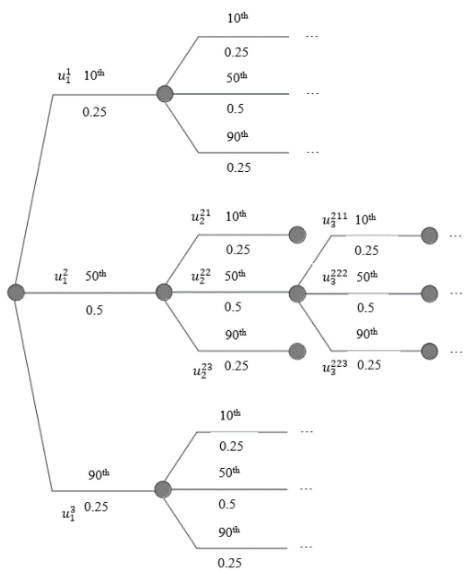

Figure 2.3 Copula-based tree structure

2.2.7. Long Short-Term Memory (LSTM) Neural Networks

LSTM is a special type of recurrent neural network that can handle the vanishing gradient problem of the recurrent neural network (RNN). The LSTM neural networks can capture long-term dependencies and the tendencies of the sequential dataset [53]. Unlike traditional RNN, LSTM networks consist of three layers; the input layer, the recurrent hidden layer, and the output layer. The main objective of LSTM is to transmit and store information in the memory over a long period of time with the use of special units that are forgotten, input, update, and output gates. The series of gates is used by LSTM neural networks to control the information flow in a data sequence.

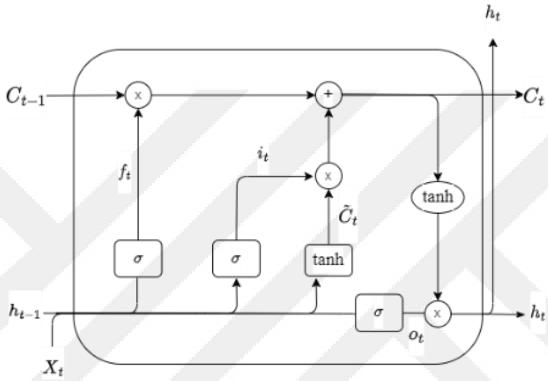

Figure 2.4 Architecture of an LSTM unit

The forgotten gate (f_t) layer calculates the information should be discarded . It takes the output of the previous layer (h_{t-1}) and the input (X_t) and calculates f_t function value. The input gate determines the information that will be stored in the current memory cell C_t. Lastly, the update gate updates the cell state, and the output gate computes the output information. The functions of the gates can be expressed mathematically as follows:

$$f_t = \sigma\left(W_f \cdot [h_{t-1}, x_t] + b_f\right) \tag{2.9}$$

$$i_t = \sigma(W_i \cdot [h_{t-1}, x_t] + b_i) \tag{2.10}$$

$$\tilde{C}_t = \tanh(W_C \cdot [h_{t-1}, x_t] + b_c) \tag{2.11}$$

$$C_t = f_t * C_{t-1} + i_t * \tilde{C}_t \tag{2.12}$$

$$o_t = \sigma(W_o \cdot [h_{t-1}, x_t] + b_o) \tag{2.13}$$

$$h_t = o_t * \tanh(C_t) \tag{2.14}$$

where W_f, W_i, W_o are the weight matrices of forgotten gate, input gate, and output gate, b_f, b_i, b_o are the bias terms of forgotten gate, input gate and output gate and σ is the sigmoid activation function, h_{t-1} the output value at the previous step, $\tilde{C}_t$ is the new candidate state and x_t is the input at the current step.

The selection of parameters for any machine learning algorithm has a significant impact on how well it performs. The best set of parameters is determined with hyperparameter optimization. Hyperparameter optimization, which significantly affects model performance and convergence, is crucial to the success of LSTM neural networks. Some hyperparameter optimization techniques adapted for LSTM neural networks include grid search, random search, genetic algorithm, Bayesian optimization, and particle swarm optimization. Thus, we applied grid search to investigate the hyperparameters that control the behavior of LSTMs, such as the units, learning rate, activation function, number of epochs, and batch size. The grid search technique extensively evaluates the model performance for all possible combinations of a predefined set of hyperparameters. The performance of the grid search is evaluated using cross-validation on the training set. The predefined hyperparameter set is determined as follows: $[\text{units} = 50,\ 100, 150]$, $[\text{activation function} = \text{relu}, \text{elu}]$, $[\text{learning rate} = 0.001, 0.01, 0.1]$, $[\text{batch size} = 32, 64, 128]$, $[\text{epochs} = 50, 100, 200]$. The optimal set of parameters with the highest accuracy is identified after the grid search algorithm has been applied.

$$P_w = \frac{1}{2}\rho\pi R_r^2 C_p w^3 \tag{2.15}$$

The power output of a single wind turbine can be calculated with the well-known Equation 2.15 where ρ, R_r, C_p, and w are respectively the density of air, the rotor radius, the power coefficient of the proportion of available power, and wind speed. Even so, the wind power output of a turbine, however, cannot be precisely estimated with the given equation due to the variable nature of wind and complex dynamics within and between turbines. In this study, LSTM neural networks were used to capture short and long-term dependencies and then to estimate wind power output using the data produced by the Copula-based dependent tree for the branches. A copula-generated dataset is processed by employing an LSTM model to gain more insights. This combination enables a more thorough understanding of complex data structures, making it especially useful in applications such as financial modeling, risk assessment, and time-series analysis in energy systems. After the output value is generated for each branch, the expected value for the tree is calculated for each type of copula structure.

2.3 Empirical Results

In this study, the proposed Copula-LSTM based decision tree framework for assessment of wind power plant energy potential was evaluated using real wind power plant data from Turkey. The hourly measured power output of the power plant as well as meteorological data from January 2021 to December 2021 are included in the study. The features in the dataset and their units are given in Table 2.4.

Table 2.4 Feature descriptions

Features	Unit
Temperature	℃
Humidity	%
Pressure	hPa
Wind Speed	m/s
Wind Gust	degree
Power Output	kWh

To reduce the computational burden of the model, a majority voting strategy is applied after the feature selection methods are used. Table 2.5 illustrates votes for every feature selection technique used in the study. The feature votes were used to determine whether the feature should be included in the final subset. If the majority (i.e., more than half) of the feature selection methods choose a given feature, then the feature is included in the final feature set. Thus, as the final set of features humidity, wind speed, and wind gust are obtained, which will be denoted by X_1, X_2, and X_3 respectively.

Table 2.5 Feature selection methods

Feature Selection Methods	Temperature	Humidity	Pressure	Wind Speed	Wind Gust
Forward Selection		●		●	●
Backward Elimination		●		●	●
Lasso Regularization		●	●	●	
Decision Tree Importance	●			●	●
Recursive Feature Elimination	●			●	●
Mutual Info			●	●	●

A multivariate distribution can be constructed with marginal distributions and a copula function that shows the dependence structure. The marginal densities for the variables must be derived to build a copula-based joint density that will be used to estimate conditional probabilities. The marginal distributions Normal, Gamma, Exponential, Lognormal, Erlang, Weibull, and Beta were used. The mean squared error used to evaluate the goodness of fit of the distribution mathematical expression can be written as follows,

$$\mathrm{MSE} = \mathrm{E}\left[X_o - X_p\right]^2 = \frac{\sum_{i=1}^{N}\left[X_o(i) - X_p(i)\right]^2}{N} \tag{2.16}$$

where N is the number of values, X_o is the observed value and X_p denotes obtained value from the distribution. The selected distributions for the variables are given in Table 2.6.

Table 2.6 Marginal distributions for the variables

Variable	Distribution	Parameters	Range
Temperature	Normal	$\mu = 11, \sigma = 9.11$	$[-15.08, 34.19]$
Pressure	Normal	$\mu = 1020, \sigma = 6.17$	$[995.8, 1036.3]$
Wind Speed	Scaled Beta	$\alpha = 2.94, \beta = 8.44,$	$[0.33, 7.87]$
Humidity	Normal	$\mu = 0.558\,, \sigma = 0.185$	$[0.07, 0.99]$
Wind Gust	Gamma	$\alpha = 0.861, \beta = 3.81$	$[0.71, 16.61]$

Since humidity, wind speed, and wind gust are approximated as different distributions in modelling their joint distribution, there are limited modelling approaches available. One of the approaches, as mentioned earlier, is using copula theory. Thus, the joint density function is constructed as a multivariate generalization of the marginals.

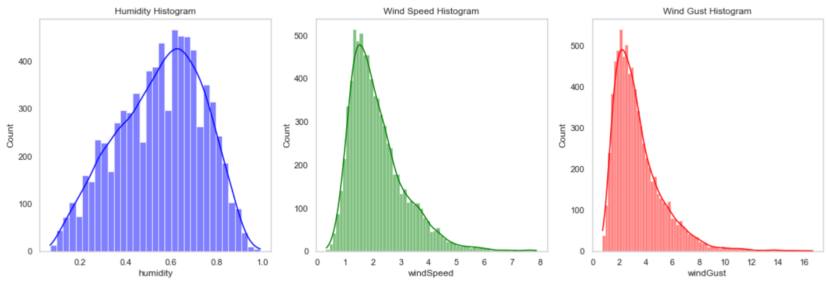

Figure 2.5 Probability distribution fitting of the variables

For modeling various types of dependencies, normal copulas from the elliptical copula family as well as Clayton and Frank copulas from the Archimedean copula family have been applied. Since parametric families of copulas are considered in the present study to build dependence structures between variables, the parameters of the specified copulas were estimated with inversion of Spearmen's rho and MOM approaches. The normal copula is generally parametrized in terms of product-moment correlation. The relation between product moment correlation and Spearman's rank order correlation is used to determine the normal copula correlation. For Archimedean copulas, the copula correlation is determined by the parameter θ. The value of θ can be easily obtained by the relation between θ and τ given in Table 2.2. The Kendall's τ is determined from the observations, whose mathematical expression given as

$$\tau_N = \binom{N}{2}^{-1} (P_n - Q_n) \tag{2.17}$$

where P_n denotes the number of concordant pairs and Q_n denotes the number of discordant pairs [54]. τ_N is the estimate of τ. The copula correlation parameters are critical since they enable us to shape the copula according to the unique structure of the data, which is essential for many statistical and financial applications. Using the specified copula and its specified parameters, a decision tree is modelled with discrete approximations to the conditional probability distributions at each branch of the tree. Figure 2.6- 2.8 illustrates the portions of constructed transient copula trees for the uniform random variables u_1, u_2, and u_3. The trees are constructed as follows: First, u_1 was estimated at three discrete points with MCS and then u_2 given that u_1 and the conditional percentiles were calculated with the equations from Table 2.1. Finally, the u_3 given that u_1 and u_2 was estimated.

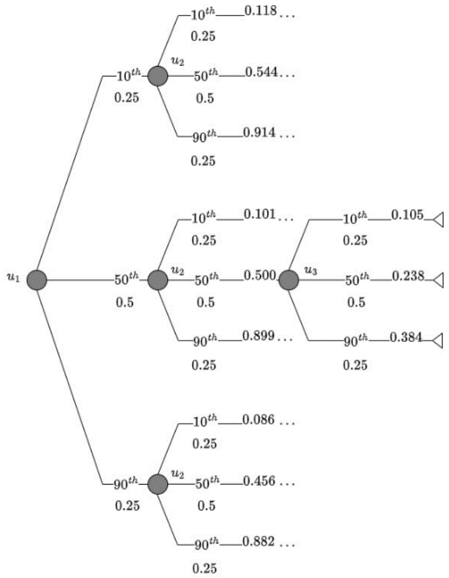

Figure 2.6 Frank copula tree

After the calculation of the uniform variables, the discrete approximations to the original variables are calculated with inverse transformation. The portion copula-based tree structures for each type of copula are shown in Figures 2.9-2.11. In the trees, the first uncertainty X_1 follows a normal distribution. The second and third uncertainties X_2 and X_3 follow beta distribution, and gamma distribution respectively. The uncertainty advances at each node in response to earlier decisions or events in a tree structure that represents a series of dependent uncertainties. The results of each node depend on the results of the preceding nodes, which produce a sequence of events.

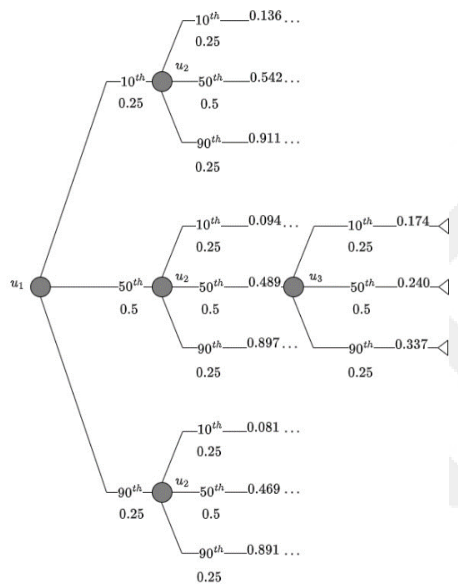

Figure 2.7 Clayton copula tree

For instance, in Frank copula, the humidity, X_1 is modeled as a three-branch discrete chance node with outcomes 0.32, 0.56, and 0.8 and with the probabilities 0.25, 0.5, and 0.25 assigned to each outcome. The wind speed, X_2, is a conditional chance node and if X_1 is 0.56 (50^{th} percentile) then X_2 given that X_1 is modeled at three points with the values 0.862, 1.951 and 3.433. If X_2 given that X_1 is 1.951 (50^{th} percentile) then X_3 given that X_1 and X_2 is modeled at three discrete points with the values 0.293, 2.335 and 8.197.

Since obtaining mathematical expressions of conditional densities is not available or computationally challenging, the dependent decision tree structure creates a practical way to create conditional distributions with discrete approximations.

To assess the potential of a wind power plant, the data generated by a copula-based tree model should be converted into corresponding power output data. The use of the

LSTM model to transform data produced by copula-based decision trees is a promising technique with the potential to improve the performance of the framework. We employed an LSTM model trained with the historical hourly data for this purpose. The Copula-based tree structure is used to obtain the test input feature set. In this study, the optimal values of the parameters have been determined through the grid search technique. The learning rate, batch size, and number of epochs are all set to 0.01, 50, and 64, respectively, for the model. The hidden layer activation function is used as a ReLU (rectifier linear unit), and Adam is used as an optimizer.

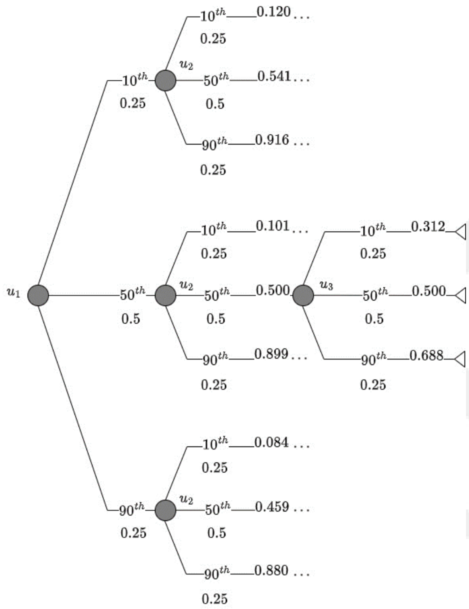

Figure 2.8 Normal copula tree

Overall, in the study, the Copula-based dependence tree approach is used to model the relationships between variables and LSTM model is used to transform the input data into power output values. The LSTM network is utilized to learn the variables (X_1, X_2 and X_3) of wind power and establish estimation model. This integrated approach allows for a more accurate representation of complex data patterns. In order to successfully recognize samples, the LSTM model first learns the existing patterns that characterize wind power and then maintains long-term memory while learning the information in the sample.

Following the acquisition of the power output values for each of the 27 branches using the LSTM and the probability values in the dependent tree structure, the expected value is calculated. The expected value is the sum of all the output values multiplied by their respective probabilities. The expected values are shown in Table 3.7 for each type of copula used in this study. All types of copulas, apart from the independence copula,

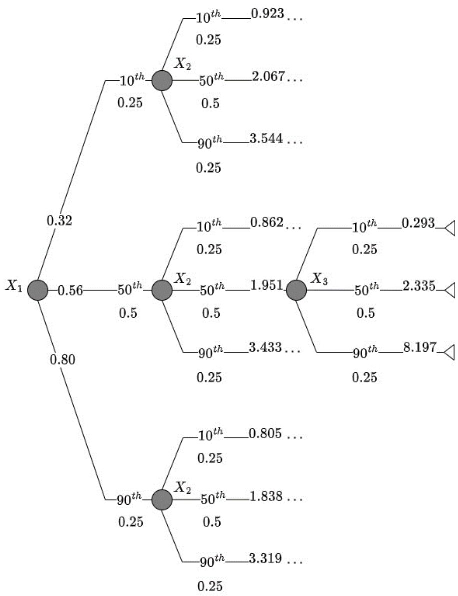

Figure 2.9 Frank copula-based tree

which consistently underestimates the true expected values, produce results that are closer to the actual mean value of historical data. The independence copula assumes that all variables are completely independent, which may not be true in many real-world situations where variables frequently exhibit some degree of interdependence or correlation.

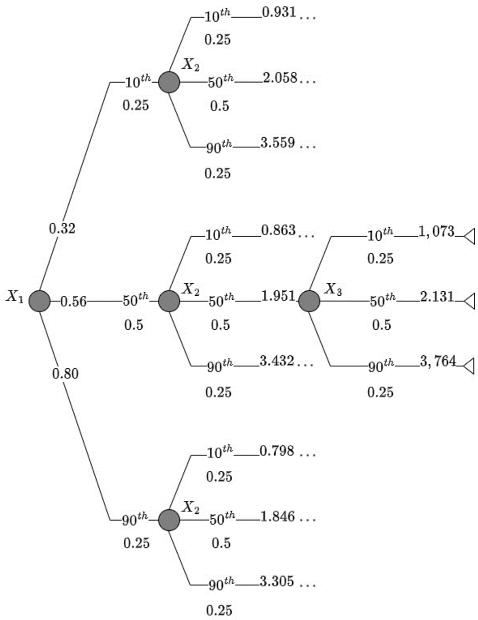

Figure 2.10 Normal copula-based tree

It is common practice for some analytical tools and models to operate under the fundamental premise of variable independence in the context of statistical modelling and analysis. This presumption makes mathematical calculations easier and frequently provides a useful starting point for many analytical tasks. However, it is crucial to acknowledge that the intricate and connected nature of real-world data may not always line up with such an assumption.

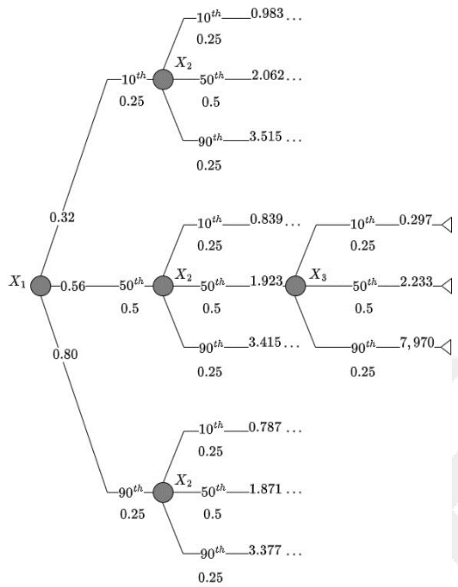

Figure 2.11 Clayton copula-based tree

Variables in a given system or dataset frequently show varying degrees of interdependence and correlation, according to empirical findings and data-driven insights. Although independence was initially assumed, actual results frequently deviate from these straightforward models. These deviations raise doubts about the validity of the analytical framework's independence assumption and its suitability for capturing the complex interrelationships between variables.

Table 2.7 Expected value of the proposed models

Model	Expected Value
Frank Copula	3566.34
Clayton Copula	3590.99
Normal Copula	3123.50
Independent Copula	2925.87
Sample Data Average	3551.00

Innovative strategies are developing in the area of statistical modeling in response to this difficulty. Utilizing a decision tree framework built on a Copula-LSTM is one such approach. Copula modeling, which captures intricate relationships between variables, is combined in this proposed framework with decision trees and LSTM networks. By

combining these components, the framework provides a more reliable way to model and analyze data, especially when dealing with non-independence among variables.
In conclusion, the independence assumption still simplifies analytical procedures, but when applied to real-world data, it has serious drawbacks. As a result of becoming aware of these inconsistencies, modeling approaches are being reevaluated, and the adoption of cutting-edge frameworks like the Copula-LSTM based decision tree approach is being encouraged. In addressing the complex interdependencies inherently present in the data, this method exhibits effectiveness and offers a convincing response to these difficulties.

2.4 Conclusion

In this study, optimal theoretical distributions of meteorological factors are evaluated as marginal probability distributions, and their ability to reproduce the properties of wind energy power output is analyzed through the Copula- LSTM based decision trees, and the effectiveness of the framework is validated. The presented framework is applicable to other research areas, enabling the integration of the Copula-LSTM based decision trees in wind energy resource assessment to achieve more accurate results. Even though the proposed framework offers valuable insights into the assessment of wind power plant site potential, it is crucial for academics to recognize the significant room for further improvement. Future studies should acknowledge and address the evolving conditions induced by climate change. The impacts of climate change introduce a dynamic layer of complexity, necessitating the inclusion of related variables such as temperature shifts and the increasing frequency of extreme weather events. Focusing on the adaptability of the framework to these changing climatic conditions is crucial for ensuring its continued accuracy and relevance in assessing wind power plant site potential. Collaborating with climate scientists and experts becomes essential to gain insights into the anticipated shifts in climate parameters. By considering the broader context of climate change, future studies can strengthen the framework to provide more robust predictions, contributing to effective assessments of wind power plant site potential amidst a changing meteorological landscape. This approach aligns with the imperative to adapt to and mitigate the impacts of climate change, making the framework a valuable tool in anticipating and managing the consequences of evolving weather patterns for wind power applications.

In conclusion, our study achieves two critical advancements. Firstly, we challenge conventional independence assumptions by recognizing and modeling the dependence between meteorological variables, considering complex and nonlinear dependencies frequently overlooked in earlier studies. Secondly, we integrate Copula and Deep Learning techniques into a decision tree framework, revolutionizing the evaluation of the energy potential of wind power plants while addressing meteorological uncertainties. This fusion framework provides a more robust and reliable way of assessing the potential for wind energy, which is a significant advancement in the field.

Our research not only contributes to scientific understanding but also facilitates the efficient utilization of wind energy resources. By shedding light on the techno-economic viability of wind power projects, it offers policymakers and stakeholders a mechanism for informed decision-making. As we navigate an era where renewable energy sources are crucial, our study emerges as a vital tool for the deployment and optimization of wind power plants, ultimately promoting a more sustainable and energy-diverse future.

Moreover, the emphasis in our study on advocating for mandatory pre-assessment requirements underscores the vital importance of adopting a proactive and thorough approach within the wind energy sector. We underscore the need for professionals to utilize sophisticated tools during comprehensive site evaluations, ensuring a holistic understanding of the environmental, technical, and economic aspects of potential wind power projects. This approach not only aids in cost-effective decision-making but also enables strategic resource allocation, optimizing the overall effectiveness wind energy initiatives. By establishing the best practices, our research aims to contribute to the long-term success and viability of wind power projects, aligning them with the broader goals of a sustainable and diversified energy landscape.

Chapter 3

Optimization of Energy Management in Heterogeneous Smart Grids: A Peer-to-Peer Trading Approach for Cost Reduction, Self-Sufficiency, and Grid Independence

Abstract

A deterministic Mixed-Integer Linear Programming based framework is designed to optimise energy flows and trading decisions among households of various configurations, including fully grid-dependent users, PV-only prosumers, and those with both PV panels and BESSs. This study demonstrated that peer-to-peer trading enhances community energy efficiency by increasing the use of local renewable resources and minimizing dependency on centralized infrastructure. Household diversity is demonstrated to have a major impact on energy trading behavior and system-level outcomes, emphasizing the essential role of diversified management measures. In particular, prosumers with BESS play an important role in balancing supply and demand in a smart grid community. The study emphasizes the necessity of incentive mechanisms in maintaining long-term engagement and operational viability. These findings contribute to enhancing decentralized, reliable, and resilient smart grid systems while also providing useful insights for future research in market design, optimization, and policy development.

3.1 Introduction

As technology advances and the population grows, global warming and energy crises pose major challenges making decarbonization and sustainability imperative. Achieving sustainability in the energy system can be accomplished through significant transformation, as traditional energy systems struggle to cope with the intermittent nature of RESs.

Integrating energy storage, smart grid technologies, and demand-side management systems is crucial to overcome these challenges. Energy storage systems can mitigate the negative effects of the intermittent nature of renewable energy resources by storing excess energy during surplus periods and supplying it during deficits, thereby enhancing grid stability. Beyond improving system reliability and balance, these systems also enable cost savings by storing energy when prices are low (typically during low-demand periods) and supplying it when prices are high (typically during peak demand).

Advancements in energy storage solutions have given rise to the energy trading models, where households have dual identities as both consumers and energy producers.

By adopting DERs such as PV panels, wind turbines, energy storage systems, and EVs, prosumers contribute to a more decentralized, resilient, and efficient energy network.

This transformation has led to a bidirectional energy flow between prosumers and consumers, which is known as Peer-to-Peer (P2P) energy trading. It is a decentralized energy trading system that enables prosumers to buy or sell energy from/to other peers within their local community. This approach enhances the utilization of renewable energy sources and other distributed energy resources (DERs) in smart grids [61]. This mechanism benefits both the seller and buyer since the P2P energy trading price is generally lower than the grid energy price and higher than the feed-in tariff, leading to savings on electricity bills and profit for prosumers [62]. For the system operator side, P2P energy trading reduces pressure on the central grids and enhances grid reliability. Efficient energy management can accommodate rising loads and DER participation, hence reducing the need for expensive grid infrastructure enhancements [63].

Despite its advantages, the integration of P2P trading and various DERs creates a new challenge for the management side in terms of coordination and optimization of energy distribution [64]. The decentralized mechanisms of P2P trading require real-time control over prosumers and consumer interactions within the smart grid. Uncoordinated actions can create grid congestion, causing voltage fluctuations, frequency deviations, and blackouts. Optimization of DERs utilization and demand response mechanism introduces a significant challenge since it requires a comprehensive and effective management model to capture the dynamics of the smart grid. Balancing storage, consumption, and trade decisions in response to supply-demand fluctuations is critical for energy management models to improve energy utilization and reduce grid dependency [65-67].

Households can be equipped with various Distributed Energy Resources (DERs) such as photovoltaic (PV) systems, battery energy storage systems (BESS), and electric vehicles (EVs) to optimize their energy usage and sustainability. The combination of the DERs can vary among households, depending on factors such as load profile and infrastructure availability [68-69]. Some households may only adopt PV panels, while others may combine PV with BESS. In [70], the crucial role of energy storage in system reliability and flexibility has been shown. The cumulative effect of storage technologies with trading may contribute to 60% savings on electricity bills [71]. This diverse community contributes to a more flexible and resilient local energy trading, optimizing the balance between supply and demand.

In literature, numerous studies have explored P2P energy trading as a decentralized energy system that leverages the benefits of DERs and renewable energy resources. The study [72] focuses on minimizing electricity cost while considering the microgrid constraints and uncertainty of renewable energy resources with the Copula model and Quantum PSO. In [73], a coalition formation game and a rational economic model have been developed to evaluate the monetary benefit of a P2P trading smart grid system. The primary focus of these studies is on the economic benefits of P2P energy trading, including electricity bill savings, financial incentives for participants, and market efficiency [74-76]. By introducing a new pricing scheme, P2P trading typically offers more favorable rates than traditional grid feed-in tariffs [77]. However, while the economic aspects of P2P energy trading have been extensively analyzed, the impact of P2P trading on broader system-level objectives such as community-supported self-sufficiency and grid dependency remain underexplored. Most of the studies about energy management with P2P trading and DER integration did not analyze how local energy trading affects self-sufficiency at the community level or to what extent it reduces grid dependency. Understanding these types of impacts is key to designing a resilient and sustainable smart grid structure.

Community-supported self-sufficiency refers to the capability of a prosumer to meet their energy demand with the support of peer-to-peer (P2P) energy trading within the community. Promoting self-sufficiency in smart grids contributes to a more sustainable future for power systems [78]. At the same time, reducing overall grid dependency should be aimed at the energy management systems. With the coordination of local energy resources and storage technology, the necessity for external support of the grid should be minimized. Reducing grid dependency enhances the resilience of smart grids while also minimizing transmission losses, leading to a more efficient and reliable smart grid system.

Most of the studies in the literature analyze small-scale smart grid communities, which provide limited insights into the scalability of the energy management system. As community size grows, the complexity of the smart grid operations increases making scalability a critical aspect that requires a deeper exploration. In addition, in a diverse community, consumer-prosumer interactions and the influence of different types of smart houses on energy trading behaviors should be investigated to provide a more realistic and comprehensive energy management system. This study evaluates how the prosumer-consumer mix affects energy management system outcomes.

In this type of optimization problem rule-based optimization [79-81], classical optimization [82,83], heuristic optimization methods such as particle swarm optimization (PSO) [84-86], and fuzzy logic [87,88], machine learning such as Deep Q Learning (DQN) [88,89], and Deep Deterministic Policy Gradient (DDPG)[90] techniques has been applied to power systems. The study employs the MILP model to establish a comprehensive energy management system for smart grids. MILP is a powerful tool that provides an optimal solution subject to the constraints of the smart grid. MILP is a powerful optimization tool that guarantees the optimal solution while maintaining the smart grid's limitations. MILP ensures robustness and precision in decision-making, which makes it a viable approach for energy management applications. Heuristic approaches, on the other hand, may yield nonoptimal solutions and lack theoretical assurances of optimality, which is not ideal for real-time energy management systems.

This study makes the following key contributions:

- A deterministic MILP-based energy management model that combines P2P energy trading with DER coordination has been proposed to enhance community-supported self-sufficiency and reduce grid dependency and electricity bills. The proposed model complies with real energy system constraints, including BESS, PV system, load profiles of smart houses, and power trading.
- The economic benefits and system-level impacts of P2P trading on grid reliability, community-supported self-sufficiency, and energy resilience have been examined.
- The effects of diverse community arrangements on energy management have been studied. This study investigates how different types of combinations of DERs affect grid dependency, community-supported self-sufficiency, and the overall operational cost of the energy system.

In light of these discussions, this study aims to develop a comprehensive energy management framework and analyze the impact of energy management with P2P trading and DER integration on electricity costs, community-supported self-sufficiency, and grid dependency in a mixed-integer linear programming framework for a heterogeneous community.

3.2 Mathematical Formulation

This section introduces the mathematical model to optimize smart grid operations. The community includes 3 types of households: houses with only PV panels, houses with both a BESS and PV panels, and houses without PV panels or a BESS. Utilising different aspects of every household type has been taken into consideration in the model to enhance overall energy management.

The objective function for this model is presented in (3.1), which minimizes the total cost of electricity and grid dependency while maximizing community-supported self-sufficiency. C_i represents the total cost of electricity and $CSSR_i$ is the self-sufficiency ratio, indicates how much of their energy needs are satisfied independently of the external grid. GDR_i represents grid dependency ratio, measures how much a household depends on the grid.

$$min\, z = z^* = \sum_i \alpha C_i - \beta CSSR_i + \theta GDR_i \tag{3.1}$$

α, β, θ are weight coefficients that adjust the relative significance of each term of the objective.

$$\begin{aligned} & Q_{i,t}^{PV} + Q_{i,t}^{fromGrid} + Q_{i,t}^{BESdisch} + \sum_{j,i\neq j} Q_{i,j,t}^{P2Pprch} \\ & = Q_{i,t}^{load} + Q_{i,t}^{toGrid} + Q_{i,t}^{BESch} + \sum_{j,i\neq j} Q_{i,j,t}^{P2Psold} \\ & \forall i \in I, \forall t \in T \end{aligned} \tag{3.2}$$

(3.2) ensures that, at every time step, the total energy supply for each household equals its total energy demand. The supply side involves energy generated from PV panels $Q_{i,t}^{PV}$ of household i at period t, energy purchased from the grid $Q_{i,t}^{fromGrid}$ by household i at period t, power discharged from battery storage $Q_{i,t}^{BESdisch}$ of household i at period t, and energy imported through peer-to-peer (P2P) trading $Q_{i,j,t}^{P2Pprch}$ where household import energy from household j at period t. On the demand side, the energy is consumed to meet household i loads at period t $Q_{i,t}^{load}$, charge battery storage $Q_{i,t}^{BESch}$ by household i at period t, sell to the grid $Q_{i,t}^{toGrid}$ by household i at period t, or trade with other prosumers $Q_{i,j,t}^{P2Psold}$ where household export energy from household j at period t. It guarantees that energy inflows are balanced by outflows at every time step for each prosumer, to maintain a balanced and efficient energy distribution within the smart grid.

$$0 \leq Q_{i,t}^{fromGrid} \leq Q_{i,t}^{MaxfromGrid} . X_{i,t}^{fromGrid}, \forall i \in I, \forall t \in T \tag{3.3}$$

$$0 \leq Q_{i,t}^{toGrid} \leq Q_{i,t}^{MaxtoGrid} . X_{i,t}^{toGrid}, \forall i \in I, \forall t \in T \tag{3.4}$$

(3.3) and (3.4) ensure that grid transactions (buying/selling) stay within predefined limits of the smart grid where $X_{i,t}^{fromGrid}$ and $X_{i,t}^{toGrid}$ are binary variables indicate whether there will be a grid transaction. If the grid transaction is allowed (i.e., the binary variable is 1) then power can be imported $Q_{i,t}^{fromGrid}$ or exported $Q_{i,t}^{toGrid}$ from grid to household i at period t must remain in the predefined maximum limit of imported power from grid $Q_{i,t}^{MaxfromGrid}$ and exported power $Q_{i,t}^{MaxtoGrid}$ to grid.

$$0 \leq Q_{i,j,t}^{P2Psold} \leq Q_{i,t}^{MaxP2Psold} . X_{i,j,t}^{P2Psold}, \quad \forall i \in I, \forall j \in J, i \neq j, \forall t \in T \tag{3.5}$$

$$0 \leq Q_{i,j,t}^{P2Pprch} \leq Q_{i,t}^{MaxP2Pprch} . X_{i,j,t}^{P2Pprch}, \quad \forall i \in I, \forall j \in J, i \neq j, \forall t \in T \tag{3.6}$$

(3.5) and (3.6) ensure the transactions in P2P energy trading market are within the limits. $X_{i,t}^{P2Psold}$ and $X_{i,t}^{P2Pprch}$ represent binary variables that enable household i to operate in P2P market. Based on the $X_{i,j,t}^{P2Psold}$ and $X_{i,j,t}^{P2Pprch}$, the values of $Q_{i,j,t}^{P2Psold}$ and $Q_{i,j,t}^{P2Pprch}$ are determined.

$$X_{i,t}^{fromGrid} + X_{i,t}^{toGrid} \leq 1, \forall i \in I, \forall t \in T \tag{3.7}$$

$$\sum_{j,i \neq j,} X_{i,j,t}^{P2Psold} + \sum_{j,i \neq j,} X_{i,j,t}^{P2Pprch} \leq 1, \forall i \in I, \forall t \in T \tag{3.8}$$

(3.7) guarantees that a household cannot simultaneously import power from the grid and export power to the grid. Similarly, (3.8) guarantees that a household cannot simultaneously import power from the P2P market and export power to the P2P market.

$$X_{i,t}^{fromGrid} + X_{i,j,t}^{P2Psold} \leq 1, \forall i \in I, \forall j \in J, i \neq j, \forall t \in T \tag{3.9}$$

$$X_{i,t}^{toGrid} + X_{i,j,t}^{P2Pprch} \leq 1, \forall i \in I, \forall j \in J, i \neq j, \forall t \in T \quad \textbf{(3.10)}$$

The constraint (3.9) ensures that a household cannot import power from the grid while exporting power in P2P market at the same time period. In addition to that, (3.10) imposes that if a household is exporting power to the grid, it cannot simultaneously import power from the P2P market or vice versa.

$$\sum_i \sum_j Q_{i,j,t}^{P2Pprch} = \sum_i \sum_j Q_{i,j,t}^{P2Psold}, \; i \neq j, \forall t \in T \quad \textbf{(3.11)}$$

(3.11) is the P2P market power balance constraint that ensures that the total power imported in the P2P market is equal to the total power exported in the P2P market, maintaining market equilibrium. This guarantees a stable and effective power trading system, protecting P2P market integrity and avoiding transaction inconsistencies.

$$S_{i,t} = S_{i,t-1} + \eta_{ch} \, Q_{i,t}^{BESch} \Delta t - (1/\eta_{disch}) Q_{i,t}^{BESdisch} \Delta t, \forall i \in I, t \in T \setminus \{1\} \quad \textbf{(3.12)}$$

The battery energy balance after charging or discharging operations at period t is determined by (3.12) where $S_{i,t}$ represents state of charge (SoC) level of BESS of household i a period t. η_{ch} and η_{disch} are charging and discharging efficiency rates.

$$Q_{i,t}^{BESch} \leq Q_{i,t}^{maxBESch} X_{i,t}^{BESch}, \forall i \in I, \forall t \in T \quad \textbf{(3.13)}$$

$$Q_{i,t}^{BESdisch} \leq Q_{i,t}^{maxBESdisch} X_{i,t}^{BESdisch}, \forall i \in I, \forall t \in T \quad \textbf{(3.14)}$$

where $Q_{i,t}^{maxBESch}$ and $Q_{i,t}^{maxBESdisch}$ refer maximum power rating of battery storage system for charging and discharging. Power ratings set the operational limits to ensure safe battery performance. The limits used to eliminate the risk of overcharging and overdischarging (See (3.13) and (3.14)). They are determined based on the specifications of the batteries, which are given by the manufacturers.

$$X_{i,t}^{BESch} + X_{i,t}^{BESdisch} \leq 1, \forall i \in I, \forall t \in T \quad \textbf{(3.15)}$$

The constraint (3.15) guarantees that a house cannot charge and discharge its battery simultaneously.

$$S_{i,t} \geq 0.2 * B_i^{cap}, \forall i \in I, \forall t \in T \quad \textbf{(3.16)}$$

$$0 \leq S_{i,t} \leq B_i^{cap}, \forall i \in I, \forall t \in T \quad \textbf{(3.17)}$$

While (3.16) imposes that the battery never discharges below 20% of the total battery capacity B_i^{cap} at any time t, (3.17) prevents battery SoC does not exceed the total battery capacity B_i^{cap}.

$$Q_{i,j,t}^{P2Pprch} = 0, i = j, \forall t \in T \quad \textbf{(3.18)}$$

$$Q_{i,j,t}^{P2Psold} = 0, i = j, \forall t \in T \quad \textbf{(3.19)}$$

(3.18) and (3.19) prevent a prosumer from exchanging power with itself in the P2P market.

$$C_i = \sum_{j,j\neq i} \sum_{t} P_t^{P2Pprch} \, Q_{i,j,t}^{P2Pprch} \Delta t + \sum_{t} P_t^{fromGrid} \, Q_{i,t}^{fromGrid} \Delta t \quad \textbf{(3.20)}$$
$$- \sum_{j,j\neq i} (\sum_t P_t^{P2Psold} \, Q_{i,j,t}^{P2Psold} \Delta t - \sum_t P_t^{toGrid} \, Q_{i,t}^{toGrid} \Delta t) + Fees\&tax,$$
$$\forall i \in I$$

The total cost of electricity for each household involves energy purchases from the grid and P2P market, energy sales to the grid and P2P market, and additional fees/taxes as shown in (3.20). $P_t^{P2Pprch}$, $P_t^{P2Psold}$ and P_t^{toGrid} are price of P2P purchase price, P2P selling price and grid purchase price, respectively. In addition to that there are fees and taxes to support electricity infrastructure.

$$CSSR_i = \frac{\sum_t \left(Q_{i,t}^{PV} + Q_{i,t}^{BESdisch} + \sum_{j,i\neq j} Q_{i,j,t}^{P2Pprch} - \sum_{j,i\neq j} Q_{i,j,t}^{P2Psold} \right)}{\sum_t Q_{i,t}^{load}}, \forall i \in I \quad \textbf{(3.21)}$$

$$GDR_i = \frac{\sum_t Q_{i,t}^{fromGrid}}{\sum_t Q_{i,t}^{load}}, \forall i \in I \quad \textbf{(3.22)}$$

(3.21) defines the CSSR measure, which indicates community-supported self-sufficiency ratios. Community-supported self-sufficiency measures how much a household meets its energy demand with local energy resources such as PV, BESS, and P2P. The value of CSSR is the indicator of the energy independence of the smart house from the grid. Self-sufficiency is a key measure for enhancing decentralized energy management in smart grids since it can strengthen system stability and lower carbon footprints. (3.22) defines the GDR measure as the grid dependency ratio. It represents the proportion of a household load that is met by the grid. A lower GDR is desired to reach a more resilient smart grid structure. Overall, these three objectives provide vital insights into the effectiveness of decentralised energy systems, which help to optimise energy distribution, storage use, and P2P energy trading techniques.

$$Q_{\mathrm{i,t}}^{\mathrm{toGrid}} \leq M\left(1 - \mathrm{X}_{\mathrm{i,t}}^{\mathrm{disch}}\right), \forall i \in I, \forall t \in T \quad \textbf{(3.23)}$$

$$Q_{\mathrm{i,t}}^{\mathrm{disch}} \leq Q_{i,t}^{load} + \sum_{j,i \neq j} Q_{i,j,t}^{P2Psold}, \forall i \in I, \forall t \in T \quad \textbf{(3.24)}$$

Exporting power to thegrid is only authorized when the BESS of household is not in discharging mode, as specified in (3.23) by a Big-M formulation. In addition to that, as stated (3.24), battery discharge is permitted only to the extent required to fulfil the household load and the energy sold in P2P to support the community's overall load.

$$\mathrm{X}_{\mathrm{i,t}}^{\mathrm{fromGrid}}, \mathrm{X}_{\mathrm{i,t}}^{\mathrm{toGrid}}, \mathrm{X}_{\mathrm{i,j,t}}^{\mathrm{P2Pprch}}, \mathrm{X}_{\mathrm{i,j,t}}^{\mathrm{P2Psold}}, \mathrm{X}_{\mathrm{i,t}}^{\mathrm{ch}}, \mathrm{X}_{\mathrm{i,t}}^{\mathrm{disch}} \in \mathit{Binary}, \\ \forall i \in I, \forall j \in J, \forall t \in T \quad \textbf{(3.25)}$$

$$Q_{\mathrm{i,t}}^{\mathrm{fromGrid}}, Q_{\mathrm{i,t}}^{\mathrm{toGrid}}, Q_{\mathrm{i,j,t}}^{\mathrm{P2Pprch}}, Q_{\mathrm{i,j,t}}^{\mathrm{P2Psold}}, Q_{\mathrm{i,t}}^{\mathrm{BESSch}}, Q_{\mathrm{i,t}}^{\mathrm{BESSdisch}} \geq 0, \\ \forall i \in I, \forall j \in J, \forall t \in T \quad \textbf{(3.26)}$$

(3.25) and (3.26) are variable definition constraints.

3.3 Experimental Study

In this section, the mathematical model developed in Section 3.2 has been implemented. The study analyzes a smart grid community consisting of 20 smart houses, categorized based on the energy generation and storage capabilities they are equipped with. The community involves five houses equipped with PV systems, eleven houses equipped with both PV systems and BESS, and four houses without PV or BESS, relying completely on grid power for their needs. This heterogeneous community structure enables a comparative evaluation of various household types regarding energy self-sufficiency, grid dependency, and economic efficiency.

The household load profiles, PV generation, BESS specifications (capacity, power ratings, etc.), and grid electricity prices used in this study are obtained from [91]. These parameters are crucial for optimizing and assessing the operation of the smart grid under various scenarios. The incorporation of various household types enables the analysis of the impact of DERs and energy storage on system performance based on the objectives introduced in Equation 3.1, particularly in the context of P2P energy trading.

The model captures dynamics within the smart grid community over 24 hours at a 15-minute resolution. A thorough evaluation of daily energy flows and system performance is made possible by this high temporal granularity.

$$P_t^{P2P} = \frac{P_t^{fromGrid} + P_t^{toGrid}}{2}, \forall t \in T \quad \textbf{(3.27)}$$

The P2P energy trading prices that are used in the study are determined using the mid-market pricing approach described in [92]. In that method, the P2P trading price is the average of the grid purchasing price and feed-in tariff and formulated in Equation 3.27.

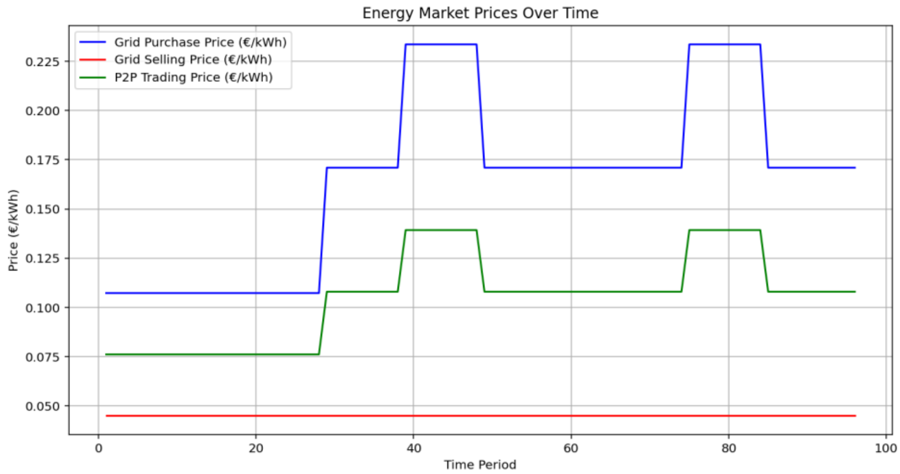

Figure 3.1 Energy market prices over time

Figure 3.1 illustrates how the P2P trading price consistently remains higher than the grid selling price and lower than the grid purchasing price. Since prosumers can import electricity in P2P market at a cheaper cost than buying from the grid, they can get a better return than exporting excess energy to the grid. This pricing mechanism guarantees that prosumers profit by participating in P2P trading. Within the smart grid community, this structure improves overall energy cost efficiency, encourages P2P energy trading, and reduces dependency on the central grid.

Figure 3.2 illustrates the power consumption and PV generation profile of an arbitrarily selected smart house over time. The peak energy consumption occurs in the afternoon and evening, which aligns with typical household energy usage patterns due to increased activity during these periods. Additionally, PV generation peaks in the afternoon, which is consistent with the classic PV profile.

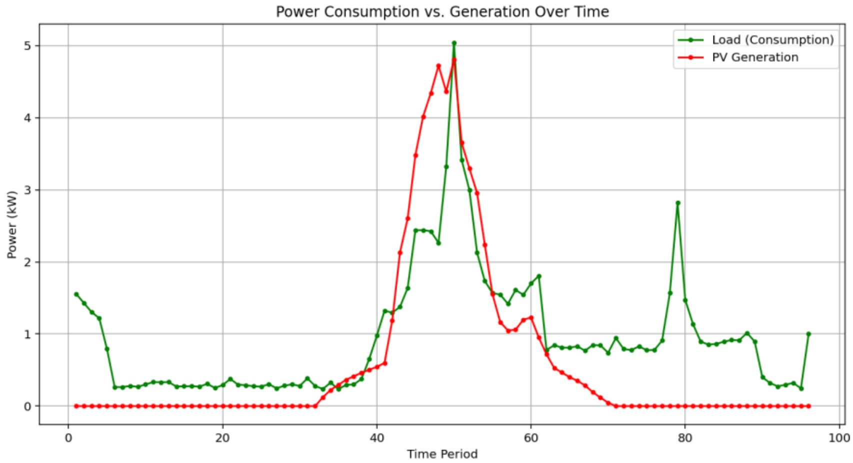

Figure 3.2 Power consumption and generation for a smart house

Table 3.1 represents the input parameters of the mathematical model, including electricity purchasing and selling prices, limits on purchasing/selling electricity for both the grid and peer-to-peer (P2P) markets, and battery energy storage system (BESS) specifications, along with additional fees and taxes.

Table 3.1 Parameters of the model

Parameters	Description	Value
B_i^{cap}	Battery capacity	6.4 – 12.9 kWh
$P_t^{fromGrid}$	Electricity purchasing price of grid	0.107 - 0.234 €/kWh
P_t^{toGrid}	Electricity selling price of grid	0.045 €/kWh
$P_t^{P2Pprch}, P_t^{P2Psold}$	Electricity purchasing/selling price of P2P market	0.07615 - 0.13930 €/kWh
$Q_{i,t}^{MaxfromGrid}, Q_{i,t}^{MaxtoGrid}$	Maximum limit for purchasing /selling electricity for grid	13.8 – 20.7 kW
$Q_{i,t}^{MaxP2Pprch}, Q_{i,t}^{MaxP2Psold}$	Maximum limit for purchasing /selling electricity for P2P market	13.8 – 20.7 kW
$Q_{i,t}^{maxBESch}, Q_{i,t}^{maxBESdisch}$	Maximum limit for BESS charge and discharge	2 – 6.5 kW
η_{ch}, η_{disch}	Charging and discharging efficiency of BESS	0.945 – 0.97
$Fees\&tax$	Fees and tax	0.258 €

3.4 Results

This section introduces and discusses the results of the model. The model was implemented in GAMS and solved with a CPLEX solver. The findings presented in Table 3.2 summarize how household behavior differs under P2P-enabled and P2P-disabled conditions, emphasizing how decentralized energy trading affects grid dependency, community-supported self-sufficiency, and total cost across various household categories.

The results show that P2P trade notably increases self-sufficiency in every category of households. In particular, households with PV and ESS experience the highest average community-supported self-sufficiency increases from 1.47 (without P2P) to 8.78 (with P2P). This result demonstrates that Battery Energy Storage Systems (BESS) are essential for enhancing self-consumption through P2P trade integration, which enables homes to balance supply and demand more effectively. In addition, the community-supported self-sufficiency ratio of PV-only households increases from 0.71 to 1.22, showing that P2P trading helps prosumers maximize energy use by utilizing locally accessible resources, even without being equipped with BESS. For households without PV or ESS, CSSR rises from 0 (without P2P) to 0.837 (with P2P), demonstrating that participation in the peer-to-peer market helps meet 84% of their energy demand despite lacking the ability to generate renewable energy.

Table 3.2 Main results of the model for P2P enabled and P2P disabled scenarios

House Category	Without P2P trading			With P2P Trading		
	Community-Supported Self-Sufficiency	**Total Cost**	**Grid Dependency**	**Community-Supported Self-Sufficiency**	**Total Cost**	**Grid Dependency**
PV + BESS	1.47	1.436	0.72	8.78	2.35	0.40
PV Only	0.71	3.75	0.73	1.22	3.42	0.23
No PV/BESS	0	3.28	1	0.84	2.67	0.16

From a financial perspective, the effect of P2P trading on total cost varies across household types. A slight total cost increase (0,91 €) exists for households equipped with PV and ESS. They are key contributors to the P2P market with their energy storage and generation capacity. Since the model aims to reach community-wide optimization, these households can import more power from the grid with P2P trading to maximize overall community benefit and system stability. This highlights that policy interventions are required to ensure that households with PV and BESS who are the main contributors of the P2P market to incentivize their contributions. Without incentives, these households may not be willing to participate in P2P trading mechanisms, as excessive usage of batteries negatively impacts the health of the battery. On the contrary, households with PV present a notable reduction in total cost, reflecting the economic advantage of participating in P2P trading. These households can sell the excess power generated by their PV system to the P2P market at higher rates than the grid feed-in tariff. The most significant cost saving is observed for prosumers without PV or ESS, whose total cost is reduced from 3.28 € (without P2P) to 2.67 € (with P2P), demonstrating a reduction of approximately 18.6%. This is because without P2P trading, the household solely depends on the conventional grid, and the P2P energy trading prices are often cheaper than grid energy prices. For households with PV, their average total cost is reduced from 3.75 € to 3.42 € (approximately 8.8 %). These results highlight how P2P trading helps make energy more affordable for all households, including those without access to PV or BESS.

Grid dependency trends emphasize the benefits of P2P trade across various household types. Households without PV or ESS experience the greatest impact, dropping their grid dependency by 84%. Similarly, households with solely PV reduce their grid dependency from 0.73 to 0.23 (68% approximately). Households equipped with PV and BESS show a more moderate reduction of approximately 44.4%. Although they tend to be more self-sufficient, these households also serve as community energy stabilizers, charging BESS for their own use and supporting other prosumers during peak demand. These findings demonstrate how P2P trade supports community-supported self-sufficiency among households while providing a decentralized alternative for traditional grid-dependent households. These findings highlight the necessity of decentralized energy markets for efficient energy distribution and economic sustainability.

Figure 3.3 illustrates the power traded between households in the smart grid community. It indicates various trading patterns and levels of participation among households. Households exhibit significant variations in trading intensity, as shown by the disparity in power exchange volumes. Some households involve significant energy trading, forming clusters with high transaction volumes, whereas others are involved rarely or not at all. The presence of several significant peak loads suggests that a group of households serves as major energy hubs distributing energy across the community. In contrast, some households present low engagement, either due to insufficient energy generation capacity or lesser needs for energy exchange.

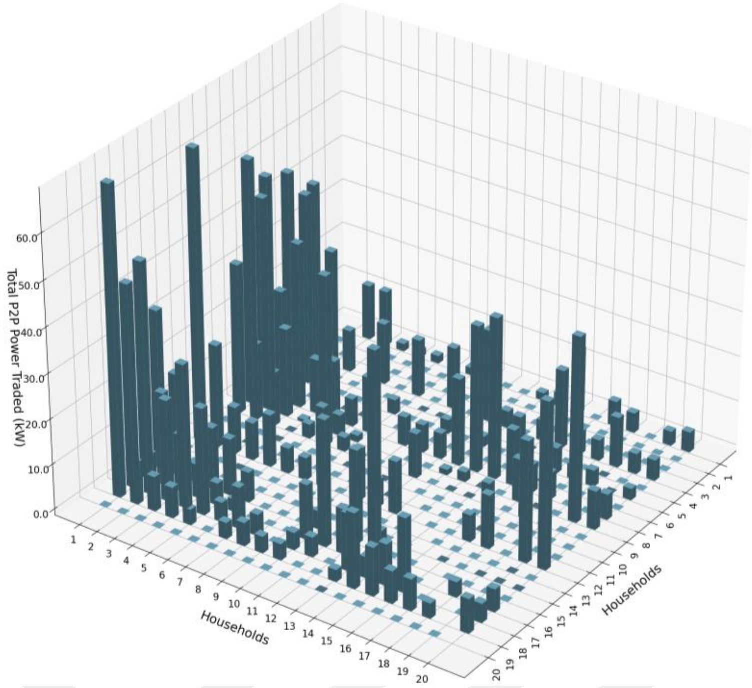

Figure 3.3 Total P2P power traded between households

The optimization of P2P energy markets is significantly influenced by the diversity in P2P energy trade behavior. Designing tailored strategies to promote higher participation, including dynamic pricing systems or incentive structures, can be enhanced with an understanding of the different levels of engagement. Future studies should examine the effects of variables including household-level energy storage, grid limitations, and real-time energy pricing on participation trends.

Figure 3.4 demonstrates a comparative analysis of energy interactions of an arbitrarily chosen household equipped with PV and BESS in a smart grid community with and without P2P trading. When the P2P trading is integrated, imported power from the grid is significantly reduced, and the share of local supply power in total supply power is increased. Since charging and discharging operations are more frequent with P2P trading, it will lead to an increased battery cycle, which leads to faster battery degradation. For this reason, a mechanism, like a battery degradation offset tariff or financial incentives, is required to encourage households with BESSs to engage in P2P trade. The behaviour of State of Charge (SoC) (%) implies that deep discharges generally happen at typically high demand with low PV generation periods (in the early morning and evening) and when energy prices are high to support the overall community benefit. Through active participation in the energy exchange process, this dynamic behavior enables the home to react more flexibly to both market prices and community demand. On the other hand, the

P2P-disabled case exhibits a higher dependence on grid import and export, more restricted battery operation, and limited export behavior, particularly during peak hours.

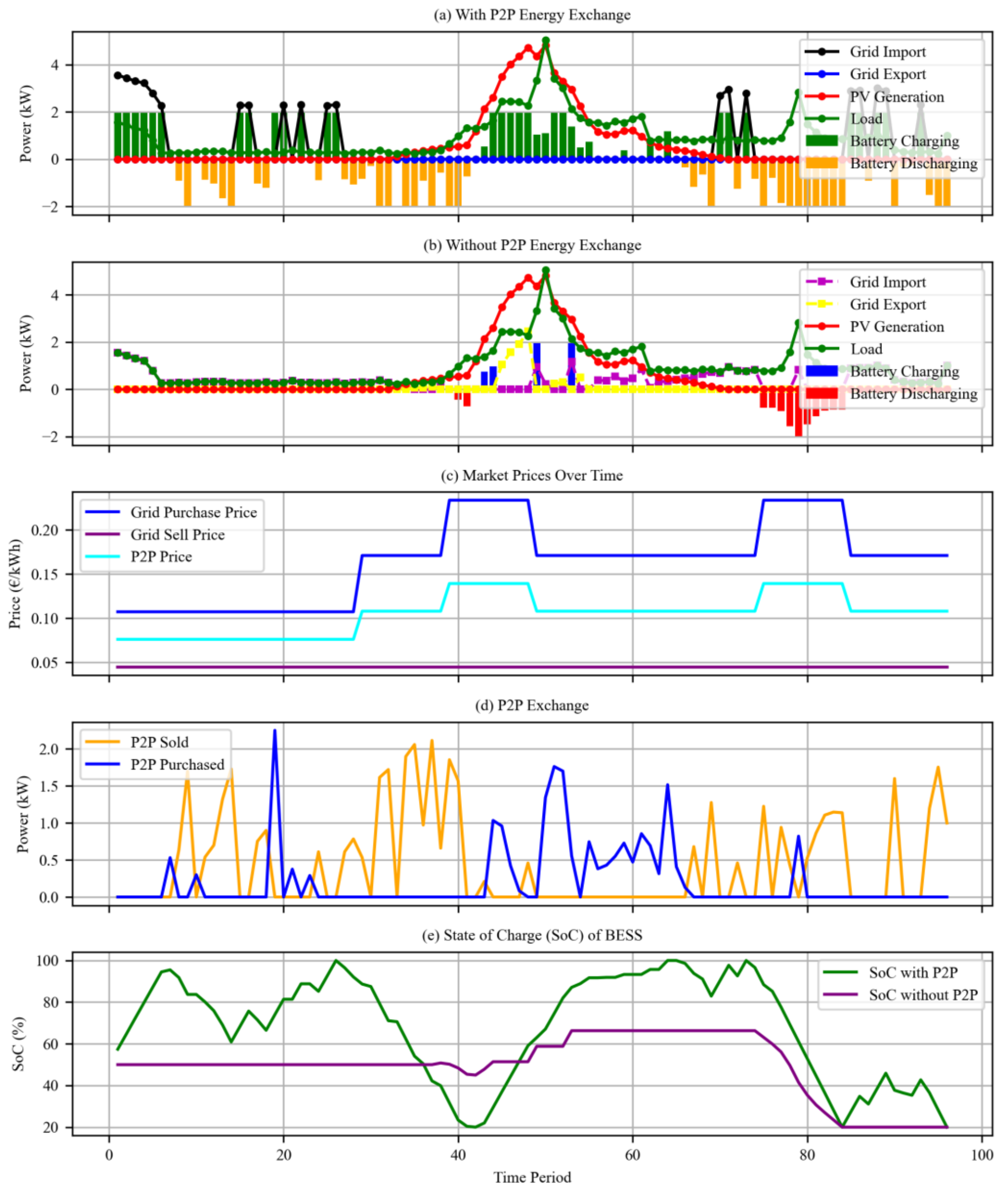

Figure 3.4 Energy storage & grid interaction for a household equipped with PV and BESS

In contrast to a traditional grid-only configuration, a household with only PV presents distinct operating behavior when engaging in P2P trading, as shown in Figure 3.5. The household decreases its dependency on grid imports when P2P trading is enabled, especially when PV generation is at its highest level. The noticeable peaks in P2P export activity show that excess solar energy is not just exported to the grid but is instead sold to the P2P market. This shift promotes local energy balancing in the community and increases the household's economic return by capturing higher peer-trading prices than traditional feed-in tariffs. Thus, even without battery storage, P2P trading improves cost efficiency and self-utilization of renewable power, as demonstrated by the household's capacity to import energy from peers during non-solar hours and export excess PV energy at better rates. The findings emphasize how PV generation reduces grid dependency, but the lack of storage restricts self-sufficiency.

As shown in Figure 3.6, a household without PV or battery storage exhibits notably different patterns of energy interaction under P2P-enabled and P2P-disabled conditions. A substantial portion of the household's energy needs are met by peer-sourced electricity when P2P trading is enabled. In times of high grid tariffs, the household deliberately reduces grid imports and instead uses more affordable energy from the P2P market. This behavior shows a conscious move toward more locally sourced and cost-effective energy usage, demonstrating an adaptive and cost-aware energy management approach. In the absence of peer energy, the household's demands are fully met by the grid. Therefore, regardless of market pricing, grid imports increase dramatically, particularly during times with high loads. Grid exports remain zero since the family is not capable of producing electricity locally. Overall, by actively engaging in the P2P market, households with no DER assets (i.e., no PV or BESS) can reduce grid dependency and the cost of energy. Decentralized access to peer-produced renewable energy benefits these households, boosting renewable energy access and community-supported self-sufficiency. This highlights how important P2P mechanisms are to extend the advantages of DER integration to players who do not generate in a smart grid setting.

3.5 Conclusion

In heterogeneous smart grid communities, this study has shown the benefits of P2P energy trading in maximizing energy efficiency, decreasing grid dependency, and improving community-supported self-sufficiency. Significant operational and financial benefits were found across various household types by incorporating a deterministic MILP-based energy management model in GAMS and using the CPLEX solver to implement it.

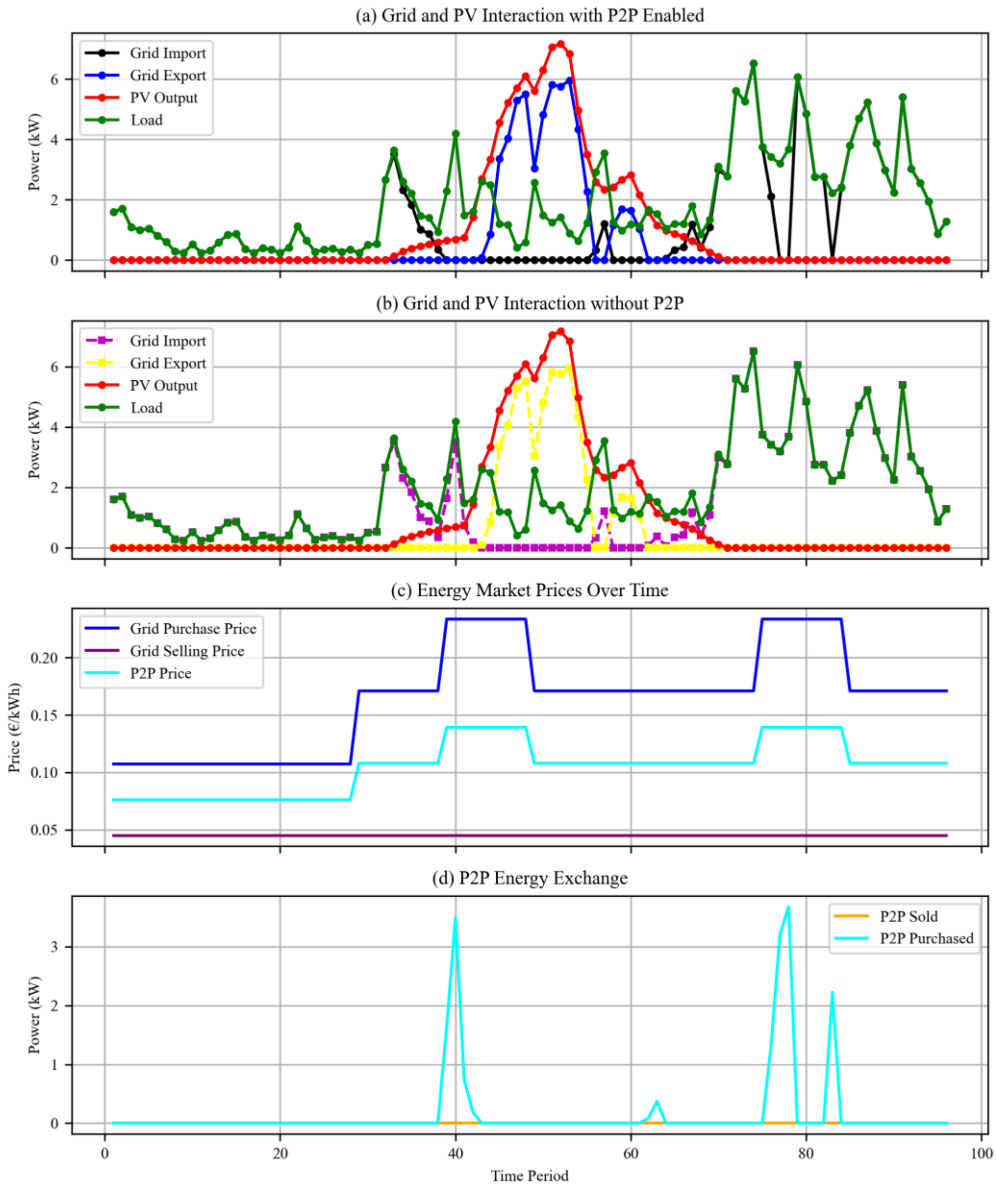

Figure 3.5 Energy storage & grid interaction for a household equipped with PV

According to the findings, P2P trading was most beneficial to households with both PV and BESS, as evidenced by the nearly six-fold increase in community-supported self-sufficiency from 1.47 to 8.78. This showed how important storage systems are for balancing supply and demand locally. With self-sufficiency rising by roughly 71.8%, PV-only households also experienced a notable improvement, which was attributed to the effective utilization of excess PV energy through P2P transactions. Decentralized trading methods enhance energy access and equality for non-generating households, as demonstrated by the fact that households with no DER assets (no PV or BESS) were able to cover 84% of their energy needs through the P2P market.

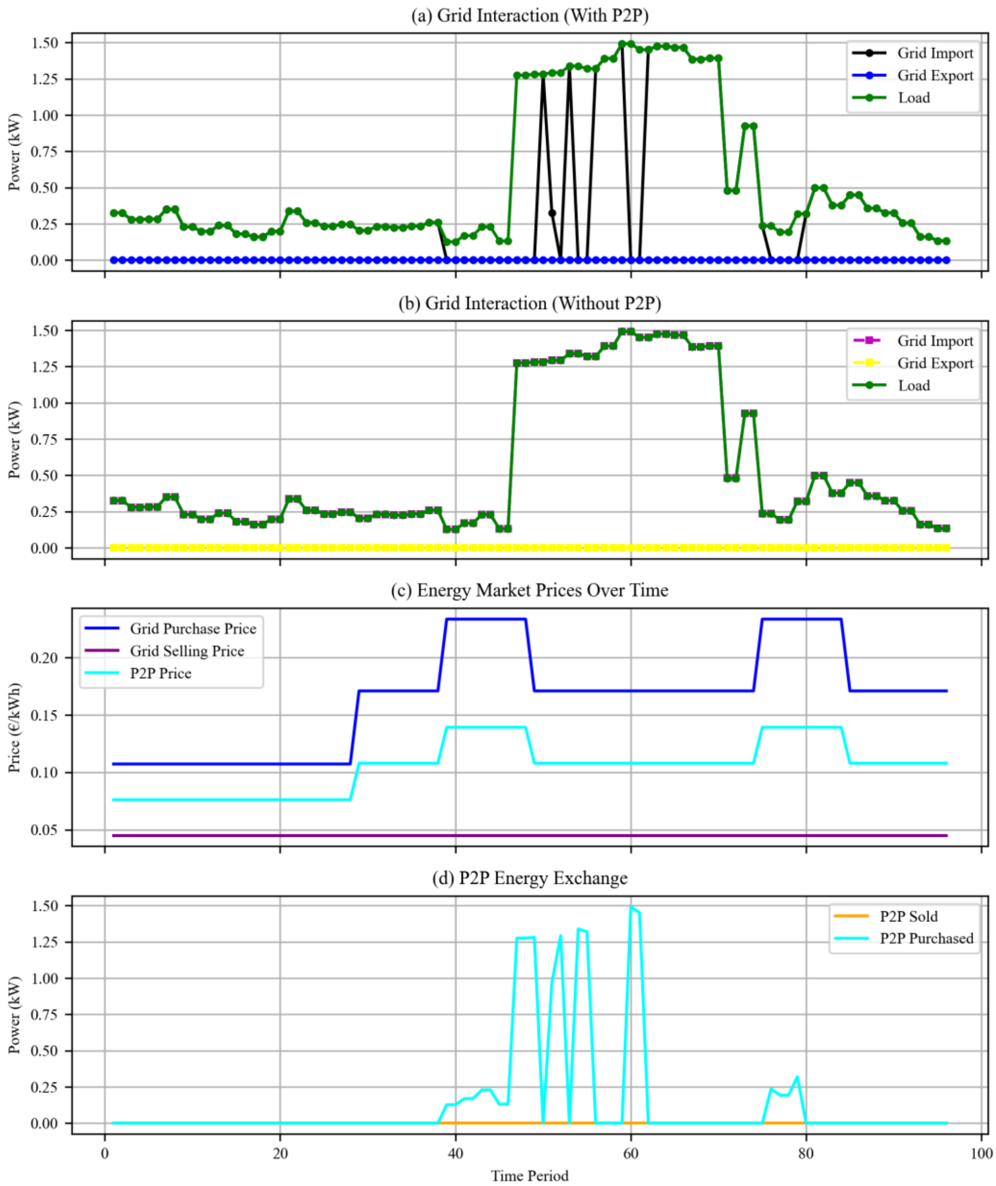

Figure 3.6 Energy storage & grid interaction for a household equipped with no PV or BESS

Participation in P2P decreased energy expenditures for most household types from a financial viewpoint. Households without DERs received the highest cost reduction, with their overall costs reducing by 18.6%. Households with solely PV also benefited from an 8.8% cost reduction. Although the total cost of households with both PV and BESS increased slightly, this result is explained by their crucial role in maintaining the community's energy balance and increasing battery degradation, emphasizing the necessity of degradation offset tariffs or other financial incentives to guarantee sustained participation.

Grid dependency was also significantly decreased by P2P trading: 84% for non-DER households, 68% for PV-only households, and 44% for PV+BESS households. To maintain long-term operational viability, energy hubs must be supported through tailored incentive programs, as seen by the growing trading activity and energy provision duties of PV+BESS households. To ensure an effective and scalable P2P energy ecosystem, future research should further analyze dynamic tariff models, adaptive incentive structures, and policy-driven frameworks combining financial sustainability with grid stability, engagement of community, and market efficiency. Reward programs and incentives that reduce operating expenses can help them continue participating, which is crucial for market stability, energy balancing, and community resilience.

To improve market transparency and operational effectiveness, future studies should investigate the scalability of the energy management models for larger communities, AI-driven optimization, and blockchain-based transaction security. To facilitate decentralized trading while maintaining grid stability, appropriate pricing, and consumer security, regulatory frameworks must also change. P2P trading has the potential to play a significant role in the shift to decentralized, low-carbon, and community-driven energy systems with the proper combination of technological advancement, legislative backing, and financial incentives.

Chapter 4

Reinforcement Learning-Driven Real-Time Pricing and Control for Decentralized Energy Systems

Abstract

A reinforcement learning-based architecture for decentralized control and real-time pricing in smart energy systems is presented in this chapter. The proposed approach is designed to address the complexity and uncertainty of grid management arising from the integration of DERs, including PVs, BESS, and EVs, into smart residential neighborhoods.

The rule-based model was developed to model and validate the operational settings, which include mechanisms like battery degradation modelling, overnight charging, and P2P energy trading. For the development and comparison of control techniques, this first layer presents a standard and a reliable testing environment.

Building on this foundation, the reinforcement learning model enables autonomous decision-making and dynamic pricing, thereby supporting decentralized, real-time energy management. Prosumers use a combination of PV systems, EVs, and optional BESS to respond adaptively to real-time pricing signals from a central system operator, altering their trading, storage, and energy consumption practices in response to market and grid conditions.

The proposed architecture demonstrates the effectiveness of real-time pricing mechanisms with learning-based control to enable adaptable, decentralized, and efficient energy system operations. The simulation findings show that the reinforcement learning model significantly reduces energy costs, optimizes peak load management, and increases self-consumption of locally generated renewable energy. Furthermore, the system's ability to dynamically coordinate prosumer behavior in response to real-time situations highlights its practical applicability in smart residential communities.

4.1 Introduction

The modern world economy is mainly built on energy, making energy systems essential instruments for economic and social development. In recent decades, developments in industrialization, urbanization, and digitalization have contributed to a persistent increase in global energy demand. Over the past two decades, total energy consumption has been consistently increasing worldwide[93]. As a consequence, all around the world, over 50 billion tonnes of greenhouse gases are released annually [6], contributing to a range of issues, including health issues, environmental disruption, sea level rise, etc.[94].

On the other hand, the world is currently witnessing a major energy crisis due to political issues, depletion of fossil fuel reserves, accelerated human population growth and global pandemics. In response to growing concerns about energy and the environment, international energy rules and regulations have been established in recent years. Many nations are setting ambitious energy system transformation targets at both the national and international levels in order to secure their future. Two notable examples of internationally agreed-upon policies are the Paris Agreement and the UN 2030 Agenda for Sustainable Development. Efficient energy management is crucial to achieving the 2030 Sustainable Development Goals, especially SDG 7, which calls for "ensuring access to affordable, reliable, sustainable, and modern energy for all" and the Paris Agreement Emission goals.

Achieving these objectives requires a paradigm shift to managing energy generation, distribution, and consumption. However, the dynamics of traditional energy systems pose significant challenges to transforming the current energy sector. In response to these challenges, smart grids have emerged as a potential solution. These systems enhance energy efficiency by enabling the integration of renewable and distributed energy resources, while also facilitating more flexible and adaptive management of energy flows. Smart grid structures aim to improve power grid management by increasing communication and collaboration among energy producers, distributors, aggregators, and consumers. With the increased use of communication sensors and data analytics technologies, energy distribution and management in smart grids have become substantially more efficient. Therefore, using energy in a sustainable way is essential for environmental sustainability and ensuring clean and accessible energy (SDG-7) [95].

Decarbonization of the energy sector while continuing to meet growing demand is possible by increasing the penetration levels of RESs and DERs, such as electric vehicles. However, high infiltration of RES can cause instability problems such as high-power swings in the feeders [96] and intolerable voltage fluctuations in the power grid due to their limited predictability, controllability and inherent variability [97]. The nature of RES makes the consideration of them in the scheduling process of power generation challenging [98].

Integrating DERs into the grid offers substantial economic and environmental benefits; however, in the absence of proper management, it can significantly jeopardize grid stability and security. In recent years, distributed energy resources, particularly electric vehicles (EVs) are becoming increasingly popular due to their efficiency and potential to reduce greenhouse gas emissions. The governmental incentives, financial benefits, and technological developments are all contributing to an increase in EV sales. The number of EVs is expected to reach 300 million globally by 2030 [99]. However, the projected dominance of EVs in the transportation sector has raised concerns regarding severe stress on the power grid, which can cause feeder congestion, increased peak demand, distribution transformer overloads and excessive voltage drops [100] when they are uncoordinated. On the other hand, aggregated batteries of EVs have a substantial energy capacity since they are mostly idle during the day[101]. Moreover, if they can be effectively monitored and coordinated via a bidirectional vehicle-to-grid system, they can have great potential to provide auxiliary functions such as peak shaving, reactive power adjustment, spinning reserve, frequency management, load balancing, and backup for intermittent renewable energy [102].

Traditional grid systems are typically designed to accommodate unidirectional energy flow, whereas smart grids can facilitate bidirectional energy exchange. This functionality enables consumers to operate as prosumers who can both consume and generate energy, while feeding the surplus back into the grid and thereby obtaining economic benefits. Advanced mechanisms, including Vehicle-to-Grid (V2G), Grid-to-Vehicle (G2V), and Home-to-Grid (H2G) systems, enable bidirectional energy transfers in smart grids. Vehicle-to-Grid (V2G) system integrates a group of electric vehicles into the grid to function as controllable loads to balance system demand during off-peak hours and as a distributed energy resource to supply energy services to the grid during peak hours [103]. V2G has the advantage of being cost-effective and faster than alternative energy storage systems, as well as providing consumers with new economic opportunities and lowering environmental damage. Furthermore, V2G applications for minimizing peak demand, increasing integration of intermittent renewable energy, and offering service with efficient EV charging / discharging control are among the possibilities. This system has a bi-directional power flow, which allows EVs to operate as both controllable loads and energy resource distributors. The system reduces grid bottlenecks and instability while increasing the grid's ability to integrate renewable energy sources.

The main advantages of smart grids, especially those associated with the coordinated integration of Distributed Energy Resources (DERs) and Renewable Energy Sources (RESs), can be summarized as follows:

- Ensuring system reliability
- Enhancing overall energy efficiency
- Establishing a sustainable and resilient grid ecosystem
- Improving grid flexibility

Despite the various benefits of smart grids and the expanding potential of DERs and RESs, their widespread implementation presents additional challenges in grid management. The unpredictable and intermittent nature of renewable sources, along with an increasing number of prosumers and the complexity of bidirectional energy flows, requires the development of comprehensive energy management systems. These systems must provide real-time coordination, stability, and resource management. Therefore, it is critical to develop an intelligent control and management framework that can handle the dynamic behaviour of distributed resources, promote grid flexibility, and maximize the economic and environmental benefits of smart energy systems.

In smart grids, reducing pollution arising from energy production, enhancing energy supply security, increasing the share of renewable energy sources in electricity generation, mitigating the fluctuations caused by distributed energy resources, and ensuring economic stability in the energy sector and its dependent sectors can be achieved through the effective management of grid operations. Smart energy system management aims to improve power network flexibility, sustainability, and reliability while also meeting financial and environmental objectives. As highlighted in various studies in the literature, a comprehensive energy management system must incorporate comprehensive demand response (DR) mechanisms to actively involve consumers and prosumers in grid balancing and optimization

Demand response (DR) management in the energy market refers to encouraging consumers to shift their energy usage over time in response to fluctuations in energy prices or to reduce consumption during periods of high prices or when grid reliability is at risk [104]. DR programs can improve system reliability, flexibility, and cost-efficiency for both consumers and system operators, and in the long term, they can reduce the need for investments aimed at increasing generation capacity. DR programs are categorised into two types: price-based and incentive-based. In incentive-based programs, system operators are allowed to regulate user demand to reduce energy consumption during peak periods. By contrast, in price-based programs, fluctuating prices are offered to consumers to flatten demand curves, and their behavior is expected to align with the system operator’s objectives through price signals. However, unlike incentive-based programs, consumers in price-based programs retain full control over their energy usage and can modify their consumption patterns based on price signals to achieve financial benefits [105]. The most well-known price-based DR programs are Real-Time Pricing (RTP), Time of Use (TOU) rates, and Critical Peak Pricing (CPP) [106]. Compared to other time-based demand participation solutions, RTP is considered one of the most effective approaches [107]. To manage energy systems effectively, the RTP system should include both the supply and demand sides [108].

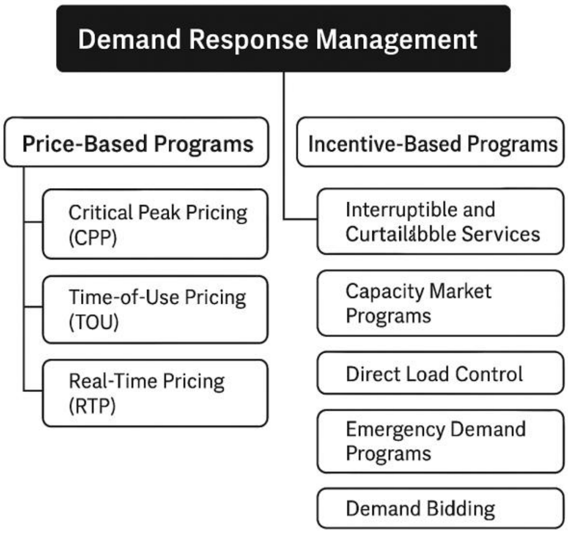

Figure 4.1 Demand response management programs

In the literature, numerous studies have investigated RTP-based demand response (DR) programs for the development of optimal energy management strategies, given that RTP is considered one of the most promising approaches for achieving system reliability and efficiency through dynamic, supply-demand-based pricing [109-111]. Price uncertainty, the nondeterministic nature of real-world systems, and the difficulty in forecasting consumer demand have attracted attention from researchers.

When smart grid energy management models in the literature are examined in terms of their objectives, several categories emerge:

- Minimization of cost [112-114],
- Maximization of social welfare [115-120] ,
- Minimization of consumption [121-124],
- Simultaneous minimization of cost and consumption [125-128],
- Maximization of social welfare and minimization of consumption [68,129].

However, the increasing integration of RESs and various types of DERs into smart energy systems has introduced significant complexity in balancing operations, thereby underscoring the need for more sophisticated and systematically formulated objective function combinations within energy management models that accurately capture system dynamics.

Most of the studies in the literature mainly focus on the interest of consumers and ignore the stochastic part of power suppliers [111], which remains a gap in that field of research. However, the penetration of stochastic power generators into the power grid (solar panel farms, wind turbines, etc.) is non-negligible. Therefore, to reflect the system holistically, a pricing mechanism must include both supply and demand sides to manage the power system effectively [108].

Moreover, classical optimization algorithms and heuristic algorithms are widely used in energy management. However, these algorithms use an approximation of reality which sometimes can fail to reflect the nature of the system environment. In addition, these algorithms suffer from the curse of dimensionality and cannot generate a solution in an acceptable time frame [130]. In fact, optimality cannot be guaranteed in nonstationary systems with these algorithms. Furthermore, intelligent optimization algorithms such as reinforcement learning are also used for solving energy management problems, and they can effectively solve most of the optimization problems.

Reinforcement learning (RL) is a data-driven intelligent control technique which learns the optimal control strategy in real time according to the varying conditions of the system environment through scalar evaluative feedback [131,132]. One of the key features of RL is to obtain user responses and learn from them. The main goal of the RL algorithm is to determine the best action in order to maximize rewards. Since RL does not require prior information, it is the most promising tool for energy management [133]. However, there are only a few studies that propose an RTP scheme with RL. When Lu [134] first applied this approach, the results showed that RTP with RL is an appropriate tool for energy management. Nevertheless, the integration of renewable energy sources, electric vehicles, and other stochastic supply-side factors was not taken into account in this analysis. There is certainly potential for improvement because RL is still in its infancy. The design environment should be representative of reality, but this is actually impossible without taking both the supply and demand sides into account.

The contribution of this study lies in the development of a novel, flexible, and reliable smart energy management system that enables holistic planning of smart grid operations through the integrated management of both supply and demand sides, an aspect often overlooked within the grid incorporating renewable and distributed energy sources.

This system incorporated a real-time bidirectional (buy/sell) pricing mechanism, where both system operations and user behaviours were guided by reward functions. A real-time energy management framework was designed to control transactions in the smart grid. One of the primary objectives of this study was to offer a new perspective on energy management research with dynamic pricing. The proposed work aimed to effectively balance energy supply and demand while supporting the global agenda of the UN 2030 for sustainable development.

4.2 Methodology

4.2.1 Dataset

The dataset utilized in this study comprises various data sources, including household load, photovoltaic energy generation, energy tariff rates, and the parameters of BESS and EVs. The household load data is collected from a UK-based home. This data is recorded at a high temporal resolution of one minute, providing a granular view of electricity consumption patterns over an entire year. The annual photovoltaic (PV) generation data is obtained from a PV panel installed at a home located in the UK. The energy tariff rates are sourced from a UK-based energy company. The parameters of battery energy storage systems and electric vehicles are sourced from the UK National Travel Survey, manufacturers, and industry reports.

4.2.1.1 Household Load Data

The household electricity load data has been collected from 22 homes in the East Midlands region of the UK [135]. This dataset, gathered at a high temporal resolution of one minute over an entire year, enables detailed insights into electricity usage patterns across different hours of the day, days of the week, and seasons. In addition to the load data, various household factors, including types of heating and cooling systems, insulation levels, construction details (e.g., detached, semi-detached, terraced houses), number of occupants, and a list of major electrical appliances, are obtained through the household characteristics survey. The household characteristic types are estimated based on the survey and electricity usage patterns, and later on, they are used to create load profiles based on the household types.

As a demonstration, the daily load profiles of a house are given in Figure 4.2. The day and house were selected arbitrarily. Consumption is noticeably low during typical working hours on a weekday, as shown in the figure, which suggests that the residents are away from home for work or other obligations.

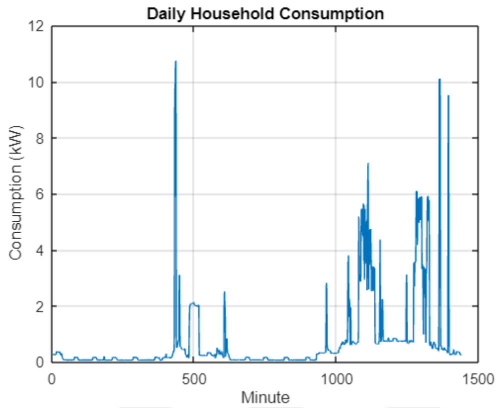

Figure 4.2 Daily household consumption for the selected day and house

4.2.1.2 PV Generation Data

PV generation data is sourced from the PVoutput.org website for a 3.8 kW residential solar system placed in Nottingham, UK [136]. The data has a one-minute resolution for a year.

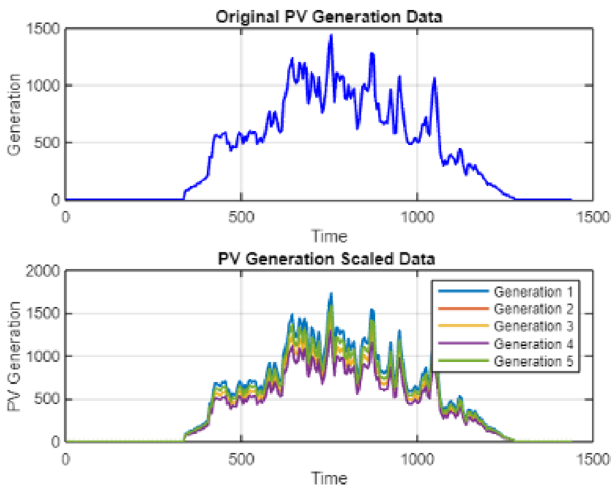

a)

To provide a PV generation profile for each home, variations resulting from panel orientation, shading effects, and other factors have been taken into consideration using scaling, additive Gaussian white noise (AGWN), and multiplicative noise. The generation values below a certain threshold are not exposed to scaling or noise to maintain the integrity of the data. When evaluating the impact of noise on PV generation data, signal-to-noise ratios (SNR) are used as a metric. Among various types of noise, multiplicative noise has been selected since it results in the lowest SNR.

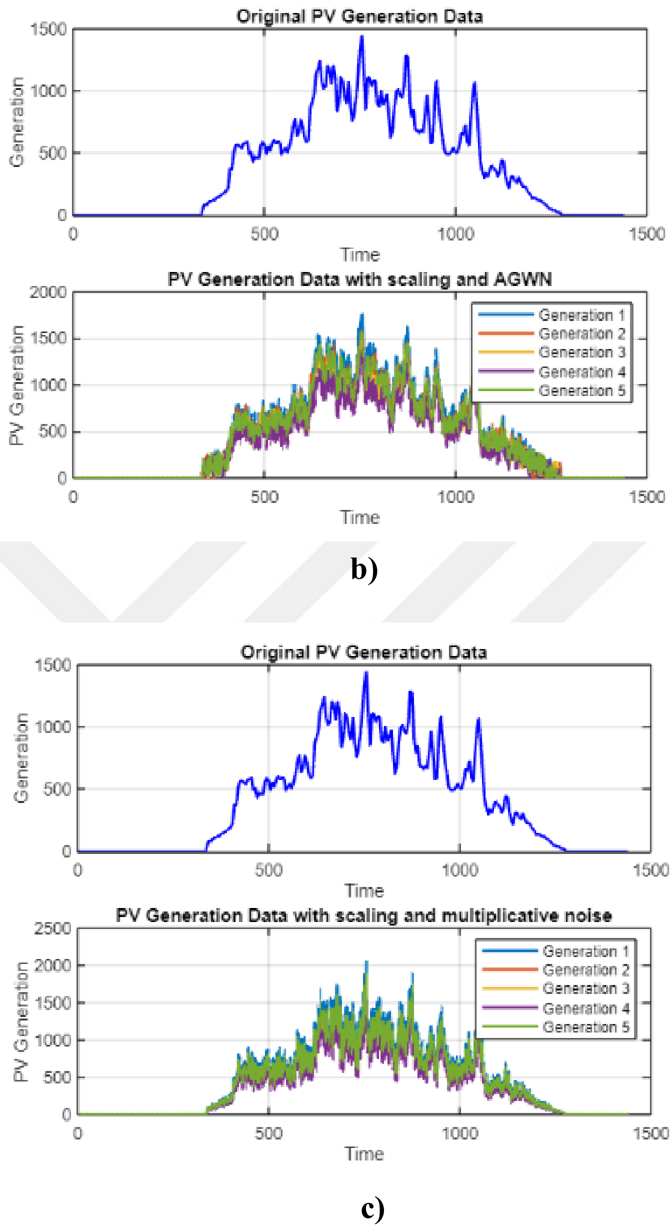

Figure 4.3 (a) Scaling, (b) Scaling and AGWN, (c) Scaling and multiplicative noise

4.2.1.3 Electricity Tariff Rates

In that study, a price-based demand response mechanism was implemented with reinforcement learning. A rule-based simulation model was used to benchmark, build, and test the program design in a controlled virtual environment before reinforcement learning implementation. In the rule-based simulation, the Time of Use (TOU) price tariff has been used.

TOU pricing sets different rates for electricity depending on the time of day and aims to shift electricity demand from peak to off-peak times. In that study, the TOU rates are gathered from the Octopus Energy Company, UK [137]. The rates are given in Figure 4.4. There are three different tariff rates: off-peak tariff between 2 am and 5 am, peak tariff between 4 pm and 7 pm, and mid-peak tariff during the remaining hours.

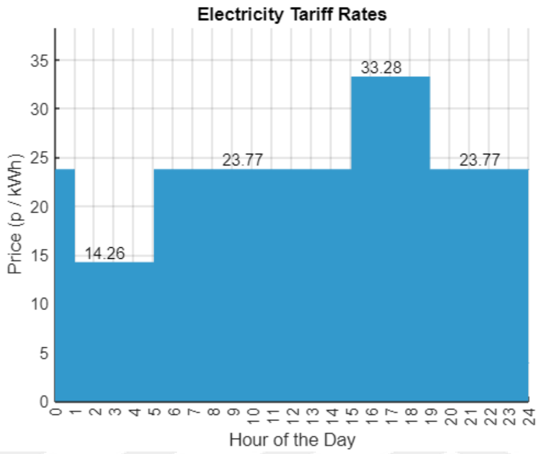

Figure 4.4 Electricity tariff rates

There is also a standing charge cost. This cost is charged to maintain the energy supply network, meter readings operations, and support governmental programs. The standing charge rate is 53.94 pence per day. The tariff rates are fixed for the contracted period. Moreover, the Feed-in Tariff in the UK, which allows consumers to sell excess power generated from renewable resources like PV to the national grid, stopped accepting new participants in 2019. This means that new installations cannot benefit from this tariff scheme. Therefore, in that study, prosumers don't make any profit from exporting power to the grid.

4.2.1.4 Electric Vehicle

In that study, every house was assumed to have at least one electric vehicle (EV). EVs in the system will act as both shiftable loads (EV charging) and Battery Energy Storage Systems (BESS) for discharging. By strategically shifting the load from peak tariff periods to low tariff periods, EVs can facilitate valley filling operations. In addition to that, by discharging during peak tariff periods, they can perform peak shaving operations. This multifunctionality helps minimize maximum peak power consumption.

To control the charging and discharging behaviors of EVs, it is essential to consider factors such as the EVs' location (whether they are at home or not), the average distance they travel per day, and the number of trips per day. Analyzing these variables enables efficient management of EV operations, leading to enhanced energy utilization and cost savings.

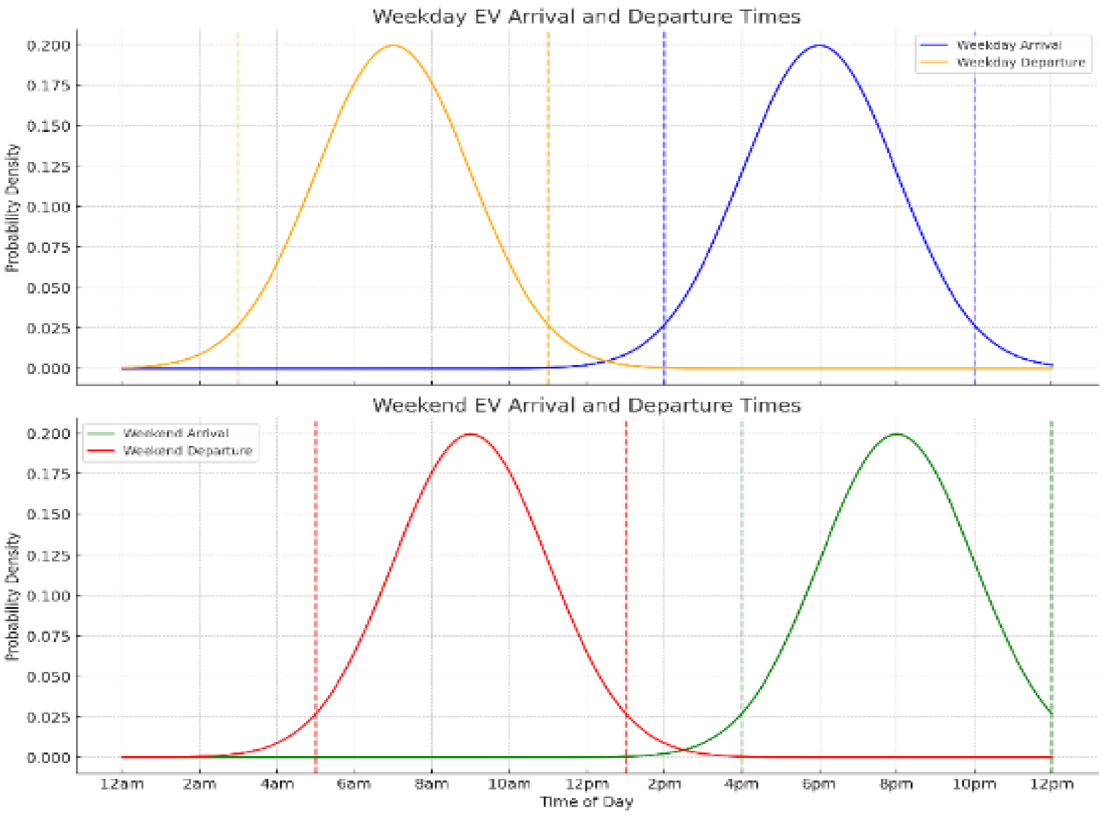

Figure 4.5 The distribution of arrival and departure times of EVs

To model the arrival and departure times of electric vehicles (EVs) on weekdays and weekends, they are assumed to follow normal distributions with specified means and standard deviations. On weekdays, the arrival times have a mean of 6 pm and a standard deviation of 2 hours, resulting in a 95% confidence interval between 2 pm and 10 pm. Weekday departure times have a mean of 7 am and the same standard deviation, leading to a 95% confidence interval between 3 am and 11 am. On weekends, the arrival times have a mean of 8 pm and a standard deviation of 3 hours, with a 95% confidence interval from 4 pm to 12 am. Weekend departure times have a mean of 9 am with the same standard deviation, resulting in a 95% confidence interval between 5 am and 1 pm. A 2-sigma level confidence interval has been set to avoid the effects of long tails of the normal distribution and provide more realistic time windows (see Figure 4.5).

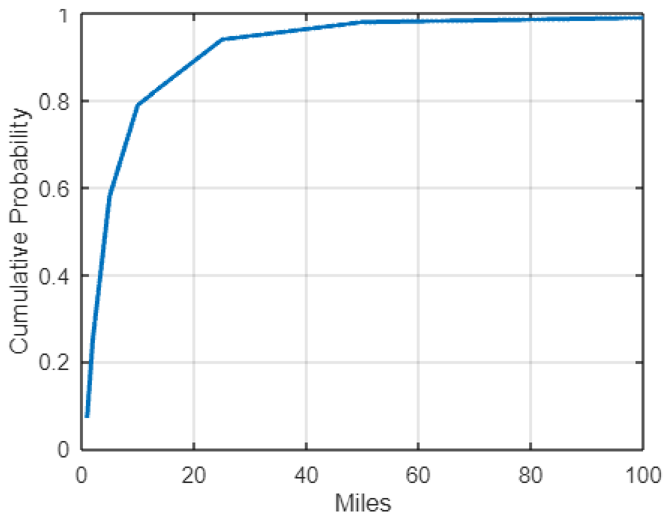

Figure 4.6 CDF of average trip distance

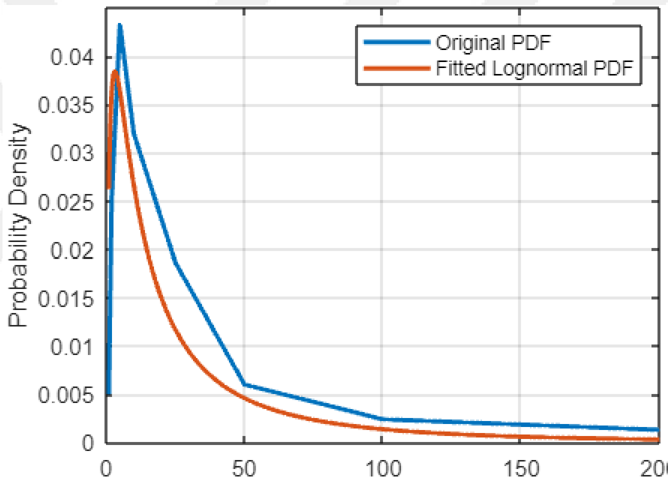

Figure 4.7 PDF of average trip distance and estimated lognormal distribution

The Cumulative distribution function (CDF) of the trip distance of EVs per day is derived from real-world data collected by the National Travel Survey, 2021 [138]. (See Figure 4.6). The probability density function (PDF) is derived from the CDF. The PDF was best fitted with a lognormal distribution. The daily trip travel distances of EVs are obtained by sampling from the estimated lognormal distribution.

A lognormal distribution must be fitted to empirical data using a number of methodical procedures based on statistical theory and numerical methods. First of all, cumulative percentages are computed from the dataset, indicating the proportion of observations less than or equal to each distance. From these cumulative percentages, the probability density function (PDF) is derived by numerically differentiating across the range of distances. This discrete differentiation approximates the PDF values by dividing differences in cumulative percentages by corresponding differences in distances. Interpolation techniques are then applied to extrapolate these PDF values across the entire range of observed distances, ensuring a smooth and continuous representation.

To fit the lognormal distribution, initial estimates for its parameters (mu and sigma) are calculated from the mean and standard deviation of the logarithm of distances. Non-linear regression methods, such as the nlinfit function in MATLAB, are utilized to optimize these parameters by minimizing the residual sum of squares between the observed cumulative percentages and those predicted by the lognormal cumulative distribution function (CDF). This fitting process ensures that the lognormal distribution closely matches the empirical data, capturing the underlying distribution's shape and characteristics effectively.

4.2.2 Rule-Based Energy Management System Model

In that section, a rule-based smart grid energy management system is designed within a residential neighbourhood in the UK. The community includes multiple houses, each equipped with rooftop PV solar panels and one EV per household. Additionally, randomly selected houses are assumed to be equipped with a BESS.

The households are categorized into three groups based on their load profile and the survey data. These categories are households with children, multiple working households, and multiple non-working households. Each household type has distinct energy consumption profiles that present their daily routines and lifestyles.

Households with children intend to consume more energy in the early evening when family members return home from school and work. During this period, activities such as cooking, heating, and entertainment lead to a peak in electricity consumption. Also, during the daytime, energy usage is generally lower as family members are often at work and school, but there can still be some consumption due to essential appliances like refrigerators, heating or cooling systems.

Multiple working households may have lower energy consumption during the daytime when adults are at work and peak consumption in the mornings and evenings. Multiple non-working households are often considered retirees. Since residents are usually at home, daytime usage is expected to be observed, and energy consumption does not fluctuate too much throughout the day.

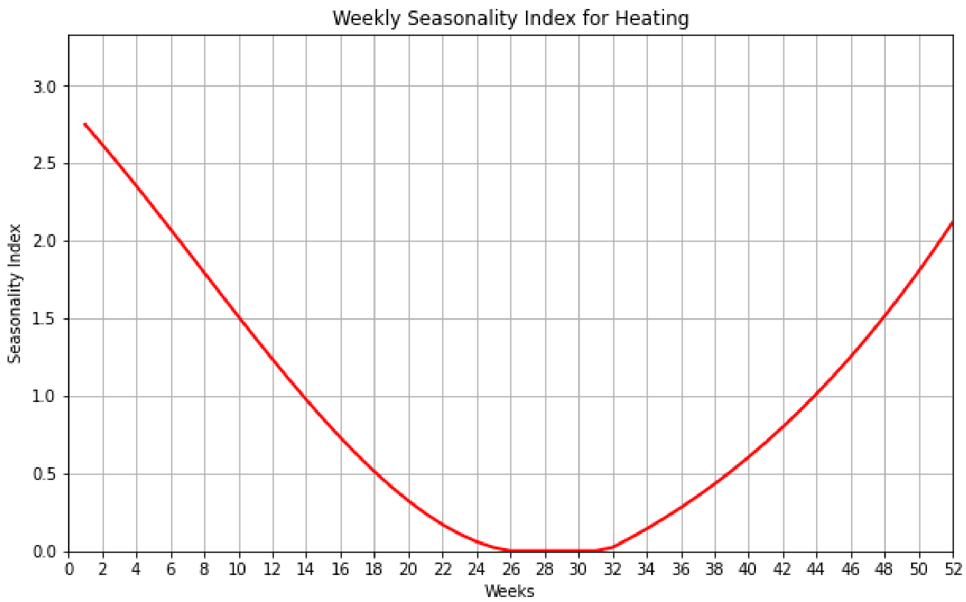

Figure 4.8 Weekly seasonality index for heating demand

The electrification of heating is one of the usage areas of this household categorization. Based on the household type of house, additional heating load is applied to the base consumption to reflect the seasonal variations in the heating demand seasonality index obtained from the Household Electricity Survey [139]. The weekly seasonality indexes are shown in Figure 4.8.

The main function of the management system is controlling energy flow both within the community and the grid system. The environment designed in that study enables peer-to-peer trading within the community to maximize the utilization of renewable energy and minimize peak consumption and load smoothing. In peer-to-peer trading, houses without BESS can share the excess energy generated by their PV to support those with storage systems. On the other hand, houses with BESS can dispatch stored energy in their battery to support households without BESS. There is no restriction on energy flow between houses. Any house can share its energy with any house and receive energy from any house. Power can flow in both directions between any houses connected to the grid, which enables real-time dispatch of generation and BESSs.

EVs plugged into the home have the ability for bidirectional energy flows. Via vehicle-to-home (V2H) and home-to-vehicle (H2V) technologies, EVs can act both as distributed energy resources and controllable loads. This implies that they may both send energy back to the grid to satisfy household energy demands and draw power from it to charge their batteries. They enable the system to balance demand during peak demand periods since they act as a storage device to provide additional capacity. Additionally, the load of EVs can be shifted to low-demand periods. In that way, they provide peak shaving and valley filling operations. Essentially, in that system EVs become a dynamic component of the system by load shifting and supporting demand response.

The proposed energy management system's rule-based control framework is designed around four periods, each with a specific set of predefined operational rules that guide household energy decisions. These periods correspond to typical household activity cycles and sun availability patterns, allowing time and behaviour-aware coordination of distributed energy resources. Figure 4.9 depicts the logic framework that defines the system's behavior in each period.

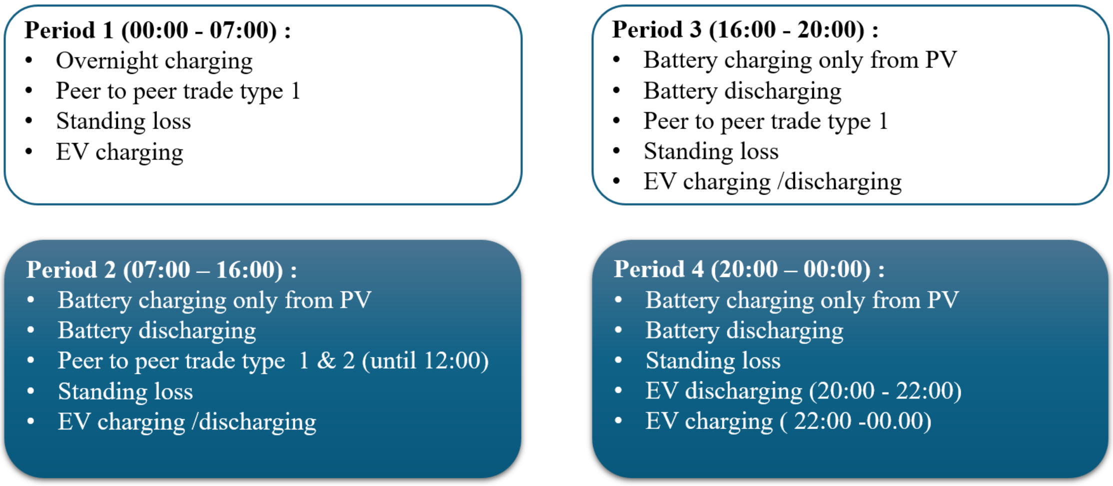

Figure 4.9 Rule-based operational strategies across different periods in the smart energy management system

Period 1 represents the overnight period when the demand is low and mostly no PV production. The system facilitates overnight charging of BESS during that period to leverage the lowest tariff rate. P2P trading type 1, which allows prosumers with PV to share their surplus PV power within the P2P market, enables the use of PV generation at the early hours of the morning. Standing losses are involved in the model for BESSs and EVs. Furthermore, EV charging is scheduled at this time to take advantage of low demand and reduce grid stress.

Period 2 facilitates battery charging only from PV sources, increasing self-consumption of renewable energy since it coincides with the daytime period and peak solar generation. In case of energy need, battery discharge operation is also allowed. Both P2P trade types 1 and 2 are operational, allowing for the sharing of excess energy until midday. Both EV charging and discharging are dynamically regulated according to prosumer schedules and system requirements, and standing losses are once more taken into account.

Period 3 presents early evening, which is generally associated with high demand. PV generation reduces, but battery charging from excess PV power and battery discharging are used to satisfy demand. P2P trading type 1 is used to improve flexibility, and EV activities, including charging and discharging, are carried out according to system balance and mobility requirements.

In Period 4 that is late evening, when photovoltaic power is no longer available, the system continues to control energy flow by charging and discharging batteries to satisfy continuous demand. The electric vehicle (EV) control method follows a more precise schedule: EVs are discharged between 20:00 and 22:00, supporting evening peak demand and contribute to network load balancing, and then charged between 22:00 and 00:00 to take advantage of lower demand periods.

The rule-based model had been developed to create a realistic smart grid simulation environment and to aid in the implementation of essential system activities such as peer-to-peer (P2P) trading, battery degradation assessments, and overnight charging schemes. This approach provided the validation of essential algorithms and system dynamics before proceeding to the reinforcement learning (RL) phase. The rule-based model enables baseline operational activities by improving PV utilization, EV and BESS scheduling, and peak demand reduction. It thus acts as an important intermediary step between static control logic and adaptive real-time learning.

The daily household cost ($Cost_{house}$) involves the grid import cost and revenue obtained from energy exported to peers. There is no revenue obtained when the excess power is exported to the main grid.

$$Cost_{house} = Cost_{house}^{buy} - Rev_{house} \tag{4.1}$$

$$Cost_{house}^{buy} = \sum_{t} \pi_{fromgrid} \ P_{import} \ \Delta t + \sum_{t} \pi_{fromp2p} \ P_{importP2P} \ \Delta t \tag{4.2}$$

$$Rev_{house} = \sum_{t} \pi_{top2p} \ P_{exportP2P} \ \Delta t \tag{4.3}$$

$$P_{import} = P_{house\ load}^{t} - P_{PVgen}^{t} + P_{BESS}^{t} + P_{EV}^{t} - P_{house\ exportP2P}^{t} \tag{4.4}$$

where $Cost_{house}$ is daily energy cost of a house , $Cost_{house}^{buy}$ is the grid import cost, Rev_{house} is the revenue obtained from energy exported to P2P market, P_{import} is the net imported power from the grid at a time t , $\pi_{fromgrid}$ is the electricity tariff price at a time t, $\pi_{fromp2p}$ is the electricity price for P2P market at time t and Δt is the sample time.

4.2.2.1 Overnight Charging Algorithm

The algorithm optimizes the overnight charging levels for battery energy storage systems (BESS) monthly, leveraging the lowest electricity tariffs. For each day, the net excess energy generated by the PV system is calculated. Net excess energy is the renewable energy available for storage. The algorithm then averages these daily values over the month for each house to determine the BESS capacity needed each night, setting the predetermined overnight charging level. The details of the algorithm are shown in Algorithm 1.

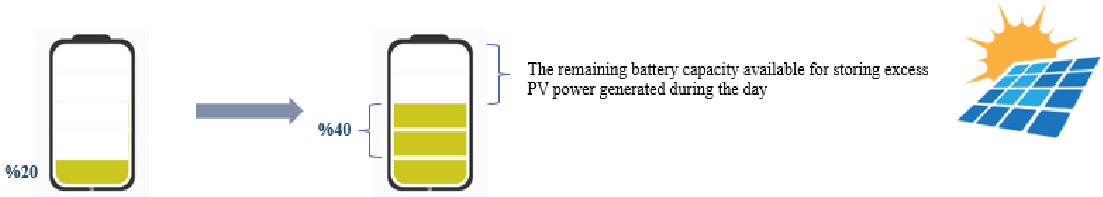

Figure 4.10 Concept of overnight battery charging strategy for PV energy utilization

During the overnight charging period (12 am to 7 am), the BESS charges until it reaches the predetermined charging level. This approach aims to fully utilize the cheaper overnight electricity while reserving capacity to store excess solar energy generated during daylight hours.

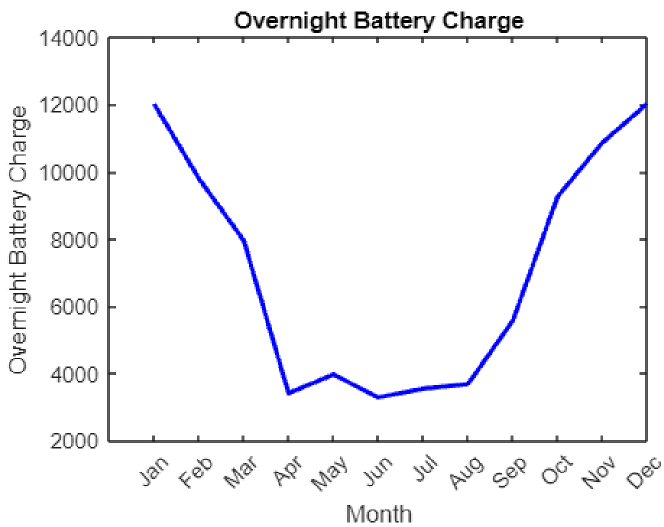

Figure 4.11 Monthly overnight battery charging

The main aims are to maximize the use of cheap overnight electricity and optimize solar energy storage. By charging the battery during the low-tariff period, the system ensures cost-effective energy use.Additionally, by keeping some capacity available in the battery, the system can store excess solar energy produced during the day, which would otherwise be exported to the grid. This strategy encourages on-site storage and self-consumption of PV generated energy to reduce reliance on grid electricity and effectively utilize clean and affordable energy. The monthly overnight charge levels determined for house 1 are given in Figure 4.11

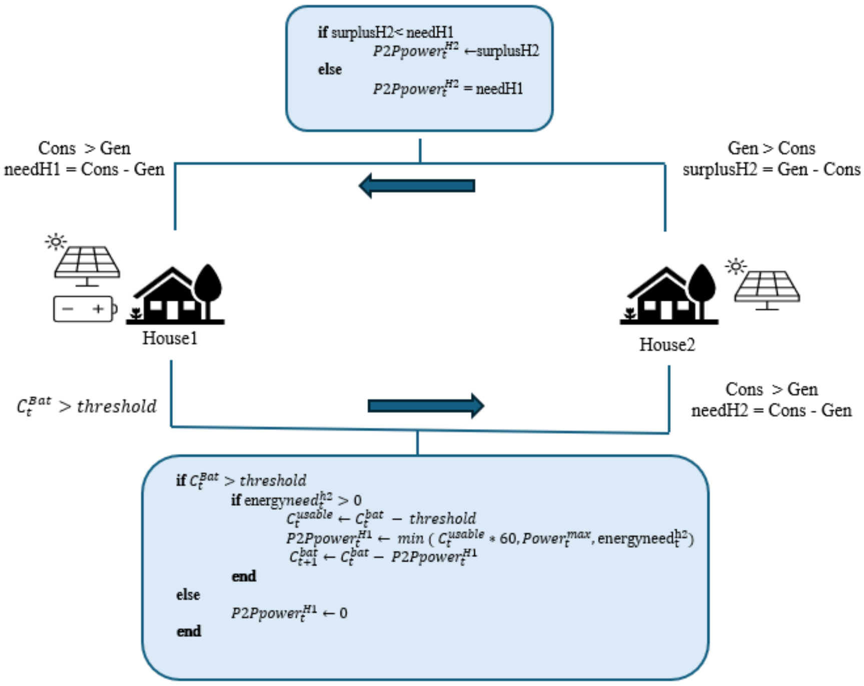

Figure 4.12 Peer-to-Peer (P2P) energy trading mechanism

4.2.2.2 Peer-to-Peer Trading Algorithms

In a peer-to-peer trading algorithm for houses with PV systems, if a house has a PV system without Battery Energy Storage Systems (BESS), it can share its excess power with other houses that need energy. The aim of this peer-to-peer trading algorithm is to efficiently utilize surplus energy generated by houses with PV systems. Allowing the sharing of excess energy among households, the algorithm reduces reliance on the main grid and promotes community-driven sustainability. This approach not only improves resource utilization but also enhances grid stability and resilience, ultimately contributing to a more sustainable and decentralized energy ecosystem. The details are provided in Algorithm 2.

Algorithm 1 Overnight charging level algorithm

for h, h ∈ *houses*
    for d, d ∈ *days*
        for t, t ∈ *minutes*
          If generation (t, h) > consumption (t, h)
                $export_{t,h}^{diff} \leftarrow Gen_{t,h} - Con_{t,h}$
          end if
          Calculate $dailyexport_{h}^{diff}$
          If $dailyexport_{h}^{diff} > Ch_{bat}^{max} - Ch_{bat}^{min}$
          $dailyexport_{h}^{diff} \leftarrow Ch_{bat}^{max} - Ch_{bat}^{min}$
          end if
        end for
    overnightBatteryCharge (d, h) ← $Ch_{bat}^{max} - dailyexport_{h}^{diff}$
    end for
end for
for h, h ∈ *houses*
    for m, m ∈ *months*
    Calculate averageovernightBatteryChargemonthly (h, m)
    end for
end for

For the houses equipped with both the PV system and BESS, if the charge level of their BESS is above the predetermined threshold, they can export energy in a peer-to-peer market mechanism by discharging their BESS. With this approach, they can support their local community, contribute the grid stability. Furthermore, the homeowners can gain profit from these transactions and foster sustainable energy practices and a collaborative approach to energy management and control. The details are provided in Algorithm 3.

Algorithm 2 Peer-to-peer trade algorithm for house with PV system

for d, d ∈ *days*
    for t, t ∈ *minutes*
        if energy$surplus_{t}^{h2} > 0$ and $energyneed_{t}^{h1} > 0$
                if energy$surplus_{t}^{h2} \leq energyneed_{t}^{h1}$
                        $P2Ppower_{t}^{h2} \leftarrow \mathrm{energysurplus}_{t}^{h2}$
                else $P2Ppower_{t}^{h2} \leftarrow energyneed_{t}^{h1}$
                end if
        end if
    end for
end for

The algorithm applied to different household types based on the installed PV and BESS in P2P market, helps the control the clean and affordable energy to decrease grid reliance and stability. Both of the peer-to-peer trading mechanisms are illustrated in Figure 4.12.

Algorithm 3 Peer-to-peer trade algorithm for houses with PV system and BESS

for d, d ∈ *days*
    for t, t ∈ *minutes*
        if $\boldsymbol{C_t^{bat}} > threshold$
            if energy$need_t^{h2} > 0$
                $\boldsymbol{C_t^{usable}} \leftarrow \boldsymbol{C_t^{bat}} - threshold$
                $P2Ppower_t^{H1} \leftarrow min\,($
                $\boldsymbol{C_t^{usable}}\Delta t\,, \boldsymbol{Power_t^{max}}, \mathrm{energyneed}_t^{h2})$
                $\boldsymbol{C_{t+1}^{bat}} \leftarrow \boldsymbol{C_t^{bat}} - P2Ppower_t^{H1}$
            end if
        else
            $P2Ppower_t^{H1} \leftarrow 0$
        end if
    end for
end for

4.2.2.3 Battery Degradation Algorithms

The battery degradation algorithm calculates various metrics to assess battery performance and degradation. It computes the total absolute battery power consumption for the week. The calculation accounts for energy usage during the charging and discharging processes. Subsequently, it calculates the effective energy throughput for the week, considering the round-trip efficiency. Additionally, it determines the number of charge-discharge cycles the battery has accumulated within the week. This metric offers insights into the battery's cycling behavior and its impact on longevity. Furthermore, the algorithm calculates the capacity fade experienced by the battery system over the week.

Capacity fade refers to the gradual reduction in the battery's maximum energy storage capacity over time, often due to repeated charge-discharge cycles (See Figure 4.13). Finally, it adjusts the maximum battery capacity for the next week based on the calculated capacity fade. This adjustment ensures accurate modeling of the battery's behavior in subsequent weeks. Overall, this algorithm provides a comprehensive analysis of battery performance and degradation.

Algorithm 4 Battery degradation algorithm

for w, w ∈ *weeks*

$\mathrm{Energy}_{\mathrm{week}}^{\mathrm{Bat}} \leftarrow \sum_{\mathrm{t}} \left|\mathrm{Power}_{\mathrm{t}}^{\mathrm{Bat}}\right|/60$

$\mathrm{EnergyThroughput}_{\mathrm{week}} \leftarrow \mathrm{Energy}_{\mathrm{week}}^{\mathrm{Bat}} * \mathrm{roundTripEfficiency}$

$\mathrm{Num}_{\mathrm{week}}^{\mathrm{cycle}} \leftarrow \mathrm{EnergyThroughput}_{\mathrm{week}}/\mathrm{C}_{\mathrm{bat}}^{\mathrm{max}}$

$\mathrm{CapacityFade}_{\mathrm{week}} \leftarrow 100 - (\mathrm{slope}_{\mathrm{bat}}\mathrm{Num}_{\mathrm{week}}^{\mathrm{cycle}} + \mathrm{intercept})$

$\mathrm{C}_{\mathrm{bat}}^{\mathrm{max}} \leftarrow \mathrm{C}_{\mathrm{bat}}^{\mathrm{max}}.(1 - \mathrm{CapacityFade}_{\mathrm{week}}/100)$

end

4.2.3 Real-time Pricing Based Energy Management System

In the modern world, the evolving global energy landscape, with increasing penetration of renewable energy resources, electrification, and the emergence of prosumers, presents both opportunities and challenges, especially in ensuring grid reliability and stability.

As the integration of DERs such as PV panels, EVs, and BESSs expands, so does the complexity of managing energy flows within the grid. Renewable energy sources are inherently variable and intermittent, leading to fluctuations in energy supply that must be balanced with demand. Additionally, the increase in prosumers adds another layer of complexity, as these entities can switch between being energy producers and consumers, depending on various factors such as energy prices and their own consumption needs. As a result, a more dynamic, adaptive, and decentralized approach to energy management is required.

The energy management framework addresses these challenges by establishing a system comprising a system operator and multiple prosumers. The system operator sets dynamic energy prices based on real-time grid conditions, while prosumers make decentralized decisions regarding their energy consumption and incorporation of BESS and EV batteries. This approach not only enhances grid stability but also maximizes the utilization of renewable energy, BESS and EV batteries, and provides both economic and social benefits to prosumers.

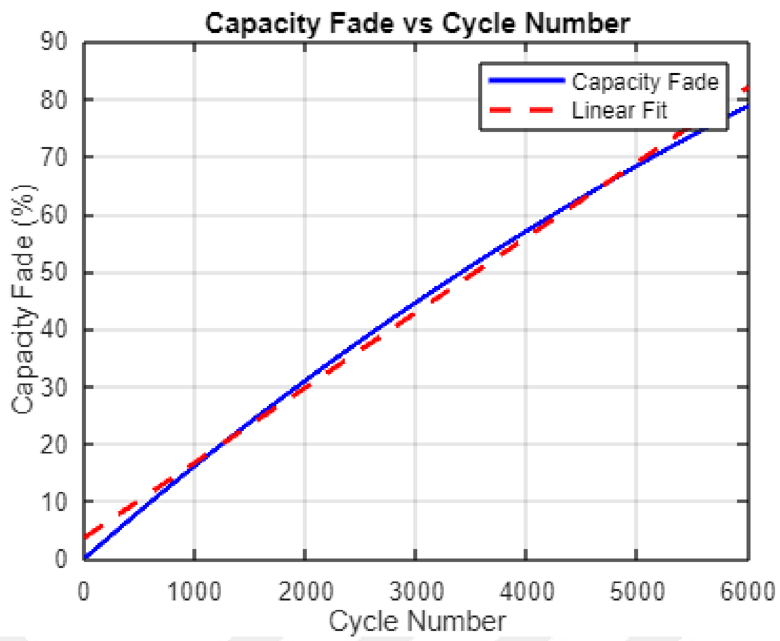

Figure 4.13 Capacity fade of battery vs. cycle number

Overall, this study introduces a real-time energy management framework that utilizes real-time pricing combined with reinforcement learning techniques to optimize the management of energy resources and improve system performance. The following sections describe the system and its components and the dynamics of energy trading strategies.

4.2.3.1 System Model

In this study, a real-time pricing-based energy management framework is designed. This framework operates with two distinct players: a system operator and multiple individual prosumers. The system operator leads by setting dynamic prices for each time interval t, and the prosumers are making informed decisions based on the market conditions.

Each prosumer $n \in N = \{1, \ldots, n\}$ is equipped with photovoltaic (PV) panels, an electric vehicle (EV), and a smart meter to monitor energy consumption and production. Additionally, some prosumers have installed battery energy storage systems (BESS) to store excess energy produced by their PV panels. The energy stored in BESS can be kept for the prosumer's own use, sold in P2P, or transferred to the grid. EV is solely for the use of the prosumer.

4.2.3.1.1 Battery Energy Storage System (BESS)

BESSs are key elements in a smart grid that provides effective demand-response management. Within this system, they are utilized to enhance the self-consumption of

PV-generated energy while supporting peak shaving and valley-filling operations. In that study, BESSs can store excess energy generated by PV panels or energy drawn from the grid or supply stored energy. The stored energy can then be used for self-consumption by prosumers or for trading within the peer-to-peer (P2P) energy market. Prosumers can decide when and how much energy to charge or discharge from their BESS to either meet their demands or supply excess energy or demand energy through the P2P trading market, or they can charge their BESS from the grid when needed. Determining the optimal levels of the states of energy in BESSs to achieve cost efficiency on bills and increasing renewable energy penetration has paramount importance in energy management systems. Within the proposed framework, the charging and discharging strategies of BESS are stated in (4.6) – (4.9).

$$\mathrm{SOE}_{\mathrm{n,t+1}}^{\mathrm{BESS}} = \begin{cases} \mathrm{SoE}_{\mathrm{n,t}}^{\mathrm{BESS}} + \eta_{\mathrm{chrg}}^{\mathrm{BESS}} \mathrm{P}_{\mathrm{n,t}}^{\mathrm{BESS}} \Delta \mathrm{t}, & \mathrm{P}_{\mathrm{n,t}}^{\mathrm{BESS}} > 0 \\ \mathrm{SoE}_{\mathrm{n,t}}^{\mathrm{BESS}} + \dfrac{\mathrm{P}_{\mathrm{n,t}}^{\mathrm{BESS}} \Delta \mathrm{t}}{\eta_{\mathrm{disch}}^{\mathrm{BESS}}}, & \mathrm{P}_{\mathrm{n,t}}^{\mathrm{BESS}} \leq 0 \end{cases} \tag{4.6}$$

$$\mathrm{SoC}_{\mathrm{n,t}}^{\mathrm{BESS}} = \frac{\mathrm{SoE}_{\mathrm{n,t}}^{\mathrm{BESS}}}{\mathrm{SoE}_{\mathrm{n,cap}}^{\mathrm{BESS}}} \tag{4.7}$$

$$\mathrm{SoC}_{min}^{\mathrm{BESS}} \leq \mathrm{SoC}_{\mathrm{n,t}}^{\mathrm{BESS}} \leq \mathrm{SoC}_{max}^{\mathrm{BESS}} \tag{4.8}$$

$$-\mathrm{P}_{min}^{\mathrm{BESS}} \leq \mathrm{P}_{\mathrm{n,t}}^{\mathrm{BESS}} \leq \mathrm{P}_{max}^{\mathrm{BESS}} \tag{4.9}$$

$\mathrm{SoE}_{\mathrm{n,t}}^{\mathrm{BESS}}$ (kWh) and $\mathrm{P}_{\mathrm{n,t}}^{\mathrm{BESS}}$ (kW) represent the state of energy level of BESS of n^{th} prosumer at time t and charge /discharge power from BESS n^{th} prosumer at time t, respectively. $\eta_{\mathrm{chrg}}^{\mathrm{BESS}}$ and $\eta_{\mathrm{disch}}^{\mathrm{BESS}}$ are charging and discharging efficiency rate of BESS (%). With the value of $\mathrm{P}_{\mathrm{n,t}}^{\mathrm{BESS}}$ the mode of a BESS is determined: a positive value indicates charging mode, while a negative value indicates discharging mode. Δt is the sample time (h). $\mathrm{SoE}_{min}^{\mathrm{BESS}}$ and $\mathrm{SoE}_{max}^{\mathrm{BESS}}$ are the minimum and maximum stored energy limits. The value of $\mathrm{P}_{\mathrm{n,t}}^{\mathrm{BESS}}$ is constrained by the power ratings of BESS, defined as $[\mathrm{P}_{max}^{\mathrm{BESS}}, -\mathrm{P}_{max}^{\mathrm{BESS}}]$ are the power ratings of BESS where $\mathrm{P}_{max}^{\mathrm{BESS}}$ represents the maximum power output. $\mathrm{SoC}_{\mathrm{n,t}}^{\mathrm{BESS}}$ is the state of charge level of the n^{th} BESS and formulated in (2) where $\mathrm{SoE}_{\mathrm{n,cap}}^{\mathrm{BESS}}$ is the capacity of the n^{th} BESS (kW). The limits of $\mathrm{SoC}_{\mathrm{n,t}}^{\mathrm{BESS}}$ and $\mathrm{P}_{\mathrm{n,t}}^{\mathrm{BESS}}$ are given in (3) and (4).

4.2.3.1.2 Electric Vehicle (EV)

Electric Vehicles (EVs) can act as both an energy source, supplying power when prosumers are in energy need, and a controllable load, dynamically adjusting their charging patterns to optimize energy usage within the system. The framework enables prosumers to strategically manage EV battery operations based on grid conditions, energy prices, and energy demand. This ensures optimal utilization of the EV's battery storage capability.

Through vehicle-to-home (V2H) and home-to-vehicle (H2V) mechanisms, prosumers can achieve cost savings and reduce their reliance on the grid by intelligently managing their EV battery usage. The charging and discharging strategies of EVs are stated in (4.9) – (4.13), where $\mathrm{SoE}_{\mathrm{n,t}}^{\mathrm{EV}}$ and $\mathrm{P}_{\mathrm{n,t}}^{\mathrm{EV}}$ represent the state of the energy level of EV of n^{th} prosumer at time t and charge /discharge power from EV n^{th} prosumer at time t, respectively.

$$\mathrm{SOE}_{\mathrm{n,t+1}}^{EV} = \left\{ \begin{array}{ll} \mathrm{SoE}_{\mathrm{n,t}}^{EV} + \eta_{\mathrm{chrg}}^{\mathrm{BESS}} \mathrm{P}_{\mathrm{n,t}}^{EV} \Delta \mathrm{t}, & \mathrm{P}_{\mathrm{n,t}}^{\mathrm{EV}} > 0, C_{n,t}^{EV} = 1, \\ \mathrm{SoE}_{\mathrm{n,t}}^{EV} + \dfrac{\mathrm{P}_{\mathrm{n,t}}^{EV} \Delta \mathrm{t}}{\eta_{\mathrm{disch}}^{EV}}, & \mathrm{P}_{\mathrm{n,t}}^{EV} \leq 0, C_{n,t}^{EV} = 1 \\ \mathrm{SoE}_{\mathrm{n,t}}^{EV} + \dfrac{\mathrm{P}_{\mathrm{n,d}}^{EVtrip} \Delta \mathrm{t}}{\eta_{\mathrm{disch}}^{EV}}, & \mathrm{t} \in \left[t_{departure}, t_{arrival}\right], C_{\mathrm{n,t}}^{EV} = 0 \end{array} \right\}, \quad \forall n, t \tag{4.9}$$

$$\mathrm{SoC}_{\mathrm{n,t}}^{EV} = \frac{\mathrm{SoE}_{\mathrm{n,t}}^{EV}}{\mathrm{SoE}_{\mathrm{n,cap}}^{\mathrm{EV}}}, \forall n, t \tag{4.10}$$

$$\mathrm{SoC}_{min}^{EV} \leq \mathrm{SoC}_{\mathrm{n,t}}^{EV} \leq \mathrm{SoC}_{max}^{EV}, \forall n, t \tag{4.11}$$

$$\mathrm{P}_{min}^{EV} C_{n,t}^{EV} \leq \mathrm{P}_{\mathrm{n,t}}^{EV} \leq \mathrm{P}_{max}^{EV} C_{n,t}^{EV}, \forall n, t \tag{4.12}$$

$$\mathrm{P}_{\mathrm{n,t}}^{EVtrip} = -\frac{L_d^n P_{cons}}{t_{n,d,arr} - t_{n,d,dep}}, d = \left\lceil \frac{\Delta t}{m_{av}} (t+1) \right\rceil, \quad \mathrm{t} \in \left[t_{n,d,dep}, t_{n,d,arr}\right], \forall n \tag{4.13}$$

$\eta_{\mathrm{chrg}}^{\mathrm{EV}}$ and $\eta_{\mathrm{disch}}^{\mathrm{EV}}$ are charging and discharging efficiency rate of EV. With the value of $\mathrm{P}_{\mathrm{n,t}}^{\mathrm{EV}}$ the mode of the EV is determined: charging mode or discharging mode. If EV is not at home, $\mathrm{SOE}_{\mathrm{n,t+1}}^{EV}$ is updated based on the total energy consumption of EV over the entire travel period. The total energy consumption is evenly distributed across all time intervals between the departure and arrival times, ensuring a consistent update to the $\mathrm{SOE}_{\mathrm{n,t}}^{EV}$ at each time step during the journey. That approach prohibits dramatic shifts in the state of energy and captures the dynamic nature of energy use, accurately representing real-world EV energy depletion. From the perspective of reinforcement learning (RL), this gradual update approach assures that the agent receives stable and gradual reward signals, minimizing variation while promoting policy learning convergence. $C_t^{EV} \in \{0,1\}$ denotes EV connection status (1: Connected, 0: Not connected). (4.11) ensures that the state of charge level of EVs stays in the upper and lower bound. (4.12) ensures that charging and discharging operations can be conducted only when the EV is at home and denotes upper and lower power ratings for EVs. The energy consumption for a trip is calculated based on L_d^n trip distance (mile) on day d for prosumer n and P_{cons} average energy consumption of EV (kWh/mile). m_{av} represents the total number of time steps available in a day. (4.13) calculates the average power consumption of EV energy consumption per trip based on travel distance and energy efficiency.

4.2.3.1.3 Peer-to-Peer Energy Trading Implementation

Peer-to-Peer energy trading is a mechanism that enables direct energy exchange between prosumers and consumers, which helps to minimize grid dependency. By leveraging DERs such as PV systems and BESS, the P2P mechanism optimizes energy generation and consumption, enhances system flexibility, efficiency, and sustainability, and unlocks new revenue streams for prosumers. This mechanism encourages prosumer interaction by allowing them to dynamically share their energy based on their demand, grid conditions, energy prices, and safety limitations. P2P trading is controlled through two algorithms that facilitate energy exchange and optimize local energy distribution.

The first algorithm, P2P PV Surplus Allocation (P2P-PSA), enables houses without BESS to share their excess energy with other houses in need. This algorithm aims to efficiently utilize surplus energy generated by houses without BESS. Facilitating energy sharing among prosumers promotes community-driven sustainability. This approach not only improves resource utilization but also enhances grid stability and resilience, ultimately contributing to a more decentralized system. (HB: houses with BESS and H: houses without BESS).

The house without BESS that has surplus energy $\left(\sum_{\boldsymbol{n}\in \boldsymbol{H}} \boldsymbol{P}_{\boldsymbol{n},\boldsymbol{t}}^{\boldsymbol{excess}} \geq \mathbf{0}\right)$ can share that energy with the BESS equipped houses that are in need $\left(\sum_{\boldsymbol{n}\in \boldsymbol{HB}} \boldsymbol{P}_{\boldsymbol{n},\boldsymbol{t}}^{\boldsymbol{need}} \geq \mathbf{0}\right)$. The surplus energy is distributed among the houses with BESS in proportion to their energy needs, where $Pr_{n,t}$ proportion rate for house n at time t. This energy trade helps smooth out fluctuations in power consumption, reducing stress on the grid. The allocation mechanism distributes the surplus energy based on the proportion of their energy demand relative to the total demand, ensuring an equitable and efficient use of surplus energy. This approach not only optimizes the overall energy usage within the community but also contributes to a more resilient and stable grid by mitigating demand fluctuations.

Algorithm 5 P2P-PSA Algorithm

if $\sum_{n\in H} P_{n,t}^{excess} \geq 0 \; and \; \sum_{n\in HB} P_{n,t}^{need} \geq 0$ **then**

for each house with BESS ($n \in HB$) and $P_{n,t}^{need} > 0$ **do**

Calculate proportions $Pr_{n,t}$:

$$Pr_{n,t} = \frac{P_{n,t}^{need}}{\sum_{n\in HB} P_{n,t}^{need}}$$

end for

for each house with BESS ($n \in HB$) **do**

for each house without BESS ($m \in H$) **do**

Calculate power will be transferred from house m to house n at time t:

$$P_{n,m,t}^{P2P\_PSA} = min\left(\left(Pr_{n,t} \cdot \left(P_{m,t}^{excess}\right)\right), P_{n,t}^{need}\right)$$

Update power need of house n:

$$P_{n,t}^{need} = P_{n,t}^{need} - P_{m,n,t}^{P2PC\_PSA}$$

end for

end for

end if

The P2P BESS-Supported Energy Trading (P2P-BSET) algorithm enables houses equipped with BESS to participate in P2P energy trading when the state of charge level of their BESS is above the predetermined threshold. The energy available in the BESS of the houses is shared proportionally based on the needs of the houses without BESS. Unlike the P2P-PSA algorithm, it only facilitates surplus PV energy sharing, this algorithm enables houses with BESS to actively discharge the stored energy in BESS to support other prosumers in need. Prosumers can generate profit from these transactions and foster sustainable energy practices and encourage a collaborative approach to energy management. The details of the algorithm are shown in Algorithm 6.

4.2.3.2 Load Management

$$P_{n,t}^{net} = P_{n,t}^{Load} - P_{n,t}^{PV} + P_{n,t}^{BESS} + P_{n,t}^{EV} - \sum_{m,m\in H} P_{m,n,t}^{P2PC_{PSA}}, \quad n \in HB, t \in T, \forall n, t \tag{4.14}$$

$$P_{m,t}^{net} = P_{n,t}^{Load} - P_{n,t}^{PV} + P_{m,t}^{EV} - \sum_{n,n\in H} P_{n,m,t}^{P2PC_{BSET}} + \sum_{n,n\in HB} P_{m,n,t}^{P2PC_{PSA}}, \quad m \in H, t \in T, \forall m, t \tag{4.15}$$

$$P_{s,t}^{import} = \begin{Bmatrix} P_{s,t}^{net}, & P_{s,t}^{net} \geq 0 \\ 0, & o.w \end{Bmatrix}, \forall s \in H \cup HB, \forall t \in T \tag{4.16}$$

$$P_{s,t}^{export} = \begin{Bmatrix} P_{s,t}^{net}, & P_{s,t}^{net} \leq 0 \\ 0, & o.w \end{Bmatrix}, \forall s \in H \cup HB, \forall t \in T \tag{4.17}$$

Load management in a smart grid is essential for sustaining system reliability and stability. It maintains that energy generation, storage, and consumption are optimally balanced for every prosumer, ensuring that energy needs are met in real time. The power balance constraints expressed in (4.14) and (4.15) ensure that the energy demand of the prosumer, regardless of whether power is supplied from the grid, EV $(P_{n,t}^{EV}, P_{m,t}^{EV})$, BESS$(P_{n,t}^{BESS}, P_{m,t}^{BESS})$, locally PV generated power $(P_{n,t}^{PV})$ or power imported from P2P market $(P_{m,n,t}^{P2PC\_PSA}, P_{m,n,t}^{P2PC\_BSET})$ is always satisfied at each time step . If the local energy sources, including P2P trading, are insufficient to satisfy the demand, the remaining energy deficit is imported from the grid. Conversely, when a prosumer generates surplus energy even after operating in the P2P market, that power is exported to the grid. $P_{n,t}^{import}$ and $P_{m,t}^{import}$ denote power import from the grid at time from house n and m based on the house type. If their values negative that indicate the house has energy surplus at the time t, exported power to the grid. Thus, $P_{n,t}^{export}$ and $P_{m,t}^{export}$ are set to $-P_{n,t}^{import}$ and $-P_{m,t}^{import}$, respectively. Additionally, $P_{n,t}^{import}$ and $P_{m,t}^{import}$ are set to zero at time t.

Algorithm 6 P2P-BSET Algorithm

for each house with BESS $(n \in HB)$ **do**
  for each house without BESS (m ∈ H) and $P_{m,t}^{need} > 0$ **do**
    if $SOE_{n,t}^{BESS} > threshold$
      Calculate proportions $Pr_{n,t}$:

$$Pr_{n,t} = \frac{P_{n,t}^{need}}{\sum_{n \in HB} P_{n,t}^{need}}$$

      if $P_{m,t}^{need} > 0$
        Calculate level of energy house n can be discharged from its BESS to share in P2P:
        $SOE_{n,t}^{dich} = SOE_{n,t}^{BESS} - threshold$
        Calculate power will be transferred from house n to house m at time t:
        $P_{n,m,t}^{P2P\_BSET} = min\ (SOE_{n,t}^{disch}\Delta t, P_{max}^{BESS}, P_{m,t}^{need})$
      end if
    end if
  end for
  Update state of energy of BESS:

$$SOE_{n,t+1}^{BES} = SOE_{n,t}^{BESS} - \sum_{m} P_{n,m,t}^{P2P\_BSET}$$

end for

4.2.3.3 Markov Decision Process Formulation

The real-time energy management framework is formulated with the Markov Decision Process (MDP) approach to train and simulate a Deep Reinforcement Model (DRL) since the next state and action of the actors are dependent on the previous state and action (Markovian Property). Each MDP tuples involve state space (S_n), action space (A_n) and immediate reward (R_n). The diagram of MDP is shown in Figure 4.14.

For each time step t, the observed information from the environment is used by the agent for strategic decision-making. This energy management framework involves both the system operator and the prosumers. For the system operator, the state space (S^{SO}) at time t stores the observed information from the environment and is formulated as follows

$$S_t^{SO} = \{P_t^{import}, P_t^{export}\} \tag{4.18}$$

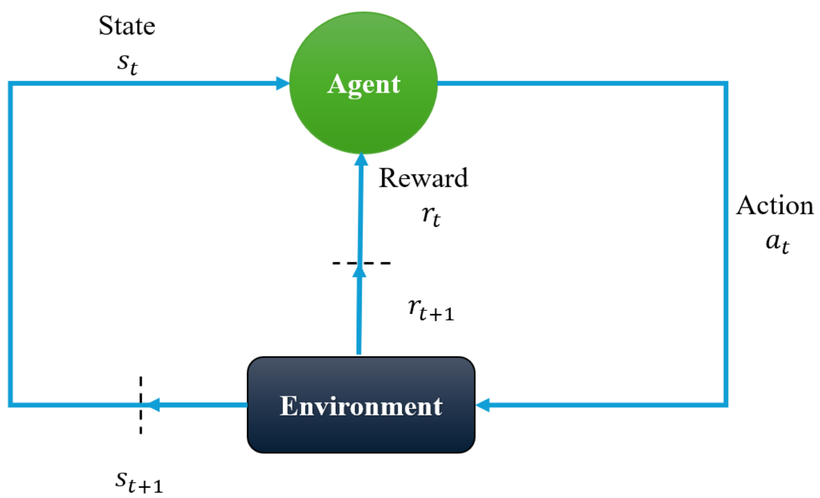

Figure 4.14 Structure of Markov Decision Process

P_t^{import} *and* P_t^{export} are represent the cumulative power imported from the grid at time t $\left(\sum_n P_{t,n}^{import}\right)$ and the cumulative power exported to the grid at time t $\left(\sum_n P_{t,n}^{export}\right)$ where $P_{t,n}^{import}$ and $P_{t,n}^{export}$ are power imported from the grid and exported to grid from prosumer n at time t respectively. Action space (A^{SO}) includes all the available actions at the current state and is formulated as follows

$$A_t^{SO} = \{\pi_t^{grid}, \pi_t^{P2P}\} \tag{4.19}$$

where π_t^{grid} and π_t^{P2P} are the price of electricity from the grid and P2P market.

Each prosumer has an identical state space (S_n), and is formulated as follows

$$S_t^n = \{SoC_{n,t}^{EV}, SoC_{n,t}^{BES}, E_{n,t}^{PV}, C_{n,t}, S_{n,t}^{EV}\} \quad \textbf{(4.20)}$$

$SoC_t^{BESS} \in [0,1]$ *and* $SoC_t^{EV} \in [0,1]$ are represent the state of charge level of BESS at time t and the state of charge level of EV at time t. E_t^{PV}, C_t and $S_t^{EV} \in \{0,1\}$ are denoted as PV generation, load and EV connection status at time t, respectively.

Action space (A_n) of a prosumer includes all the available actions at the current state. It involves power charge or discharge at time t for EV and BESS and a flag to determine the participation of the prosumer in P2P market. Each prosumer has an identical action space and is formulated as follows:

$$A_t^n = \{P_{n,t}^{EV}, P_{n,t}^{BESS}, F_{n,t}^{P2P}\} \quad \textbf{(4.21)}$$

where $P_{n,t}^{EV}$ and $P_{n,t}^{BESS}$ represent the power charged or discharged from the electric vehicle (EV) and the battery energy storage system (BESS), respectively. Their values can be positive, representing charging, or negative, representing discharging. $F_{n,t}^{P2P}$ is a binary flag that shows whether the prosumer participates in the P2P energy market based on market conditions.

Accordingly, the final form of the state space and action space, integrating both the system operator's and prosumers' components into a unified representation, is formulated as follows:

$$S_t = \{SoC_t^{BESS}, SoC_t^{BES}, P_t^{import}, P_t^{export}, S_t^{EV}, C_t, E_t^{PV}\} \quad \textbf{(4.22)}$$

$$A_t^n = \{\pi_t^{grid}, P_t^{BESS}, P_t^{EV}, F_{n,t}^{P2P}, \pi_t^{P2P}\} \quad \textbf{(4.23)}$$

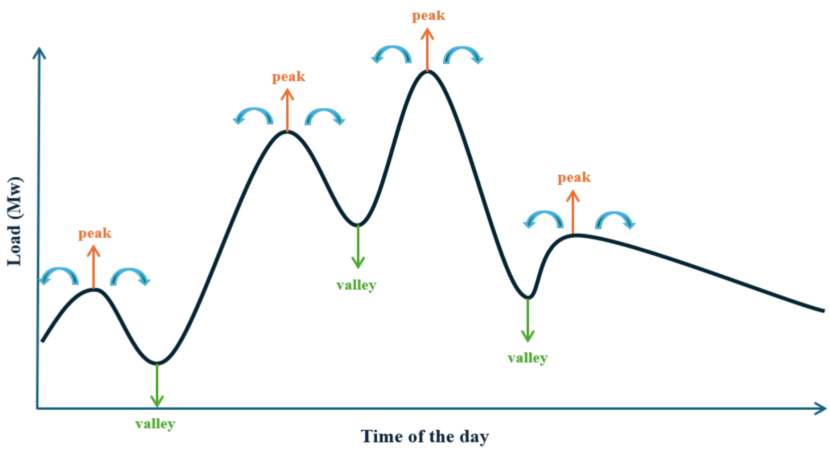

Figure 4.15 Demonstration of peak shaving and valley filling operations

The main objective of the system operator is to achieve a more flattened load curve by minimizing fluctuations in net load with peak shaving and valley filling. This approach helps reduce operational and maintenance costs, mitigate load fluctuations over time, and minimize the need for distribution system upgrades. Since peaks rarely occur during the day (typically in the morning and evening hours), upgrading the infrastructure is often economically infeasible and can disrupt the community. Instead, by smoothing the net load in the grid, the system operator enhances system reliability while ensuring efficient grid operation.

To achieve this objective, the system operator's reward function is formulated to penalize sharp deviations in net load between consecutive periods. By discouraging sudden increases or decreases in the net load, the function promotes a gradual and controlled load adjustment, which also contributes to peak shaving and valley filling. The formulation of the reward function is as follows:

$$R_t^{SO} = -\log\left(\frac{|P_t^{net} - P_{t-1}^{net}|}{|P_{t-1}^{net}| + \varepsilon} + \varepsilon\right) \tag{4.24}$$

The objective of a prosumer consists of multiple components to capture the constraints of the system comprehensively. These include energy bills, SoC limits for EV and BESS, and P2P trade volume.

The energy bill involves the cost of electricity imported from both the main grid and the P2P market, as well as revenue generated from electricity exported to the P2P market. This objective term refers to the electricity bill of prosumers by incentivizing prosumers to reduce grid usage, encouraging them to share the excess energy in the P2P market, and managing their energy consumption effectively and is formulated as follows:

$$R_{n,t}^{bill} = -P_{n,t}^{import} \Delta t\, \pi_t^{grid} - P_{n,t}^{importP2P} \Delta t\, \pi_t^{P2P} + P_{n,t}^{exportP2P} \Delta t\, \pi_t^{P2P} \tag{4.25}$$

The EV battery compliance penalty ensures that the SoC of the EV remains within its operational limits. If the SoC drops below or exceeds predefined limits, a penalty is applied to discourage excessive charging or discharging and preserve the health of the battery.

$$R_{n,t}^{EV} = -\left\{\begin{matrix} \mathrm{SoC}_{min}^{EV} - \mathrm{SoC}_{\mathrm{n,t}}^{EV} & \mathrm{SoC}_{\mathrm{n,t}}^{EV} < \mathrm{SoC}_{min}^{EV} \\ \mathrm{SoC}_{\mathrm{n,t}}^{EV} - \mathrm{SoC}_{max}^{EV} & \mathrm{SoC}_{\mathrm{n,t}}^{EV} > \mathrm{SoC}_{max}^{EV} \\ 0 & \mathrm{SoC}_{min}^{EV} \le \mathrm{SoC}_{\mathrm{n,t}}^{EV} \le \mathrm{SoC}_{max}^{EV} \end{matrix}\right\} \tag{4.26}$$

Similarly, the BESS SoC limits penalty term has the same structure that ensures the BESS operates within safe SoC boundaries.

$$R_{n,t}^{BESS} = -\left\{\begin{matrix} \mathrm{SoC}_{min}^{BESS} - \mathrm{SoC}_{\mathrm{n,t}}^{BESS} & \mathrm{SoC}_{\mathrm{n,t}}^{BESS} < \mathrm{SoC}_{min}^{BESS} \\ \mathrm{SoC}_{\mathrm{n,t}}^{BESS} - \mathrm{SoC}_{max}^{BESS} & \mathrm{SoC}_{\mathrm{n,t}}^{BESS} > \mathrm{SoC}_{max}^{BESS} \\ 0 & \mathrm{SoC}_{min}^{BESS} \le \mathrm{SoC}_{\mathrm{n,t}}^{BESS} \le \mathrm{SoC}_{max}^{BESS} \end{matrix}\right\} \tag{4.27}$$

To encourage local energy exchange, the P2P Trade volume rewards prosumers who actively participate in peer-to-peer trading. By increasing the proportion of energy traded within the local network, prosumers can minimize dependency on the grid, enhancing energy resilience and grid stability.

$$R_{n,t}^{P2P} = \frac{P_{n,t}^{importP2P}}{P_{n,t}^{import} + P_{n,t}^{importP2P} + \varepsilon} \tag{4.28}$$

The reward function of a prosumer can be expressed as:

$$R_t^n = \alpha_1 R_{n,t}^{bill} + \alpha_2 R_{n,t}^{EV} + \alpha_3 R_{n,t}^{BESS} + \alpha_4 R_{n,t}^{P2P} \tag{4.29}$$

where α_1, α_2,α_3,α_4 are scaling factors.

The reward function used in the energy management model is

$$R_t = \beta R_t^{SO} + R_t^n = \beta R_t^{SO} + \alpha_1 R_{n,t}^{bill} + \alpha_2 R_{n,t}^{EV} + \alpha_3 R_{n,t}^{BESS} + \alpha_4 R_{n,t}^{P2P} \tag{4.30}$$

Overall, the objective structure encourages prosumers to optimize energy consumption and trading behavior while satisfying the constraints of the system. This approach contributes to efficient energy management systems while fostering a more resilient and sustainable energy network.

4.2.3.4 Deep Deterministic Policy Gradient Algorithm for Real-Time Energy Management Framework

Deep Reinforcement Learning (DRL) frameworks are generally used for handling decision-making problems since they can produce effective solutions by learning optimal policies through experience obtained from the environment. They can adapt to complex, dynamic environments due to their ability to extract high-dimensional features and produce effective solutions even when uncertainty, nonlinearity and large state-action spaces exist. This makes the DRL structure appropriate for real-time energy management framework.

In this study, to solve the MDP model described, a DDPG-based real-time energy management framework is used. In the DDPG algorithm, a dual network structure is adopted. The DDPG algorithm integrates the strengths of the Actor Critic algorithm, Deep Q learning (DQN) algorithm, and Deep Policy Gradient (DPG) algorithm.

In the DDPG, the transition (s_t, a_t, r_t, s_{t+1}) is stored in the replay buffer, and when the actor and critic network are updated, a mini-batch of transitions is randomly sampled. The critic network $Q(s_i, a_i|\theta^Q)$ is a Q-value function and is used to evaluate the agent based on the current state and the action taken by the agent. The sampled transactions are used to calculate the estimated Q-value $Q(s_i, a_i|\theta^Q)$. The critic network is updated by minimizing the loss between the target y_i and the estimated Q value $Q(s_i, a_i|\theta^Q)$. The loss function and the target Q value y_i are shown in (4.31) and (4.32) where $Q'\big(s_{i+1}, \mu'\big(s_{i+1}|\theta^{\mu'}\big)|\theta^{Q'}\big)$ is the Q value calculated from target critic network Q' and k is the number sampled transitions from the replay buffer.

$$L = \frac{1}{k}\sum_{i=1}^{k}\big(y_i - Q(s_i, a_i|\theta^Q)\big)^2 \tag{4.31}$$

$$y_i = r_i + \gamma(1-d)Q'\big(s_{i+1}, \mu'\big(s_{i+1}|\theta^{\mu'}\big)|\theta^{Q'}\big) \tag{4.32}$$

Algorithm 7 DDPG Algorithm

Initialize the actor network $\mu(s, a|\theta^\mu)$ and critic network $Q(s, a|\theta^Q)$ and randomly assign weights
Duplicate the actor and critic networks to construct the target actor network $\mu': Q' \leftarrow Q, \mu' \leftarrow \mu$ and target critic network Q' .
Set a memory pool M and adjust the capacity to Memory_max
for epoch=1,..,n **do**
    Set noise for exploration $\mathcal{N}$
    Receive the initial state s_1
    for t=1, T **do**
        Determine action $a_t = \mu(s_t|\theta^\mu) + \mathcal{N}$
        Take action a_t and receive reward r_t and proceed to next state s_{t+1}
        In the memory pool, store (s_t, a_t, r_t, s_{t+1}).
        Sample minibatch from the memory pool.
        Determine
        $L = \frac{1}{k}\sum_{i=1}^{k}\big(y_i - Q(s_i, a_i|\theta^Q)\big)^2$
        $y_i = r_i + \gamma(1-d)Q'\big(s_{i+1}, \mu'\big(s_{i+1}|\theta^{\mu'}\big)|\theta^{Q'}\big)$
        Adjust Q net such that L minimized.
        Adjust actor μ based on the gradient.
        Adjust the actor and critic target networks.
        $\theta^{Q'} \leftarrow \tau\theta^Q + (1-\tau)\theta^{Q'}$
        $\theta^{\mu'} \leftarrow \tau\theta^\mu + (1-\tau)\theta^{\mu'}$
    end for
end for

While the critic network parameters are learned using error backpropagation, the actor-network parameters θ^{μ} is learned through the policy gradient method.

The target networks of the critic and the actor networks are updated with soft update strategy as follows:

$$\theta^{Q'} \leftarrow \tau\theta^{Q} + (1-\tau)\theta^{Q'} \tag{4.33}$$

$$\theta^{\mu'} \leftarrow \tau\theta^{\mu} + (1-\tau)\theta^{\mu'} \tag{4.34}$$

τ is the soft update parameter and $\theta^{Q'}$ and $\theta^{\mu'}$ are the target critic and actor networks parameters, respectively. The soft update strategy improves the stability of the learning process. The details of the algorithm are given in Algorithm 7.

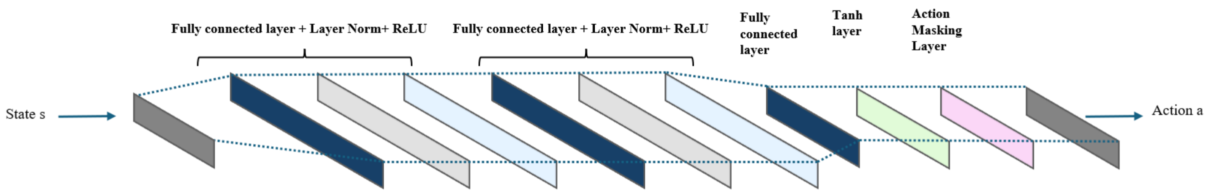

Figure 4.16 Modified actor network structure

The structure of the actor-network that is used in the energy management framework is given in Figure 4.16. The structure is a modified version of the classical actor-network structure of the DDPG algorithm. It is designed to efficiently map states to valid continuous actions while maintaining stability and ensuring compliance with predefined model constraints. The action masking layer dynamically filters the action vector, enforcing hard constraints that the agent must always satisfy. Unlike imposing penalties for constraint violations, this layer completely filters invalid actions for hard constraints.

4.2.4 Results and Analysis

In this study, the data is collected for a year with 1-minute and 30-minute resolution. The dataset includes energy load (C_t in kWh) kWh, solar energy generation (kWh), EVs connection status ($S_t^{EV} \in \{0,1\}$), trip durations of EVs, arrival and departure times of EV. For a rule-based model, TOU pricing has been used. The details of the specifications of EVs and BESSs are given under the dataset section. The initial SoC levels of EVs and BESSs are determined by a random variable using a uniform distribution.

4.2.4.1 Rule-based Energy Management Model Results

The rule-based model has been developed as a baseline framework to build key algorithms such as peer-to-peer trading, overnight charging, and battery degradation algorithms. This model uses predefined rules and algorithms. These rules and algorithms are tested with different scenarios to identify potential limitations and validate the algorithms. It serves as a testing ground. Thus, these algorithms are tested through the rule-based model before being implemented into the more advanced reinforcement-based model.

To understand how peer-to-peer trading dynamics shape the energy system rule-based model is used as a foundational reference point. The effectiveness of P2P trading can be evaluated by the level of power imported within the P2P market rather than relying on a traditional grid supply. The effect of P2P trading on energy transactions of a single house on a randomly chosen winter day is given in Figure 4.17. The figure illustrates how the integration of P2P energy transactions within the rule-based energy management framework shows a considerable reduction in grid dependency, although PV generation is low during the winter, which may result in a lower volume of P2P trade. The household shows increased grid imports when P2P transactions are absent, especially during high-demand periods, demonstrating its total dependence on the grid. However, these grid imports are significantly decreased when P2P trading is implemented, suggesting that local energy exchanges effectively meet part of the household's energy needs. The difference between the power import with and without P2P trading shows that, even in a scenario with limited renewable energy generation, P2P energy trading contributes to load smoothing by distributing locally generated energy more efficiently. This reduces peak demand stress on the grid and promoting a more resilient and decentralized energy system.

The impact of P2P trading on energy imports across different households, segmented into four distinct periods of the day, is shown in Figure 4.18. The bar charts compare energy consumption with and without P2P trading, while the difference plots on the right quantify how much additional energy must be imported from the grid when P2P trading is absent. The analysis highlights the critical role of P2P transactions in reducing grid dependency and balancing energy demand within the microgrid.

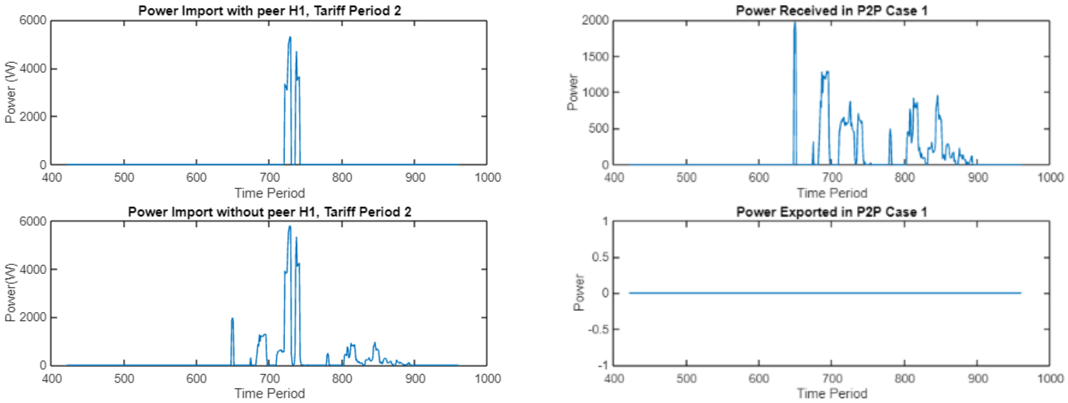

Figure 4.17 P2P Trading Effect on a Single House

Due to low demand and limited renewable generation, P2P trading has a limited impact during Periods 1 (12 AM–7 AM) and Period 4 (8 PM–12 AM). However, P2P trading considerably decreases grid imports during Period 2 (7 AM–4 PM) by sharing excess PV generation among prosumers, which reduces reliance on external supplies. For instance, House 4 and House 5, which are not equipped with Battery Energy Storage Systems (BESS), reported weekly reductions of up to 20 kWh, indicating that a significant portion of their daytime demand was met through local peer-sourced energy. On the contrary, the other houses, which have BESS installed, show low import profiles due to their ability to store and utilize excess renewable energy locally. The most significant impact is observed during Period 3 (4 PM to 8 PM), when evening activities such as cooking, heating, and lighting cause household demand to rise, increasing grid imports in the absence of P2P trading. This emphasizes the importance of peer transactions in reducing the stress caused by peak loads and improving grid flexibility.

The movements of power within the P2P trading framework, showing the exchange between multiple houses, are illustrated in Figure 4.19. As shown by the yellow circles, power is exported by House 4 and imported by House 1 within the P2P market. This transaction serves as an example of how direct power transfers made possible by peer-to-peer energy trading promote decentralized energy management and lessen dependency on the centralized grid. Furthermore, as the green circle shows, House 1 exports power as well, powering House 5. This two-way energy flow highlights how houses play a dynamic role in the P2P market, acting as both prosumers and consumers based on their consumption and availability.

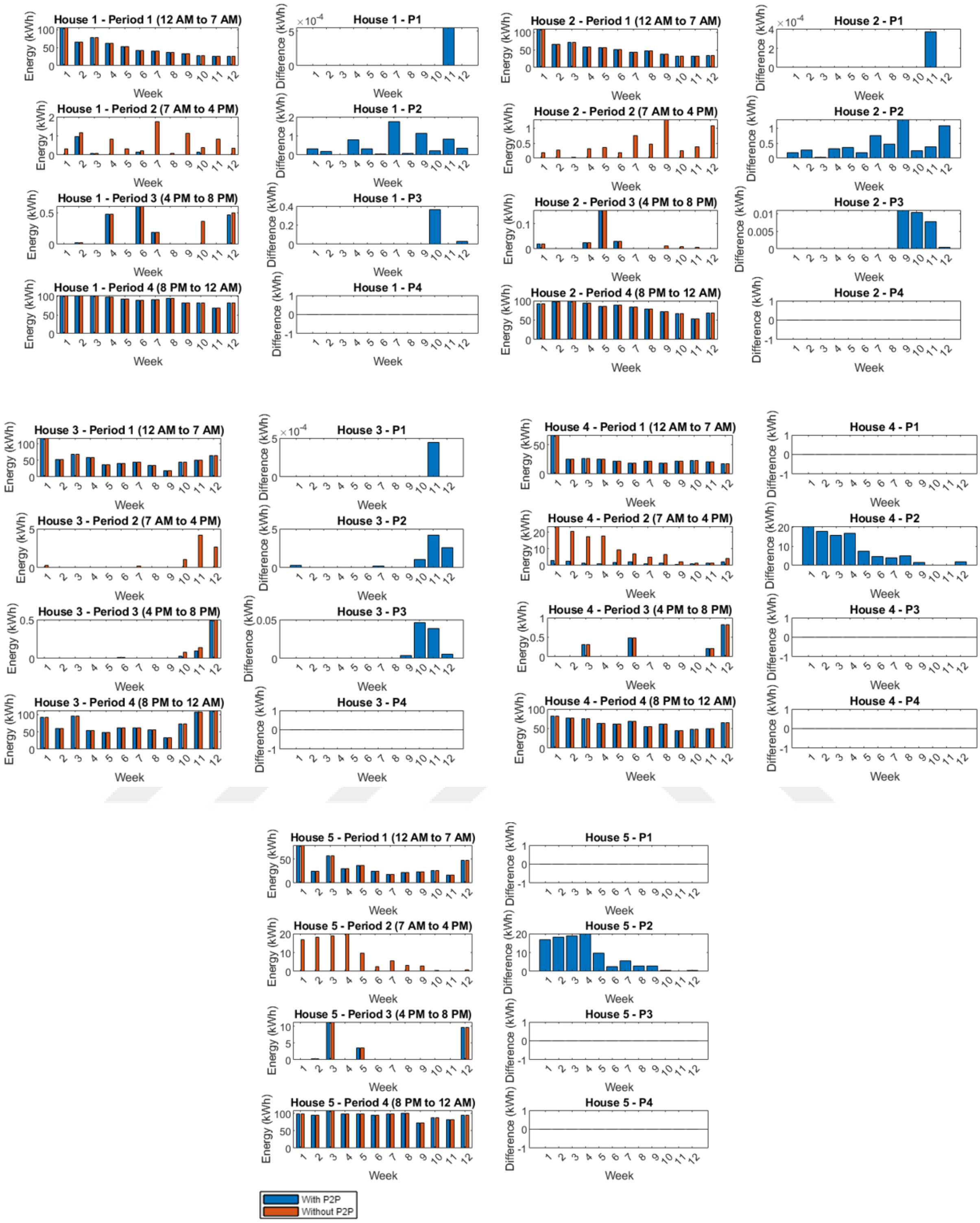

Figure 4.18 P2P Trading effect on multiple houses

Table 4.1 Effect of P2P trading on average daily cost

	Average Daily Cost with Peer (£)	Average Daily Cost without Peer (£)	Difference (%)
House 1	4.51	4.66	3.17
House 2	4.24	4.43	4.07
House 3	3.87	4.04	4.22
House 4	3.48	3.53	1.54
House 5	4.76	4.82	1.15

According to Table 4.1, P2P trading effectively reduces daily energy expenses for all prosumers, with savings ranging from 1.15% to 4.22%. The largest cost reductions are attained by Houses 3, 2, and 1, demonstrating active peer trading by lowering dependency on grid imports or using cheaper and cleaner surplus energy from others. Houses 5 (1.15%) and 4 (1.54%), on the other hand, save the least, as a result of their lack of battery energy storage systems (BESS) and the restricted availability of extra PV energy from peers. This finding further emphasises the possible benefits of BESS integration, since stored energy could enhance trading opportunities by enabling prosumers to engage in P2P transactions outside of daylight hours, hence decreasing reliance on the grid and increasing cost savings.

These results provide additional evidence that the rule-based energy management approach works well for facilitating localized energy optimization and distributed coordination in a smart grid community. Peer-to-peer energy exchanges based on specified rules are made possible by the system, which not only decreases electricity bills but also demonstrates how structured trade logic may decrease peak grid loads and encourage prosumer participation. The overall decrease in grid dependency across all family types validates the importance of comprehensive control mechanisms, even though the benefits are more noticeable in households with BESS, because of their capacity to store and trade energy after daylight hours. The rule-based model was initially developed to test the main operational algorithms and provide a realistic modelling environment, but the findings also show that it can provide real-world system-level and economic benefits in decentralized smart grid setups.

Figure 4.19 Energy transitions between houses and the grid

4.2.4.2 Real-time Pricing based DDPG Model Results

The RL-based real-time pricing mechanism and its effects on grid interactions, pricing patterns, and P2P energy trading are examined in this section. This analysis covers essential system dynamics, such as power imports and exports, effects of renewable generation, and price fluctuations in both P2P and grid markets. The findings provide light on the Deep Deterministic Policy Gradient (DDPG) algorithm's ability to adjust prices in real-time in response to system dynamics reflected in the reward function.

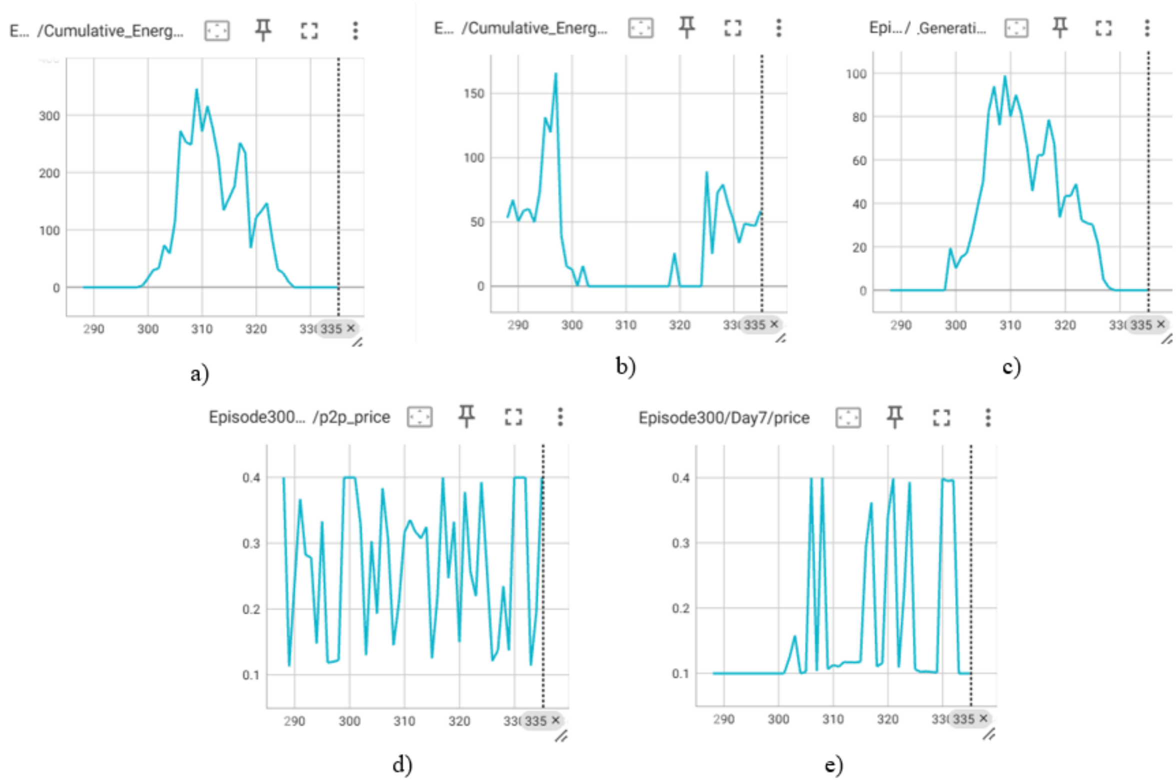

Figure 4.20 Real-time Pricing Based DDPG model

Figure 4.20(a) represents cumulative energy exports to the grid, while Figure 4.20(b) illustrates cumulative energy imports from the grid, depicting the extent of household reliance on external energy sources. Figure 4.20(a) represents cumulative energy exports to the grid, while Figure 4.20(b) illustrates cumulative energy imports from the grid, depicting the extent of household reliance on external energy sources. Figure 4.20(c) displays the renewable generation profile, which plays a critical role in shaping both export and import behaviors. The cumulative energy export curve (Figure 4.20(a)) exhibits a sharp increase between 6 am and 4 pm, aligning with the peak renewable generation period (Figure 4.20(c)). This suggests that when local PV energy production is high, households primarily utilize their generation for self-consumption and

P2P trading, exporting only surplus energy to the grid. Conversely, the cumulative energy import curve (Figure 4.20(b)) follows an inverse trend, with grid dependency decreasing during peak generation and rising before and after the high production window. This pattern indicates that households predominantly rely on grid electricity when renewable supply is insufficient. The interaction between generation, cumulative energy export, and cumulative energy import suggests that P2P trading helps optimize local energy utilization, as evidenced by the temporary reduction in grid imports during the high-generation period.

P2P market price changes are depicted in Figure 4.20(d), whereas grid pricing fluctuations are shown in Figure 4.20(e). While grid prices stay within the upper and lower boundaries established by the rule-based model, P2P prices show greater volatility and sensitivity to real-time trading situations, illustrating adaptive price formation in the RL-based pricing mechanism. According to the findings, grid pricing follows a more regulated pattern that reacts to market conditions, but P2P trading permits more flexible pricing adjustments that are directly driven by local energy supplies and demand.

A specific trend shows that P2P prices fall at times of significant renewable generation, which is indicative of peer transactions and the availability of excess energy. Grid prices, on the other hand, rise sharply during peak demand hours but exhibit comparatively less sensitivity to changes in real-time generation. These results demonstrate that, in situations where excess energy is available, P2P trading offers a more affordable option to grid dependency by facilitating localized energy trades at lower price points.

A collection of graphs in Figure 4.21 shows how energy is transferred between both prosumers and the grid, offering information on how energy is traded, used, and stored in a decentralized trading system. The patterns in the graphs demonstrate how prosumers dynamically switch between the roles of consumer and producer based on demand and local generation availability. Prosumers redistribute energy within the community by either exporting excess renewable energy to the grid or engaging in peer-to-peer (P2P) trade. On the other hand, prosumers depend on grid electricity to keep a supply balance during times of low generation or high local demand. A more sustainable and economical energy ecology is made possible by this adaptive behavior, which also improves system resilience and lessens grid dependency.

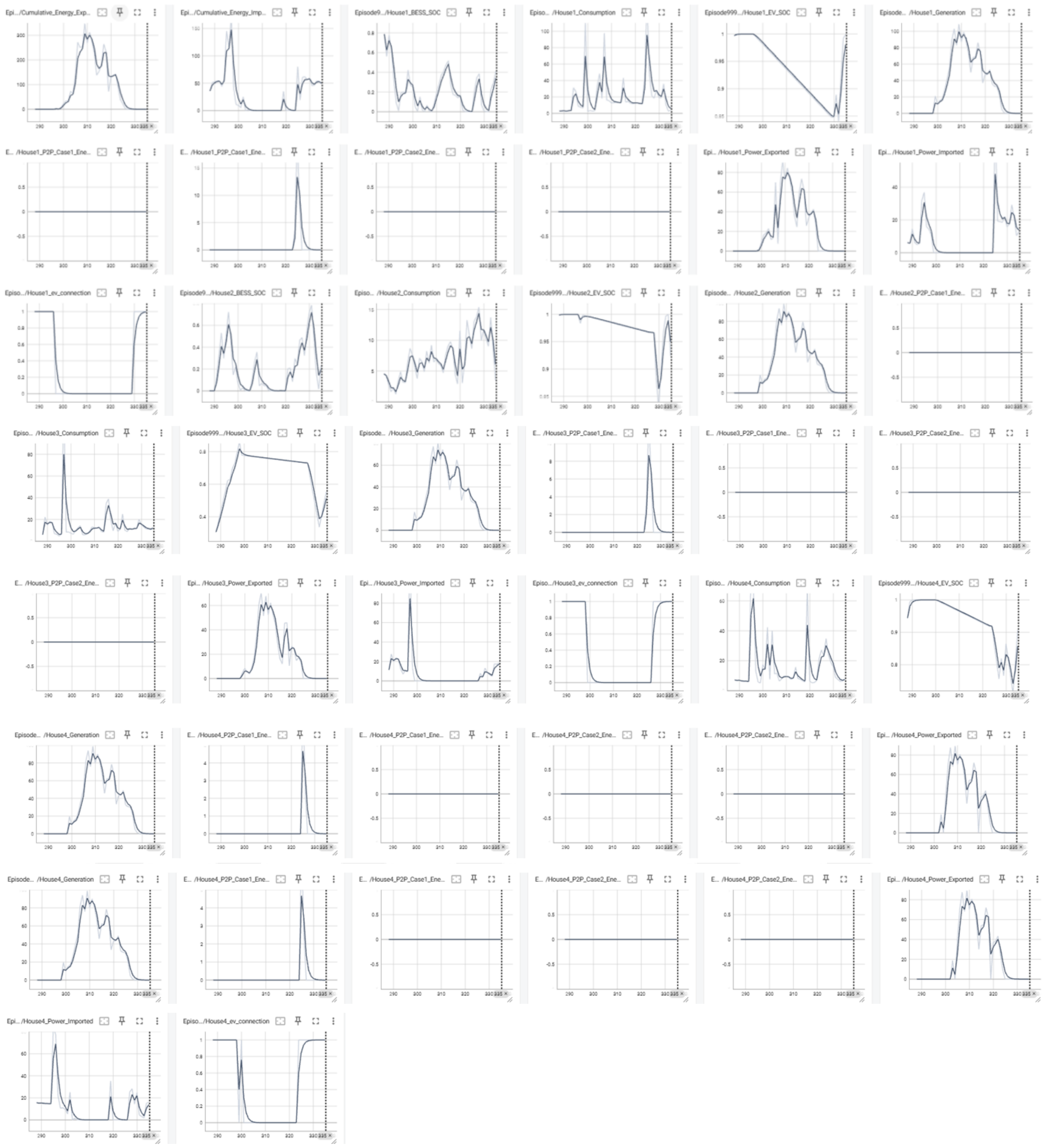

Figure 4.21 Energy flow between grid and prosumers in an RL-based trading framework

Furthermore, the EV state-of-charge (SOC) graphs demonstrate a linear decline in SOC over time, which is directly connected with the length of the trip and the EV's departure from home. By preventing needless unpredictability from entering the RL agent's training process, our approach guarantees that SOC depletion preserves model learning stability. Prosumers actively manage extra energy by either feeding it into the grid or discharging stored energy from batteries to satisfy local energy requirements, according to P2P trade patterns. This behavior demonstrates how surplus generation and managed battery discharge contribute to a more robust and cooperative decentralized energy market, highlighting the significance of P2P trade in improving community-wide energy availability.

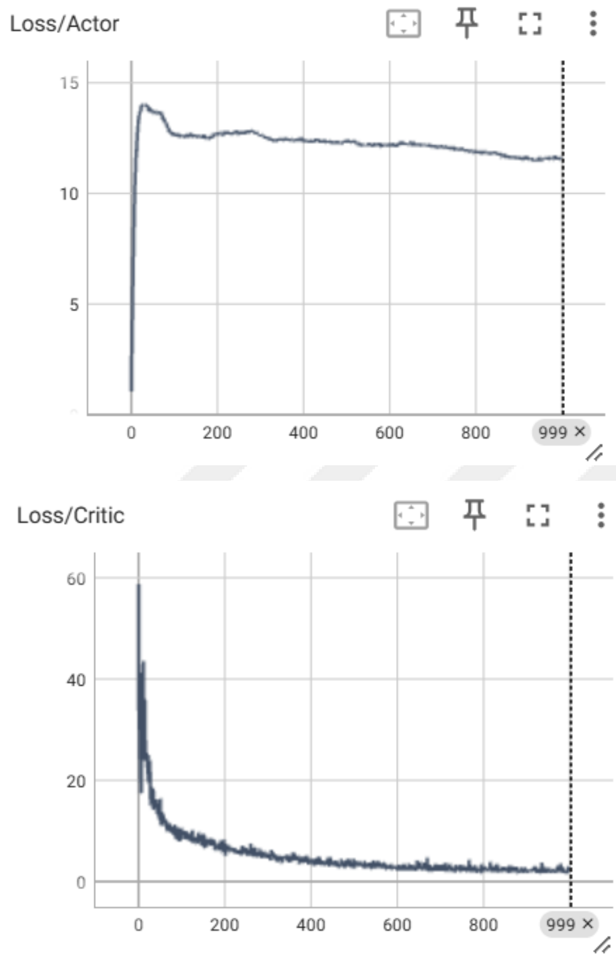

Figure 4.22 Actor and critic loss of the DDPG model

In order to evaluate the effectiveness and convergence of the proposed model, the actor and critic loss curves are presented in Figure 4.22. It can be observed that the losses decrease continuously as the number of training episodes increases, eventually converging. In particular, the critic loss decreases suddenly in the early stage of the learning process, which indicates fast learning, whereas the actor loss converges after the initial fluctuation. Convergence begins at 600 episodes, implying that the model gradually improves its policy and value estimates over time. This pattern demonstrates the usefulness of the learning process in optimizing energy management decisions.

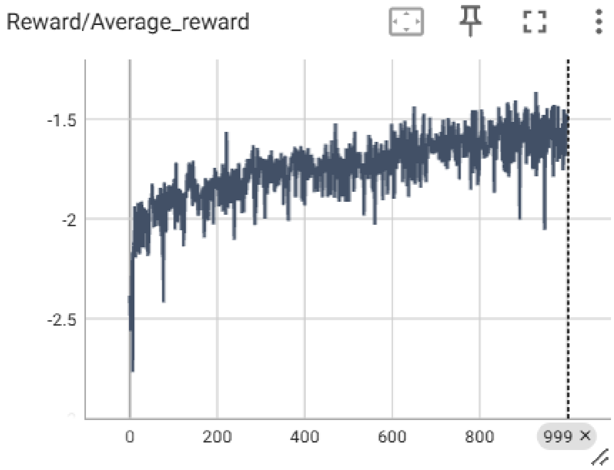

Figure 4.23 Average reward of the DDPG model

The average reward shows some variability in the early episodes, which is generally due to exploration and exploitation of trade-offs in reinforcement learning. The increasing trend in the average reward indicates that the DDPG model is learning effectively and improving its policy for energy management. While some fluctuations are observed, the overall progression suggests that the model is converging towards an optimal strategy.

The real-time pricing-based energy management model, created with the Deep Deterministic Policy Gradient (DDPG) algorithm, displays a high level of responsiveness and adaptability in a dynamic smart grid setting. Unlike the rule-based model, which uses fixed Time-of-Use (TOU) tariffs, the DDPG model employs a real-time pricing mechanism that constantly adjusts based on system conditions. Due to the difference in pricing, direct comparisons between the two models are not conducted since they would not produce a fair or meaningful evaluation.

Instead, the DDPG model's performance is evaluated according to how well it can accomplish important control goals within its particular price environment. In real time, the model is able to strategically coordinate the operation of EVs and BESSs, boost self-consumption of locally generated renewable energy, and decrease energy imports during periods of high prices. The learning process is stable and successful, as evidenced by the convergence of the actor and critic loss functions and the increasing trend of the average reward signal.

Moreover, the model's policy demonstrates intelligent behavior by dynamically adjusting prosumer actions in response to real-time price fluctuations. EV charging and discharging schedules align with low and high price periods, respectively, while peer-to-peer (P2P) trading becomes more active during times of local surplus. These patterns suggest that the agent not only internalizes the reward structure but also generalizes well across varying operational scenarios.

Overall, the DDPG-based technique provides a more adaptable and economical control strategy for decentralized energy systems. The model makes autonomous, cost-sensitive decisions that support system-wide objectives, including cost effectiveness, grid stability, and renewable integration by learning in a highly changeable and uncertain environment. This shows that the model is suitable for next-generation smart grid applications.

4.2.5 Conclusion

In order to maximize the coordination of distributed energy resources in smart grid communities, a smart energy management paradigm was presented in this chapter. The strategy was carried out in two stages: a rule-based baseline model and a reinforcement learning-based real-time pricing control model. The rule-based model, which was originally designed to create a realistic simulation environment and test control algorithms, proved useful in allowing peer-to-peer (P2P) energy trading, increasing PV self-consumption, and reducing reliance on the central grid. Its structured and strategic approach enabled the targeted deployment of electric vehicles (EVs) and energy storage, boosting operational efficiency and optimizing load balancing.

A Deep Deterministic Policy Gradient (DDPG)-based model was created to add data-driven, adaptive control under dynamic pricing, building on this basis. The RL agent improved P2P energy trading, optimized charging and discharging schedules, and matched prosumer behavior with price signals by learning to react to real-time grid and market conditions. In contrast to the rule-based system's fixed TOU scheme, the DDPG framework allowed for flexible energy management that was adapted to user activity, renewable generation, and fluctuating demand.

Simulation results validated the model's convergence and ability to optimize long-term rewards, resulting in practical benefits such as decreased electricity bills, improved load shaping, and improved system resilience. The results showed that static operational models may be effectively transformed into intelligent, self-governing control systems through reinforcement learning, making this framework a viable option for decentralized, sustainable energy management in the future.

Chapter 5

Conclusion and Future Prospects

5.1 Conclusion

This thesis provided a comprehensive, multi-stage intelligent energy management system for modern smart grid systems, emphasizing the enhancement of real-time operational intelligence, planning efficiency, and forecasting accuracy. As energy systems transition toward higher shares of renewable generation and prosumer-driven architectures, there is a growing need for methods that can manage uncertainty, improve resource coordination, and respond adaptively to dynamic conditions. This thesis addressed these challenges by progressively developing probabilistic, optimization-based, and learning-based frameworks, each contributing a distinct layer to a unified energy management vision.

In Chapter 2, a hybrid probabilistic forecasting model was proposed for determining the energy potential of wind power plants. The model accurately captured the nonlinear interactions between meteorological factors and wind power output by combining copula theory, deep learning, and decision tree approaches. This combination of statistical learning and artificial intelligence resulted in robust, high-resolution forecasts under uncertainty, making it a useful decision-support tool for renewable energy planning, risk management, and investment evaluation.

Chapter 3 advanced the research to a system-level optimization context by constructing a MILP model to coordinate power flows within residential communities with heterogeneous household profiles. The model incorporated multiple household types including grid-only users, PV-only prosumers, and PV–BESS prosumers and optimized both energy scheduling and peer-to-peer (P2P) trading. Results demonstrated the critical role of storage deployment and user diversity in shaping system performance and underscored the importance of incentive mechanisms in maintaining long-term user engagement. This centralized planning approach laid a structured foundation for decision-making in distributed energy environments.

With an emphasis on creating a framework for real-time smart grid management, Chapter 4 proceeded from planning to control. A rule-based model was initially used to represent community-level coordination of PV, BESS, EVs, and P2P energy exchange. This paradigm defined the operational logic and temporal segmentation required to manage distributed energy resources. Building on this foundation, a Deep Deterministic Policy Gradient (DDPG) reinforcement learning model was established to allow for dynamic pricing and decentralized decision-making. The agent developed optimal control techniques in real time, modifying prosumer behavior in response to system conditions, pricing signals, and storage availability. The simulation findings validated the model's capacity to reduce energy bills, increase local renewable self-consumption, and minimize grid dependency, demonstrating the importance of data-driven adaptive management in complex environments.

These chapters are integrated to create a coherent research narrative that addresses the three critical dimensions of smart energy system development: planning, control, and evaluation. Finally, the thesis presents a scalable and intelligent technique for facilitating the emergence of future energy systems that are resilient, adaptive, and aligned with long-term sustainability objectives.

5.2 Societal Impact and Contribution to Global Sustainability

This thesis aims to evaluate the potential of renewable energy sources (especially wind energy) with more sensitive and uncertain models, thus making significant contributions in line with the United Nations Sustainable Development Goals (SDGs).

SDG 7 - Accessible and Clean Energy: This thesis facilitates the integration of RES into the grid by increasing the accuracy of wind power plant production estimates. Accurate and reliable energy estimates make renewable energy investments more attractive, accelerating the transition to sustainable energy.

SDG 13 - Climate Action: Reducing dependence on fossil fuels is critical to reducing greenhouse gas emissions. Thanks to the Copula-deep learning-based models developed in the study, more effective use of wind energy becomes possible and contributes to the transition to low-carbon energy systems.

SDG 9 - Industry, Innovation and Infrastructure: The advanced modelling techniques based on artificial intelligence and machine learning used in the study contribute to the digitalisation of energy infrastructures. This will enable the development of more innovative, flexible and resilient systems in energy markets and microgrids.

SDG 11 - Sustainable Cities and Communities: This study increases the sustainability and resilience of urban energy systems through the support it provides for applications such as smart grids and P2P energy trading. This will ensure more equitable and accessible access to energy resources.

In addition, economically, this thesis contributes to reducing costs arising from energy supply-demand imbalances and providing more affordable energy, which indirectly serves **SDG 8 - Decent Work and Economic Growth.**

As a result, this thesis provides a multidimensional and holistic contribution to sustainable development in the energy sector. Fostering innovative and technological solutions represents a significant step forward in the global effort to combat climate change and build a more sustainable future. Beyond its technical advancements, the study offers valuable insights for policymakers, investors, and energy planners seeking to promote renewable energy integration and market flexibility. Moreover, its methodological framework can serve as a reference for future research aiming to address the growing complexity and uncertainty in decentralized energy systems.

5.3 Future Prospects

Building on the approaches established in this thesis, a number of exciting avenues for future research in the subject of smart energy systems become apparent. Across the planning, operation, and control layers, these future paths seek to improve system intelligence, adaptability, and practicality.

Integrating multi-vector energy systems is one appealing approach, extending the existing models that concentrate on electricity to include infrastructures for heating, cooling, and hydrogen. In order to enable more robust and efficient energy communities, future research can address the co-optimization of various sectors under a single energy management approach by utilizing hybrid optimization and control frameworks.

The field of human-centric modeling presents further opportunities. Demand response mechanisms that incorporate comfort preferences and behavioural data may significantly enhance the effectiveness and accuracy of smart grid control strategies. By incorporating behavioural economics into reinforcement learning settings, the system would be able to learn from user-driven variability in energy use patterns in addition to technical constraints.

Through edge computing and federated learning, the reinforcement learning system presented in this thesis can also be modified to function in decentralized and privacy-preserving environments. With these modifications, remote agents might work together to train energy management rules without exchanging raw data, opening the door for safe and scalable deployments across large-scale prosumer networks.

Furthermore, resilience-aware control can be the subject of future studies, with an emphasis on how systems behave in extreme situations like natural catastrophes, heat waves, and grid outages. Reinforcement learning agents can be trained to emphasize stability and recovery by integrating resilience indicators into reward structures, which will help create smart grids that are more resilient.

Finally, the implementation of blockchain-based energy markets can be supported by expanding the optimization and trading frameworks suggested in this study. Secure, transparent, and automated energy exchanges could be made possible by integrating distributed ledger and smart contract technology with peer-to-peer energy trading platforms, particularly under deregulated or community-owned grid models.

Collectively, these prospects provide a road map for transforming today's intelligent energy systems into fully adaptive, user-centric, and climate-resilient infrastructures, thereby facilitating the worldwide transition to sustainable and decentralized energy ecosystems.

BIBLIOGRAPHY

[1] "Transforming Our World: Interdisciplinary Insights on the Sustainable Development Goals - Sustainable Development Solutions Network." Accessed: Apr. 24, 2025. [Online]. Available: https://www.unsdsn.org/resources/transforming-our-world-interdisciplinary-insights-on-the-sustainable-development-goals/?gad_source=1&gbraid=0AAAABdu6wzbSbMVJFis-MKJy4lAYqOdf&gclid=CjwKCAjwwqfABhBcEiwAZJjC3lk4UEGS1tH_ThR6Gzv1Q6H2u_cV3-9HNW4pVKb3V44KD5x3RcAvRxoCN6YQAvD_BwE

[2] "The Paris Agreement | UNFCCC." Accessed: Apr. 24, 2025. [Online]. Available: https://unfccc.int/process-and-meetings/the-paris-agreement

[3] X. Fang, S. Misra, G. Xue, and D. Yang, "Smart grid - The new and improved power grid: A survey," *IEEE Communications Surveys and Tutorials*, vol. 14, no. 4, pp. 944–980, 2012, doi: 10.1109/SURV.2011.101911.00087.

[4] P. Siano, "Demand response and smart grids—A survey," *Renewable and Sustainable Energy Reviews*, vol. 30, pp. 461–478, Feb. 2014, doi: 10.1016/J.RSER.2013.10.022.

[5] K. N. Şahin and M. Sutcu, "Probabilistic assessment of wind power plant energy potential through a copula-deep learning approach in decision trees," *Heliyon*, vol. 10, no. 7, pp. 2405–8440, Apr. 2024, doi: 10.1016/j.heliyon.2024.e28270.

[6] H. Ritchie, P. Rosado, and M. Roser, "CO_2 and Greenhouse Gas Emissions - Our World in Data." Accessed: Apr. 11, 2025. [Online]. Available: https://ourworldindata.org/co2-and-greenhouse-gas-emissions#article-citation

[7] K. S. R. Murthy and O. P. Rahi, "A comprehensive review of wind resource assessment," *Renewable and Sustainable Energy Reviews*, vol. 72, pp. 1320–1342, May 2017, doi: 10.1016/J.RSER.2016.10.038.

[8] E. Vanvyve, L. Delle Monache, A. J. Monaghan, and J. O. Pinto, "Wind resource estimates with an analog ensemble approach," *Renew Energy*, vol. 74, pp. 761–773, Feb. 2015, doi: 10.1016/J.RENENE.2014.08.060.

[9] D. Astolfi, F. Castellani, A. Garinei, and L. Terzi, "Data mining techniques for performance analysis of onshore wind farms," *Appl Energy*, vol. 148, pp. 220–233, Jun. 2015, doi: 10.1016/J.APENERGY.2015.03.075.

[10] A. Kusiak, H. Zheng, and Z. Song, "Models for monitoring wind farm power," *Renew Energy*, vol. 34, no. 3, pp. 583–590, Mar. 2009, doi: 10.1016/J.RENENE.2008.05.032.

[11] H. Oh and B. Kim, "Comparison and verification of the deviation between guaranteed and measured wind turbine power performance in complex terrain," *Energy*, vol. 85, pp. 23–29, Jun. 2015, doi: 10.1016/J.ENERGY.2015.02.115.

[12] A. Altunkaynak, T. Erdik, I. Dabanli, and Z. Şen, "Theoretical derivation of wind power probability distribution function and applications," *Appl Energy*, vol. 92, pp. 809–814, Apr. 2012, doi: 10.1016/J.APENERGY.2011.08.038.

[13] C. Jung, D. Schindler, J. Laible, and A. Buchholz, "Introducing a system of wind speed distributions for modeling properties of wind speed regimes around the world," *Energy Convers Manag*, vol. 144, pp. 181–192, Jul. 2017, doi: 10.1016/J.ENCONMAN.2017.04.044.

[14] D. Ganger, J. Zhang, and V. Vittal, "Statistical characterization of wind power ramps via extreme value analysis," *IEEE Transactions on Power Systems*, vol. 29, no. 6, pp. 3118–3119, Nov. 2014, doi: 10.1109/TPWRS.2014.2315491.
[15] B. Safari, "Modeling wind speed and wind power distributions in Rwanda," *Renewable and Sustainable Energy Reviews*, vol. 15, no. 2, pp. 925–935, Feb. 2011, doi: 10.1016/J.RSER.2010.11.001.
[16] R. O. Fagbenle, J. Katende, O. O. Ajayi, and J. O. Okeniyi, "Assessment of wind energy potential of two sites in North-East, Nigeria," *Renew Energy*, vol. 36, no. 4, pp. 1277–1283, Apr. 2011, doi: 10.1016/J.RENENE.2010.10.003.
[17] O. O. Ajayi, "Assessment of utilization of wind energy resources in Nigeria," *Energy Policy*, vol. 37, no. 2, pp. 750–753, Feb. 2009, doi: 10.1016/J.ENPOL.2008.10.020.
[18] A. Serban, L. S. Paraschiv, and S. Paraschiv, "Assessment of wind energy potential based on Weibull and Rayleigh distribution models," *Energy Reports*, vol. 6, pp. 250–267, Nov. 2020, doi: 10.1016/J.EGYR.2020.08.048.
[19] M. A. Saeed, Z. Ahmed, J. Yang, and W. Zhang, "An optimal approach of wind power assessment using Chebyshev metric for determining the Weibull distribution parameters," *Sustainable Energy Technologies and Assessments*, vol. 37, p. 100612, Feb. 2020, doi: 10.1016/J.SETA.2019.100612.
[20] L. Bilir, M. Imir, Y. Devrim, and A. Albostan, "Seasonal and yearly wind speed distribution and wind power density analysis based on Weibull distribution function," *Int J Hydrogen Energy*, vol. 40, no. 44, pp. 15301–15310, Nov. 2015, doi: 10.1016/J.IJHYDENE.2015.04.140.
[21] S. H. Pishgar-Komleh, A. Keyhani, and P. Sefeedpari, "Wind speed and power density analysis based on Weibull and Rayleigh distributions (a case study: Firouzkooh county of Iran)," *Renewable and Sustainable Energy Reviews*, vol. 42, pp. 313–322, Feb. 2015, doi: 10.1016/J.RSER.2014.10.028.
[22] T. P. Chang, "Estimation of wind energy potential using different probability density functions," *Appl Energy*, vol. 88, no. 5, pp. 1848–1856, May 2011, doi: 10.1016/J.APENERGY.2010.11.010.
[23] S. Moradian, A. I. Olbert, S. Gharbia, and G. Iglesias, "Copula-based projections of wind power: Ireland as a case study," *Renewable and Sustainable Energy Reviews*, vol. 175, p. 113147, Apr. 2023, doi: 10.1016/J.RSER.2023.113147.
[24] M. M. N. S. B. McWilliams, "The Probability Distribution of Wind Velocity and Direction on JSTOR," *Wind Engineering*, vol. 3, no. 4, pp. 269–273, 1979, Accessed: Sep. 08, 2023. [Online]. Available: https://www.jstor.org/stable/43749150
[25] R. Weber, "Estimator for the Standard Deviation of Wind Direction Based on Moments of the Cartesian Components," *J Appl Meteorol Climatol*, vol. 30, no. 9, pp. 1341–1353, Sep. 1991, doi: 10.1175/1520-0450(1991)030.
[26] E. Erdem and J. Shi, "Comparison of bivariate distribution construction approaches for analysing wind speed and direction data," *Wind Energy*, vol. 14, no. 1, pp. 27–41, Jan. 2011, doi: 10.1002/WE.400.
[27] X. Bai and J. S. L. Lam, "Portfolio value-at-risk estimation for spot chartering decisions under changing trade patterns: A copula approach," *Risk Analysis*, vol. 43, no. 6, pp. 1278–1292, Jun. 2023, doi: 10.1111/RISA.13989.
[28] H. Nguyen and F. Javed, "Dynamic relationship between Stock and Bond returns: A GAS MIDAS copula approach," *J Empir Finance*, vol. 73, pp. 272–292, Sep. 2023, doi: 10.1016/J.JEMPFIN.2023.07.004.

[29] K. Xie *et al.*, “Assessment of the Joint Impact of Rainfall Characteristics on Urban Flooding and Resilience Using the Copula Method,” *Water Resources Management*, vol. 37, no. 4, pp. 1765–1784, Mar. 2023, doi: 10.1007/S11269-023-03453-9/TABLES/5.
[30] J. Seo, J. Won, J. Choi, J. Lee, and S. Kim, “A copula model to identify the risk of river water temperature stress for meteorological drought,” *J Environ Manage*, vol. 311, p. 114861, Jun. 2022, doi: 10.1016/J.JENVMAN.2022.114861.
[31] R. T. Clemen and T. Reilly, “Correlations and Copulas for Decision and Risk Analysis,” *https://doi.org/10.1287/mnsc.45.2.208*, vol. 45, no. 2, pp. 208–224, Feb. 1999, doi: 10.1287/MNSC.45.2.208.
[32] T. Wang and J. S. Dyer, “A Copulas-Based Approach to Modeling Dependence in Decision Trees,” *https://doi.org/10.1287/opre.1110.1004*, vol. 60, no. 1, pp. 225–242, Feb. 2012, doi: 10.1287/OPRE.1110.1004.
[33] C. Emeksiz and B. Demirci, “Sustainable Energy Technologies and Assessments journal homepage The determination of offshore wind energy potential of Turkey by using novelty hybrid site selection method,” 2019, doi: 10.1016/j.seta.2019.100562.
[34] G. Şahin, A. Koç, and W. van Sark, “Multi-criteria decision making for solar power - Wind power plant site selection using a GIS-intuitionistic fuzzy-based approach with an application in the Netherlands,” *Energy Strategy Reviews*, vol. 51, p. 101307, Jan. 2024, doi: 10.1016/J.ESR.2024.101307.
[35] Y. A. Solangi, C. Longsheng, and S. A. A. Shah, “Assessing and overcoming the renewable energy barriers for sustainable development in Pakistan: An integrated AHP and fuzzy TOPSIS approach,” *Renew Energy*, vol. 173, pp. 209–222, Aug. 2021, doi: 10.1016/J.RENENE.2021.03.141.
[36] M. R. Islam, M. Tareq Aziz, M. Alauddin, and Z. Kader, “Site suitability assessment for solar power plants in Bangladesh: A GIS-based analytical hierarchy process (AHP) and multi-criteria decision analysis (MCDA) approach,” 2023, doi: 10.1016/j.renene.2023.119595.
[37] M. G. Kendall, “A New Measure of Rank Correlation,” *Biometrika*, vol. 30, no. 1/2, p. 81, Jun. 1938, doi: 10.2307/2332226.
[38] K. Pearson, “VII. Note on regression and inheritance in the case of two parents,” *Proceedings of the Royal Society of London*, vol. 58, no. 347–352, pp. 240–242, Dec. 1895, doi: 10.1098/RSPL.1895.0041.
[39] M. Sklar, “Fonctions de répartition à N dimensions et leurs marges,” *Annales de l’ISUP*, pp. 229–231, 1959, Accessed: Sep. 11, 2023. [Online]. Available: https://hal.science/hal-04094463
[40] M. M. J. Zavareh, N. Mahjouri, M. Rahimzadegan, and M. Rahimpour, “A drought index based on groundwater quantity and quality: Application of multivariate copula analysis,” *J Clean Prod*, vol. 417, p. 137959, Sep. 2023, doi: 10.1016/J.JCLEPRO.2023.137959.
[41] R. B. Nelsen, *An Introduction to Copulas*, Springer. Springer New York, 2006. doi: 10.1007/0-387-28678-0.
[42] M. J. Frank, “On the simultaneous associativity of F(x, y) and x+y-F(x, y),” *Aequ Math*, vol. 19, no. 1, pp. 194–226, Dec. 1979, doi: 10.1007/BF02189866/METRICS.
[43] E. J. Gumbel, “Bivariate Exponential Distributions,” *J Am Stat Assoc*, vol. 55, no. 292, pp. 698–707, 1960, doi: 10.1080/01621459.1960.10483368.
[44] D. G. Clayton, “A model for association in bivariate life tables and its application in epidemiological studies of familial tendency in chronic disease incidence,”

Biometrika, vol. 65, no. 1, pp. 141–151, Apr. 1978, doi: 10.1093/BIOMET/65.1.141.
[45] E. M. Scheuer and D. S. Stoller, "On the Generation of Normal Random Vectors," *Technometrics*, vol. 4, no. 2, pp. 278–281, 1962, doi: 10.1080/00401706.1962.10490011.
[46] B. Biller and C. Gunes Corlu, "Copula-based multivariate input modeling," *Surveys in Operations Research and Management Science*, vol. 17, no. 2, pp. 69–84, Jul. 2012, doi: 10.1016/J.SORMS.2012.04.001.
[47] C. Genest and L. P. Rivest, "Statistical inference procedures for bivariate Archimedean copulas," *J Am Stat Assoc*, vol. 88, no. 423, pp. 1034–1043, 1993, doi: 10.1080/01621459.1993.10476372.
[48] G. Fu and D. Butler, "Copula-based frequency analysis of overflow and flooding in urban drainage systems," *J Hydrol (Amst)*, vol. 510, pp. 49–58, Mar. 2014, doi: 10.1016/J.JHYDROL.2013.12.006.
[49] A. Nazemi and A. Elshorbagy, "Application of copula modelling to the performance assessment of reconstructed watersheds," *Stochastic Environmental Research and Risk Assessment*, vol. 26, no. 2, pp. 189–205, Feb. 2012, doi: 10.1007/S00477-011-0467-7.
[50] K. Xu, D. Yang, X. Xu, and H. Lei, "Copula based drought frequency analysis considering the spatio-temporal variability in Southwest China," *J Hydrol (Amst)*, vol. Complete, no. 527, pp. 630–640, Aug. 2015, doi: 10.1016/J.JHYDROL.2015.05.030.
[51] C. Genest, K. Ghoudi, and L. p. Rivest, "A semiparametric estimation procedure of dependence parameters in multivariate families of distributions," *Biometrika*, vol. 82, no. 3, pp. 543–552, Sep. 1995, doi: 10.1093/BIOMET/82.3.543.
[52] W. H. Kruskal, "Ordinal Measures of Association," *J Am Stat Assoc*, vol. 53, no. 284, pp. 814–861, 1958, doi: 10.1080/01621459.1958.10501481.
[53] P. J. McNamee, *Decision analysis with supertree: Instructor's manual*. The Scientific Press, 1991.
[54] A. Hurst, G. C. Brown, and R. I. Swanson, "Swanson's 30-40-30 Rule," *Am Assoc Pet Geol Bull*, vol. 84, no. 12, pp. 1883–1891, Dec. 2000, doi: 10.1306/8626C70D-173B-11D7-8645000102C1865D.
[55] D. L. Keefer and S. E. Bodily, "Three-Point Approximations for Continuous Random Variables," *https://doi.org/10.1287/mnsc.29.5.595*, vol. 29, no. 5, pp. 595–609, May 1983, doi: 10.1287/MNSC.29.5.595.
[56] N. A. Zaino and J. D'Errico, "Optimal Discrete Approximations for Continuous Outcomes with Applications in Decision and Risk Analysis," *https://doi.org/10.1057/jors.1989.56*, vol. 40, no. 4, pp. 379–388, 1989, doi: 10.1057/JORS.1989.56.
[57] J. R. D'Errico and N. A. Zaino, "Statistical Tolerancing Using a Modification of Taguchi's Method," *Technometrics*, vol. 30, no. 4, p. 397, Nov. 1988, doi: 10.2307/1269802.
[58] A. C. Miller and T. R. Rice, "Discrete Approximations of Probability Distributions," *https://doi.org/10.1287/mnsc.29.3.352*, vol. 29, no. 3, pp. 352–362, Mar. 1983, doi: 10.1287/MNSC.29.3.352.
[59] S. Hochreiter and J. Schmidhuber, "Long Short-Term Memory," *Neural Comput*, vol. 9, no. 8, pp. 1735–1780, Nov. 1997, doi: 10.1162/NECO.1997.9.8.1735.
[60] Y. Wang, H. Ma, D. Sheng, and D. Wang, " Assessing the Interactions between Chlorophyll a and Environmental Variables Using Copula Method ," *J Hydrol Eng*, vol. 17, no. 4, pp. 495–506, Apr. 2012, doi: 10.1061/(ASCE)HE.1943-

5584.0000387/ASSET/5BAB9F9C-2236-4186-878B-FD6F7CB27D66/ASSETS/IMAGES/LARGE/FIGURE7.JPG.

[61] T. International Renewable Energy Agency, "Peer-to-peer electricity trading - Innovation Landscape Brief," 2020, Accessed: Mar. 24, 2025. [Online]. Available: www.irena.org

[62] W. Amin, Q. Huang, M. Afzal, A. A. Khan, K. Umer, and S. A. Ahmed, "A converging non-cooperative & cooperative game theory approach for stabilizing peer-to-peer electricity trading," *Electric Power Systems Research*, vol. 183, p. 106278, Jun. 2020, doi: 10.1016/J.EPSR.2020.106278.

[63] X. Jin, Q. Wu, and H. Jia, "Local flexibility markets: Literature review on concepts, models and clearing methods," *Appl Energy*, vol. 261, p. 114387, Mar. 2020, doi: 10.1016/J.APENERGY.2019.114387.

[64] Y. Wang, C. Gu, D. Xie, M. Alhazmi, J. Kim, and X. Wang, "Enhancing peer-to-peer energy trading in Integrated Energy Systems: Gamified engagement strategies and differentiable robust optimization," *Energy Reports*, vol. 13, pp. 3225–3236, Jun. 2025, doi: 10.1016/J.EGYR.2025.02.034.

[65] C. Zhang, J. Wu, C. Long, and M. Cheng, "Review of Existing Peer-to-Peer Energy Trading Projects," *Energy Procedia*, vol. 105, pp. 2563–2568, May 2017, doi: 10.1016/J.EGYPRO.2017.03.737.

[66] T. Sousa, T. Soares, P. Pinson, F. Moret, T. Baroche, and E. Sorin, "Peer-to-peer and community-based markets: A comprehensive review," *Renewable and Sustainable Energy Reviews*, vol. 104, pp. 367–378, Apr. 2019, doi: 10.1016/J.RSER.2019.01.036.

[67] Z. Li, S. Bahramirad, A. Paaso, M. Yan, and M. Shahidehpour, "Blockchain for decentralized transactive energy management system in networked microgrids," *The Electricity Journal*, vol. 32, no. 4, pp. 58–72, May 2019, doi: 10.1016/J.TEJ.2019.03.008.

[68] S. Nguyen, W. Peng, P. Sokolowski, D. Alahakoon, and X. Yu, "Optimizing rooftop photovoltaic distributed generation with battery storage for peer-to-peer energy trading," *Appl Energy*, vol. 228, pp. 2567–2580, Oct. 2018, doi: 10.1016/J.APENERGY.2018.07.042.

[69] C. Long, J. Wu, C. Zhang, M. Cheng, and A. Al-Wakeel, "Feasibility of Peer-to-Peer Energy Trading in Low Voltage Electrical Distribution Networks," *Energy Procedia*, vol. 105, pp. 2227–2232, May 2017, doi: 10.1016/J.EGYPRO.2017.03.632.

[70] H. Vaikund and S. G. Srivani, "Trends in Energy Management System for Smart Microgrid—An Overview," *Lecture Notes in Electrical Engineering*, vol. 703, pp. 15–28, 2021, doi: 10.1007/978-981-15-8391-9_2.

[71] J. M. Zepter, A. Lüth, P. Crespo del Granado, and R. Egging, "Prosumer integration in wholesale electricity markets: Synergies of peer-to-peer trade and residential storage," *Energy Build*, vol. 184, pp. 163–176, Feb. 2019, doi: 10.1016/J.ENBUILD.2018.12.003.

[72] A. Hasankhani and S. M. Hakimi, "Stochastic energy management of smart microgrid with intermittent renewable energy resources in electricity market," *Energy*, vol. 219, p. 119668, Mar. 2021, doi: 10.1016/J.ENERGY.2020.119668.

[73] W. Tushar *et al.*, "A coalition formation game framework for peer-to-peer energy trading," *Appl Energy*, vol. 261, p. 114436, Mar. 2020, doi: 10.1016/J.APENERGY.2019.114436.

[74] W. Tushar *et al.*, “A coalition formation game framework for peer-to-peer energy trading,” *Appl Energy*, vol. 261, p. 114436, Mar. 2020, doi: 10.1016/J.APENERGY.2019.114436.
[75] F. S. Ali, M. Aloqaily, O. Alfandi, and O. Ozkasap, “Cyberphysical Blockchain-Enabled Peer-to-Peer Energy Trading,” *Computer (Long Beach Calif)*, vol. 53, no. 9, pp. 56–65, Sep. 2020, doi: 10.1109/MC.2020.2991453.
[76] C. Zhang, J. Qiu, and Y. Yang, “A Peer-to-Peer Joint Kilowatt and Negawatt Trading Framework Incorporating Battery Cycling Degradation,” *IEEE Transactions on Power Systems*, vol. 39, no. 5, pp. 6386–6398, 2024, doi: 10.1109/TPWRS.2024.3360606.
[77] M. R. Alam, M. St-Hilaire, and T. Kunz, “Peer-to-peer energy trading among smart homes,” *Appl Energy*, vol. 238, pp. 1434–1443, Mar. 2019, doi: 10.1016/J.APENERGY.2019.01.091.
[78] S. Dorahaki, M. MollahassaniPour, and M. Rashidinejad, “Optimizing energy payment, user satisfaction, and self-sufficiency in flexibility-constrained smart home energy management: A multi-objective optimization approach,” *e-Prime - Advances in Electrical Engineering, Electronics and Energy*, vol. 6, p. 100385, Dec. 2023, doi: 10.1016/J.PRIME.2023.100385.
[79] M. J. Sanjari, H. Karami, and H. B. Gooi, “Analytical rule-based approach to online optimal control of smart residential energy system,” *IEEE Trans Industr Inform*, vol. 13, no. 4, pp. 1586–1597, Aug. 2017, doi: 10.1109/TII.2017.2651879.
[80] D. M. Minhas, J. Meiers, and G. Frey, “A Rule-based Expert System for Home Power Management Incorporating Real-Life Data Sets,” *3rd International Conference on Smart Grid and Renewable Energy, SGRE 2022 - Proceedings*, 2022, doi: 10.1109/SGRE53517.2022.9774212.
[81] S. Y. Chen and C. H. Chang, “Optimal Power Flows Control for Home Energy Management With Renewable Energy and Energy Storage Systems,” *IEEE Transactions on Energy Conversion*, vol. 38, no. 1, pp. 218–229, Mar. 2023, doi: 10.1109/TEC.2022.3198883.
[82] R. Hemmati and H. Saboori, “Stochastic optimal battery storage sizing and scheduling in home energy management systems equipped with solar photovoltaic panels,” *Energy Build*, vol. 152, pp. 290–300, Oct. 2017, doi: 10.1016/J.ENBUILD.2017.07.043.
[83] D. Zhang, S. Evangelisti, P. Lettieri, and L. G. Papageorgiou, “Economic and environmental scheduling of smart homes with microgrid: DER operation and electrical tasks,” *Energy Convers Manag*, vol. 110, pp. 113–124, Feb. 2016, doi: 10.1016/J.ENCONMAN.2015.11.056.
[84] A. Salem, A. El-Shenawy, and M. S. Hamad, “Energy Management Strategy for Grid Connected DC Hybrid Micro Grid Using Particle Swarm Optimization Technique,” *Proceedings of the International Conference on Microelectronics, ICM*, vol. 2020-December, Dec. 2020, doi: 10.1109/ICM50269.2020.9331823.
[85] A. Ignat, E. Lazar, and D. Petreus, “Energy Management for an Islanded Microgrid Based on Particle Swarm Optimization,” *2018 IEEE 24th International Symposium for Design and Technology in Electronic Packaging, SIITME 2018 - Proceedings*, pp. 213–216, Jul. 2018, doi: 10.1109/SIITME.2018.8599272.
[86] A. J. Litchy and M. H. Nehrir, “Real-time energy management of an islanded microgrid using multi-objective Particle Swarm Optimization,” *IEEE Power and Energy Society General Meeting*, vol. 2014-October, no. October, Oct. 2014, doi: 10.1109/PESGM.2014.6938997.

[87] A. Soetedjo, Y. I. Nakhoda, and C. Saleh, "Simulation of Fuzzy Logic Based Energy Management for the Home with Grid Connected PV-Battery System," *2nd International Conference on Smart Grid and Smart Cities, ICSGSC 2018*, pp. 122–126, Nov. 2018, doi: 10.1109/ICSGSC.2018.8541271.
[88] H. Xiao, X. Pu, W. Pei, L. Ma, and T. Ma, "A Novel Energy Management Method for Networked Multi-Energy Microgrids Based on Improved DQN," *IEEE Trans Smart Grid*, vol. 14, no. 6, pp. 4912–4926, Nov. 2023, doi: 10.1109/TSG.2023.3261979.
[89] Y. Liu, D. Zhang, and H. B. Gooi, "Optimization strategy based on deep reinforcement learning for home energy management," *CSEE Journal of Power and Energy Systems*, vol. 6, no. 3, pp. 572–582, Sep. 2020, doi: 10.17775/CSEEJPES.2019.02890.
[90] D. Bousnina and G. Guerassimoff, "Deep Reinforcement Learning for Optimal Energy Management of Multi-energy Smart Grids," *Lecture Notes in Computer Science (including subseries Lecture Notes in Artificial Intelligence and Lecture Notes in Bioinformatics)*, vol. 13164 LNCS, pp. 15–30, 2022, doi: 10.1007/978-3-030-95470-3_2.
[91] R. Faia, C. Goncalves, L. Gomes, and Z. Vale, "Dataset of an energy community with prosumer consumption, photovoltaic generation, battery storage, and electric vehicles," *Data Brief*, vol. 48, p. 109218, Jun. 2023, doi: 10.1016/J.DIB.2023.109218.
[92] C. Long, J. Wu, C. Zhang, L. Thomas, M. Cheng, and N. Jenkins, "Peer-to-peer energy trading in a community microgrid," *IEEE Power and Energy Society General Meeting*, vol. 2018-January, pp. 1–5, Jan. 2018, doi: 10.1109/PESGM.2017.8274546.
[93] IEA, "World Energy Outlook 2021," 2021, Accessed: Apr. 11, 2025. [Online]. Available: www.iea.org/weo
[94] A. G. Olabi and M. A. Abdelkareem, "Renewable energy and climate change," *Renewable and Sustainable Energy Reviews*, vol. 158, p. 112111, Apr. 2022, doi: 10.1016/J.RSER.2022.112111.
[95] H. Kanneganti *et al.*, "Specification of energy assessment methodologies to satisfy ISO 50001 energy management standard," *Sustainable Energy Technologies and Assessments*, vol. 23, pp. 121–135, Oct. 2017, doi: 10.1016/J.SETA.2017.09.003.
[96] Y. Li and Y. W. Li, "Power management of inverter interfaced autonomous microgrid based on virtual frequency-voltage frame," *IEEE Trans Smart Grid*, vol. 2, no. 1, pp. 30–40, 2011, doi: 10.1109/TSG.2010.2095046.
[97] B. Dupont, K. Dietrich, C. De Jonghe, A. Ramos, and R. Belmans, "Impact of residential demand response on power system operation: A Belgian case study," *Appl Energy*, vol. 122, pp. 1–10, Jun. 2014, doi: 10.1016/J.APENERGY.2014.02.022.
[98] A. S. Anees, "Grid integration of renewable energy sources: Challenges, issues and possible solutions," *India International Conference on Power Electronics, IICPE*, 2012, doi: 10.1109/IICPE.2012.6450514.
[99] "Electric vehicles - IEA." Accessed: Mar. 27, 2025. [Online]. Available: https://www.iea.org/energy-system/transport/electric-vehicles
[100] E. Vega-Fuentes and M. Denai, "Enhanced Electric Vehicle Integration in the UK Low-Voltage Networks With Distributed Phase Shifting Control," *IEEE Access*, vol. 7, pp. 46796–46807, 2019, doi: 10.1109/ACCESS.2019.2909990.
[101] M. B. Babu and R. M. Shereef, "Optimal Scheduling of Electric Vehicles for Peak Clipping Services," *2020 IEEE International Conference on Power Electronics,*

Smart Grid and Renewable Energy, PESGRE 2020, Jan. 2020, doi: 10.1109/PESGRE45664.2020.9070736.
[102] P. Thomas and P. K. Shanmugam, "A review on mathematical models of electric vehicle for energy management and grid integration studies," *J Energy Storage*, vol. 55, p. 105468, Nov. 2022, doi: 10.1016/J.EST.2022.105468.
[103] C. Guille and G. Gross, "A conceptual framework for the vehicle-to-grid (V2G) implementation," *Energy Policy*, vol. 37, no. 11, pp. 4379–4390, Nov. 2009, doi: 10.1016/J.ENPOL.2009.05.053.
[104] M. A. Lee, "Assessment of demand response and advanced metering," Washington, DC, USA, 2016.
[105] N. G. Paterakis, O. Erdinç, and J. P. S. Catalão, "An overview of Demand Response: Key-elements and international experience," *Renewable and Sustainable Energy Reviews*, vol. 69, pp. 871–891, Mar. 2017, doi: 10.1016/J.RSER.2016.11.167.
[106] P. Siano, "Demand response and smart grids—A survey," *Renewable and Sustainable Energy Reviews*, vol. 30, pp. 461–478, Feb. 2014, doi: 10.1016/J.RSER.2013.10.022.
[107] L. Zhang, Y. Gao, H. Zhu, and L. Tao, "A distributed real-time pricing strategy based on reinforcement learning approach for smart grid," *Expert Syst Appl*, vol. 191, p. 116285, Apr. 2022, doi: 10.1016/J.ESWA.2021.116285.
[108] K. Zhang, S. Hanif, C. M. Hackl, and T. Hamacher, "A Framework for Multi-Regional Real-Time Pricing in Distribution Grids," *IEEE Trans Smart Grid*, vol. 10, no. 6, pp. 6826–6838, Nov. 2019, doi: 10.1109/TSG.2019.2911996.
[109] Q. Tang, K. Yang, D. Zhou, Y. Luo, and F. Yu, "A Real-Time Dynamic Pricing Algorithm for Smart Grid with Unstable Energy Providers and Malicious Users," *IEEE Internet Things J*, vol. 3, no. 4, pp. 554–562, Aug. 2016, doi: 10.1109/JIOT.2015.2452960.
[110] Y. Dai, L. Li, P. Zhao, and J. Duan, "Real-time pricing in smart community with constraint from the perspective of advertising game," *International Transactions on Electrical Energy Systems*, vol. 29, no. 9, p. e12043, Sep. 2019, doi: 10.1002/2050-7038.12043.
[111] L. Zhang, Y. Gao, H. Zhu, and L. Tao, "A distributed real-time pricing strategy based on reinforcement learning approach for smart grid," *Expert Syst Appl*, vol. 191, p. 116285, Apr. 2022, doi: 10.1016/J.ESWA.2021.116285.
[112] A. Molderink, V. Bakker, M. G. C. Bosman, J. L. Hurink, and G. J. M. Smit, "Domestic energy management methodology for optimizing efficiency in smart grids," *2009 IEEE Bucharest PowerTech: Innovative Ideas Toward the Electrical Grid of the Future*, 2009, doi: 10.1109/PTC.2009.5281849.
[113] M. Behrangrad, H. Sugihara, and T. Funaki, "Analyzing the system effects of optimal demand response utilization for reserve procurement and peak clipping," *IEEE PES General Meeting, PES 2010*, 2010, doi: 10.1109/PES.2010.5589597.
[114] A. H. Mohsenian-Rad and A. Leon-Garcia, "Optimal residential load control with price prediction in real-time electricity pricing environments," *IEEE Trans Smart Grid*, vol. 1, no. 2, pp. 120–133, Sep. 2010, doi: 10.1109/TSG.2010.2055903.
[115] P. Tarasak, "Optimal real-time pricing under load uncertainty based on utility maximization for smart grid," *2011 IEEE International Conference on Smart Grid Communications, SmartGridComm 2011*, pp. 321–326, 2011, doi: 10.1109/SMARTGRIDCOMM.2011.6102341.
[116] H. Zhu, Y. Gao, Y. Hou, and L. Tao, "Multi-time slots real-time pricing strategy with power fluctuation caused by operating continuity of smart home appliances,"

Eng Appl Artif Intell, vol. 71, pp. 166–174, May 2018, doi: 10.1016/J.ENGAPPAI.2018.02.010.
[117] M. Ansari, A. T. Al-Awami, M. A. Abido, and E. Sortomme, “Optimal charging strategies for unidirectional vehicle-to-grid using fuzzy uncertainties,” *Proceedings of the IEEE Power Engineering Society Transmission and Distribution Conference*, Jul. 2014, doi: 10.1109/TDC.2014.6863314.
[118] C. Cecati, C. Citro, and P. Siano, “Combined operations of renewable energy systems and responsive demand in a smart grid,” *IEEE Trans Sustain Energy*, vol. 2, no. 4, pp. 468–476, Oct. 2011, doi: 10.1109/TSTE.2011.2161624.
[119] Q. Dong, L. Yu, W. Z. Song, L. Tong, and S. Tang, “Distributed demand and response algorithm for optimizing social-welfare in smart grid,” *Proceedings of the 2012 IEEE 26th International Parallel and Distributed Processing Symposium, IPDPS 2012*, pp. 1228–1239, 2012, doi: 10.1109/IPDPS.2012.112.
[120] P. Samadi, H. Mohsenian-Rad, R. Schober, and V. W. S. Wong, “Advanced demand side management for the future smart grid using mechanism design,” *IEEE Trans Smart Grid*, vol. 3, no. 3, pp. 1170–1180, 2012, doi: 10.1109/TSG.2012.2203341.
[121] S. Choi, S. Park, D. J. Kang, S. J. Han, and H. M. Kim, “A microgrid energy management system for inducing optimal demand response,” *2011 IEEE International Conference on Smart Grid Communications, SmartGridComm 2011*, pp. 19–24, 2011, doi: 10.1109/SMARTGRIDCOMM.2011.6102317.
[122] P. O. Kriett and M. Salani, “Optimal control of a residential microgrid,” *Energy*, vol. 42, no. 1, pp. 321–330, Jun. 2012, doi: 10.1016/J.ENERGY.2012.03.049.
[123] M. Silva, H. Morais, and Z. Vale, “An integrated approach for distributed energy resource short-term scheduling in smart grids considering realistic power system simulation,” *Energy Convers Manag*, vol. 64, pp. 273–288, Dec. 2012, doi: 10.1016/J.ENCONMAN.2012.04.021.
[124] T. Sousa, H. Morais, Z. Vale, P. Faria, and J. Soares, “Intelligent energy resource management considering vehicle-to-grid: A simulated annealing approach,” *IEEE Trans Smart Grid*, vol. 3, no. 1, pp. 535–542, Mar. 2012, doi: 10.1109/TSG.2011.2165303.
[125] B. Wang, Y. Li, W. Ming, and S. Wang, “Deep Reinforcement Learning Method for Demand Response Management of Interruptible Load,” *IEEE Trans Smart Grid*, vol. 11, no. 4, pp. 3146–3155, Jul. 2020, doi: 10.1109/TSG.2020.2967430.
[126] M. G. Kallitsis, G. Michailidis, and M. Devetsikiotis, “Optimal power allocation under communication network externalities,” *IEEE Trans Smart Grid*, vol. 3, no. 1, pp. 162–173, Mar. 2012, doi: 10.1109/TSG.2011.2169995.
[127] T. H. Chang, M. Alizadeh, and A. Scaglione, “Coordinated home energy management for real-time power balancing,” *IEEE Power and Energy Society General Meeting*, 2012, doi: 10.1109/PESGM.2012.6345639.
[128] J. Wang, Z. Sun, Y. Zhou, and J. Dai, “Optimal dispatching model of smart home energy management system,” *2012 IEEE Innovative Smart Grid Technologies - Asia, ISGT Asia 2012*, 2012, doi: 10.1109/ISGT-ASIA.2012.6303266.
[129] N. Gatsis and G. B. Giannakis, “Cooperative multi-residence demand response scheduling,” *2011 45th Annual Conference on Information Sciences and Systems, CISS 2011*, 2011, doi: 10.1109/CISS.2011.5766245.
[130] F. Alfaverh, M. Denaï, and Y. Sun, “Electrical vehicle grid integration for demand response in distribution networks using reinforcement learning,” 2021, doi: 10.1049/els2.12030.
[131] R. S. Sutton and A. G. Barto, “The Reinforcement Learning Problem,” 1998.

[132] B. Ravindran, “Relativized hierarchical decomposition of Markov decision processes,” *Prog Brain Res*, vol. 202, pp. 465–488, Jan. 2013, doi: 10.1016/B978-0-444-62604-2.00023-X.
[133] X. Kong, D. Kong, J. Yao, L. Bai, and J. Xiao, “Online pricing of demand response based on long short-term memory and reinforcement learning,” *Appl Energy*, vol. 271, p. 114945, Aug. 2020, doi: 10.1016/J.APENERGY.2020.114945.
[134] R. Lu, S. H. Hong, and X. Zhang, “A Dynamic pricing demand response algorithm for smart grid: Reinforcement learning approach,” *Appl Energy*, vol. 220, pp. 220–230, Jun. 2018, doi: 10.1016/J.APENERGY.2018.03.072.
[135] Richardson Ian and M. Thomson, “One-Minute Resolution Domestic Electricity Use Data, 2008-2009,” 2022, *UK Data Service*.
[136] “Generation profiles for a 3.8 kW PV station located in Nottingham.” Accessed: Apr. 15, 2025. [Online]. Available: https://pvoutput.org/ladder.jsp
[137] “Octopus Flux | Octopus Energy.” Accessed: Apr. 15, 2025. [Online]. Available: https://octopus.energy/smart/flux/
[138] “National Travel Survey 2021: Mode share, journey lengths and public transport use - GOV.UK.” Accessed: Apr. 15, 2025. [Online]. Available: https://www.gov.uk/government/statistics/national-travel-survey-2021/national-travel-survey-2021-mode-share-journey-lengths-and-public-transport-use#journey-lengths
[139] “Household Electricity Survey - GOV.UK.” Accessed: Apr. 15, 2025. [Online]. Available: https://www.gov.uk/government/collections/household-electricity-survey

CURRICULUM VITAE

2014 – 2019	B.Sc., Industrial Engineering, Abdullah Gül University, Kayseri, TURKEY
2020 – 2025	Ph.D., Industrial Engineering, Abdullah Gül University, Kayseri, TURKEY
2021 – Present	Research Assistant, Industrial Engineering, Abdullah Gül University, Kayseri, TURKEY

SELECTED PUBLICATIONS AND PRESENTATIONS

J1) Şahin, K. N., & Sutcu, M. (2024). Optimization of Energy Management in Heterogeneous Smart Grids: A Peer-to-Peer Trading Approach for Cost Reduction, Self-Sufficiency, and Grid Independence submitted in IEEE Access.

J2) Şahin, K. N., & Sutcu, M. (2024). Probabilistic Assessment of Wind Power Plant Energy Potential Through a Copula-Deep Learning Approach in Decision Trees published in *Heliyon*, *10*(7).

J3) Sütçü, M., **Şahin, K. N.,** Koloğlu, Y., Çelikel, M. E., & Gülbahar, İ. T. (2022). Electricity load forecasting using deep learning and novel hybrid models published in Sakarya University Journal of Science, 26(1), 91-104.

C1) Şahin, K. N., & Sutcu, M., Strategic Coordination of P2P Energy Trading in Smart Microgrids in International Conference on Engineering, Natural Sciences, and Technological Developments (ICENSTED 2024) (July 2024).

C2) Şahin, K. N., Short Term System Marginal Electricity Price Forecasting Using Deep Neural Networks and a Hybrid Model in 41. Yöneylem Araştırması Endüstri Mühendisliği Kongresi (YAEM 2022), (October 2022)